

MICROBORE HPLC METHODOLOGY AND TEMPERATURE PROGRAMMED

MICROBORE HPLC

by

Jeffrey Bowermaster,

Dissertation submitted to the Faculty of the  
Virginia Polytechnic Institute and State University  
in partial fulfillment of the requirements for the degree of

DOCTOR OF PHILOSOPHY

in

Chemistry

APPROVED:

---

Harold M. McNair, Chairman

---

John G. Dillard

---

Paul E. Field

---

John G. Mason

---

Larry T. Taylor

December, 1984

Blacksburg, Virginia

MICROBORE HPLC METHODOLOGY AND TEMPERATURE PROGRAMMED MICRO-  
BORE HPLC

by

Jeffrey Bowermaster

(ABSTRACT)

Small diameter LC columns provide rapid thermal equilibration and are ideal candidates for temperature programmed LC. Special instrumentation requirements are presented and details of column assembly are given to permit the preparation of highly efficient, stable microbore columns. Three LC temperature control systems are described and their individual strengths and weaknesses are discussed. Problems encountered in raising the temperature of an LC column are addressed and solutions are described. Experimental results of column and instrumentation evaluation are given and the effects of temperature on speed, efficiency, stability and retention of a broad range of samples is reported. Temperature and solvent programming are compared directly.

## ACKNOWLEDGEMENTS

I would like to thank all those people who have helped me along the way. (6th grade teacher who turned me on to science); , (high school math teacher) for teaching me to understand complex systems; and (UNCC Chemistry Professors) for their attention and support; , for insisting I go to graduate school, (EPA personnel) for being such good people to work with, E. M. Science, for giving me my own company to play with, , for taking me seriously, , yes, and even and for being stimulating graduate school types, the secretaries and , for their sympathy and concern, to , for keeping me supplied during the ordeal and earning her angel wings, and most of all, the Doc, Harold McNair, for keeping the wolves at bay, for letting me go wild, for not screaming too much, and for really coming through when it counted.

## CONTENTS

1.0	INTRODUCTION . . . . .	1
2.0	HISTORICAL . . . . .	6
2.1	Microbore LC . . . . .	6
2.1.1	Resolution and Cost . . . . .	8
2.1.2	Sensitivity . . . . .	8
2.1.3	Speed . . . . .	10
2.1.4	Gradient Elution . . . . .	13
2.1.5	Temperature Gradients . . . . .	14
2.2	Temperature Programmed LC . . . . .	15
2.2.1	Observed Temperature Effects . . . . .	16
2.2.2	Equilibration Time . . . . .	18
2.2.3	Comparison of Programming Techniques . . . . .	19
2.2.4	Uses of Temperature Programmed LC . . . . .	22
2.2.5	Column Efficiency and Temperature . . . . .	24
2.2.6	Microcolumn Temperature Programming . . . . .	28
2.2.7	Column and Sample Stability . . . . .	30
2.2.8	Summary . . . . .	33
3.0	THEORY . . . . .	35
3.1	Isothermal Microbore Instrumentation Requirements . . . . .	35
3.1.1	Plate Theory . . . . .	35

3.1.2	Extracolumn Variance . . . . .	38
3.1.3	Theoretical Extracolumn Variance Evaluation . . . . .	40
3.1.4	Injector Volume . . . . .	45
3.1.5	Non-eluting Sample Solvent . . . . .	45
3.1.6	Detector Volume . . . . .	47
3.2	Retention Mechanism . . . . .	50
3.2.1	Thermodynamics . . . . .	52
3.2.2	Measurement of the Temperature Effect . . . . .	53
3.2.3	Void Volume . . . . .	54
3.2.4	Void Volume via Linearization of Homologous Series . . . . .	57
3.2.5	Column Efficiency vs Temperature . . . . .	58
3.3	Conclusions . . . . .	65
4.0	EXPERIMENTAL . . . . .	67
4.1	Instrumentation . . . . .	67
4.1.1	Solvent Reservoir . . . . .	67
4.1.2	Pump . . . . .	68
4.1.3	Pulse Dampener . . . . .	71
4.1.4	Injector . . . . .	73
4.1.5	Frits . . . . .	73
4.1.5.1	Kel-F® Surrounded Frits . . . . .	80
4.1.6	Columns . . . . .	84
4.1.7	Tubing Cutter . . . . .	87

4.1.8	Column Packer	89
4.1.9	Detector	89
4.1.10	Thermal Isolation	94
4.1.11	Back Pressure Regulator	95
4.2	Column Temperature Control	98
4.2.1	Electrical Heating	98
4.2.2	Water Bath Circulation	105
4.2.3	Hot Air Blower System	109
4.3	Reagents and Materials	113
4.3.1	Homologous Series	113
4.3.2	LC Solvents	117
4.3.3	Sorbents	117
4.4	Procedures	117
4.4.1	Column Polishing	117
4.4.2	Column Packing	126
4.4.3	Retention versus Temperature Study	133
4.4.3.1	Calculations	135
4.4.4	Adsorption Isotherm Study	136
4.4.4.1	Calculations	140
4.4.5	Density Data	140
4.4.6	Empty Column Volume	140
4.4.7	Packed Column Volume	143
4.4.8	Column Conditioning	144
4.4.9	Flow Measurement	146

4.4.10	Temperature Response Time . . . . .	147
5.0	RESULTS AND DISCUSSION . . . . .	151
5.1	Microbore Equipment Performance . . . . .	152
5.1.1	Injection Volume . . . . .	152
5.1.2	Weak Solvent (Mobile Phase) . . . . .	154
5.1.3	Weak Solvent (Sample Solvent) . . . . .	158
5.1.4	Detector Cell Volume . . . . .	163
5.1.5	Polished versus Non-Polished Tubing Performance . . . . .	163
5.2	Temperature Effects . . . . .	166
5.2.1	Effect of Temperature on Retention . . . . .	166
5.2.2	Excessive Void Volume Estimates . . . . .	168
5.2.2.1	Pendant Group Effects . . . . .	168
5.2.2.2	Precision of Retention Volume Measurements	172
5.2.2.3	Sorbent Change on Conditioning . . . . .	176
5.2.2.4	Temperature Gradients . . . . .	179
5.2.3	Temperature Equivalence to Composition . . . . .	183
5.2.4	Efficiency vs Temperature . . . . .	186
5.2.5	Adsorption Isotherm Change with Temperature	188
5.2.6	Temperature Programming . . . . .	192
5.2.7	Temperature Programming vs Solvent Programming	192
5.3	Future Work . . . . .	196

6.0	CONCLUSIONS . . . . .	199
A.0	VOID VOLUME DETERMINATION . . . . .	205
A.1	.Berendsen's Method . . . . .	206
A.2	.Grobler's Method . . . . .	207
A.3	.Mockel's Method . . . . .	208
B.0	HOMOLOGOUS SERIES PROGRAM . . . . .	210
C.0	ISOTHERM PROGRAM . . . . .	218
D.0	RETENTION VOLUMES . . . . .	223
	REFERENCES . . . . .	230
	VITA . . . . .	239

## List of Figures

Figure	Page
1. Speed for 1 mm and 4.6 mm ID columns . . . . .	12
2. Formation of three dimensional concentration profiles with radial temperature gradients . .	27
3. Variables used to calculate N . . . . .	36
4. Velocity profile of laminar fluid flow through a tube . . . . .	41
5. Effect of laminar flow on the width of an initially narrow sample zone . . . . .	42
6. The effect of laminar flow on the injection profile from an open sample loop . . . . .	45
7. Calculated diffusion coefficients of benzene in methanol as a function of temperature . . .	63
8. Plot of plate height versus linear velocity and reduced plate height versus reduced linear velocity . . . . .	64
9. Solvent splitter system used to form microbore compatible gradients . . . . .	70
10. Flush volume requirements of a 11.7 ml pulse dampener . . . . .	72
11. Direct column attachment to a sample valve according to Scott and Kucera . . . . .	75
12. Nut and Ferrule used to seal the column to the valve . . . . .	76
13. Inside column end frit . . . . .	78
14. ISCO's threaded in-column frit design . . . . .	79
15. Safe top-column connection of a microbore column to a sample valve . . . . .	81

Figure	page
16. Frit before insertion into a column end-fitting . . . . .	82
17. Frit after insertion into a column end-fitting . . . . .	83
18. Kel-F surrounded frit . . . . .	85
19. Beveled microbore column end and the seal made with the kel-f surrounded frit . . . . .	88
20. Column packing equipment . . . . .	90
21. Special column end-fitting for direct column-to-detector cell connection . . . . .	92
22. The 0.5 and 8.0 $\mu$ l UV detector cells . . . . .	93
23. Vapor pressures versus temperatures for methanol and water . . . . .	96
24. Temperature programmed chromatograms using two different types of back pressure regulators . . . . .	97
25. Stable microbore back pressure regulator . . . . .	99
26. Electrical column heating system . . . . .	100
27. Power versus temperature for an electrically heated microbore column . . . . .	102
28. Multiple electrical contact system for offsetting longitudinal temperature gradients with electrical heating . . . . .	104
29. Circulating water microbore column temperature control system . . . . .	106
30. Brass insert allowing polyethylene tubing to be used with swagelock fittings leak free at 100 $^{\circ}$ C . . . . .	108
31. Heated air column temperature control system . . . . .	110

Figure	Page
32. Inside surface of commercial 1/16" ID stainless steel tubing . . . . .	119
33. Inside tubing finish after polishing . . . . .	124
34. Automatic column polisher . . . . .	125
35. Column packing instrumentation . . . . .	127
36. Means of loading the slurry into the column and reservoir excluding air . . . . .	129
37. Chromatogram from a 50 cm, 5 $\mu$ m column which was made using the temperature programmed column packing technique . . . . .	134
38. Batch extraction system for isotherm determination . . . . .	137
39. Conditions of analysis and a typical chromatogram of the column extract . . . . .	139
40. Density versus temperature for 50/50, 70/30 and 90/10 methanol/water mixtures . . . . .	142
41. Temperature programmed chromatogram showing the effects of detector cell blockage by wax solidifying inside the detector cell . . . . .	145
42. Side-arm pipette used to measure low flow rates . . . . .	148
43. Temperature response times for conventional 4.6 mm ID columns and 1 mm ID microbore columns . . . . .	149
44. Efficiency versus injection volume for microbore columns . . . . .	153
45. Step gradient chromatogram . . . . .	156
46. Non-eluting solvent effect . . . . .	159

Figure	Page
47. Effect of the difference between the mobile phase and sample solvent strength on observed efficiency as a function of capacity factor . . . . .	161
48. PTH-amino acid analysis using a large volume injection (25 $\mu$ l) on a 50 cm microbore column . . . . .	162
49. Chromatograms from a microbore column using 0.5 and 8.0 $\mu$ l cells . . . . .	164
50. Observed column efficiency versus $k'$ from 0.5 and 8.0 $\mu$ l cells . . . . .	165
51. Van Deemter Plots from microbore columns constructed from polished and non-polished tubing . . . . .	167
52. Effect of a 1% relative error in retention volume on the resulting $V_0$ estimate . . . . .	175
53. Effect of column conditioning on chromatographic performance . . . . .	178
54. $\ln k'$ versus $n_c$ plots for alkyl benzenes as a function of temperature at three different mobile phase compositions . . . . .	184
55. $\ln \alpha$ versus temperature . . . . .	185
56. Observed column efficiency as a function of the flow rate, the capacity factor, and temperature of the column and the mobile phase using an air heating system . . . . .	187
57. Column efficiency versus temperature for a water jacketed microbore column . . . . .	189
58. Composite adsorption isotherms for methanol/water mixtures on RP-18 as a function of temperature . . . . .	191
59. Temperature programmed microbore HPLC . . . . .	193
60. Comparison of solvent and temperature gradients . . . . .	197

## List of Tables

Table	Page
1. Injector and detector volumes for micro LC instrumentation . . . . .	3
2. Maximum tubing length (cm.) producing less than a 5% increase in observed peak width. . . . .	44
3. Percent increase in the width of a microbore peak caused by a 0.5, 2.5 and 8.0 $\mu$ l detector cells as a function of capacity factor. . . . .	49
4. $k/(k + 1)$ and $k^2/(k + 1)^2$ as a function of capacity factor $k$ . . . . .	60
5. Viscosity of methanol as a function of temperature. . . . .	62
6. Homologous Series Used . . . . .	114
7. UV absorbance and sample concentrations for homologous series samples. . . . .	116
8. Density as a function of temperature for methanol-water mixtures. . . . .	141
9. Plate counts for constant solvent and step gradient solvent injection techniques . . .	157
10. $V_0$ estimates from homologous series as a function of temperature and mobile phase composition. . . . .	169-171
11. $V_0$ Estimation using the Mockel method using $nc \geq 5$ . . . . .	173
12. Void volume prediction using Berendsens method for every conceivable combination of homologs. . . . .	174

List of Tables (cont.)

13. Adjustments to retention times to cause all combinations of homologs in figure XII to predict the same void volume of 176 ul. . . . .	177
14. Retention volume as a function of flow rate . .	181
15. Void volume estimates from retention volume by the Berendsen method and resulting capacity factors. . . . .	183
16. Temperature programmed versus isothermal retention times as a function of mobile phase composition . . . . .	194
17. Peak Widths vs carbon number for alkyl benzenes in temperature programmed LC . . . . .	196

## 1.0 INTRODUCTION

This dissertation has three main objectives: first, to describe the effect that particular instrumental design has on the observed performance of microbore columns; second, to outline in detail procedures that have been successfully employed for packing stable, high efficiency microbore columns; and third, to report on the potential of temperature programmed LC, as an inexpensive alternative to solvent programmed LC.

The current popularity of microbore HPLC can be attributed to the pioneering work of Scott and Kucera (1) who described column packing procedures, instrumental requirements and experimental results using 1 mm ID packed LC columns. They emphasized the necessity to miniaturize the component volumes (injectors, detectors) and connection volumes, concurrent with reducing the column diameter, in order to maintain resolution. At the time (1979) of their original publication (1), no commercial manufacturer sold an integrated LC instrument package which met their requirements. However, at this writing, at least 10 companies now market micro LC instrumentation with small volume injectors and detectors. Micro LC defines any LC with a column diameter less than 2.1 mm ID. Microbore LC is

assumed here to mean 1 mm ID LC. A listing of the injector volumes and and detector configurations are listed in Table I.

All of these micro LC instruments use 0.2-1.0  $\mu$ l injectors and 0.06-2.9  $\mu$ l detector cells. In contrast, typical conventional instrumentation uses 10  $\mu$ l injectors and 8  $\mu$ l detector cells. Reduction in injector and detector volumes will lead to a reduction in the overall sensitivity of microbore LC. Since a potential gain in sensitivity is one of microbore LC's major advantages, micro LC instrumentation using small volume injectors and detectors reduce the utility of microbore LC. The decision to market micro LC with the specifications in Table I is seen as a failure to fully appreciate the actual requirements of microbore LC with respect to the injection volume, the detector volume, and their influence on sensitivity and resolution. Both a theoretical evaluation and experimental results will show that conventional instrumentation delivers higher sensitivity and almost the same resolution as micro LC instrumentation with the advantage that no special instrumentation needs to be implemented.

It has been stated that microbore columns are more difficult to pack than conventional bore columns. The early columns that came on the market shortly following Scott and Kucera's publi-

Table I.

Injector and Detector Volumes (in  $\mu\text{l}$ )  
and detector cell pathlengths for  
Micro LC Instrumentation

	ISCO	LDC	LKB	Kratos	Beckman
Injector Volume	0.06	0.5	0.5	--	0.5
Detector Volume	0.25	2.9	0.8	0.5	2.2
Optical Pathlength (mm)	5	1	3	1	5
	Brownlee	Varian	Shimadzu	Waters	JASCO
Injector Volume	0.2	0.5	0.5	--	1.0
Detector Volume	1.0	0.5	0.5	1.9	1.0
Optical Pathlength (mm)	5	2	1	1	5

cation had low performance and developed voids after only a few hours operation. The reasons for these failures was not so much due to an intrinsic property of the reduced column diameter as it was a failure of the manufacturers to pay attention to small details. The relative importance of the inner wall finish for microbore columns is magnified since the ratio of volume to surface area increases as the inverse of the radius of the column. The surface area of the frits used to terminate the column decreases by a factor of twenty-one going from 4.6 mm to 1 mm ID, so care must be taken to see to it that the smaller surface area remains porous. With the proper attention to the inner wall finish, the mode of column termination and the packing technique, microbore columns have been packed routinely in this lab with 5, 7 and 10  $\mu\text{m}$  particles of LiChrosorb® RP-8, RP-18, Si-60, CN,  $\text{NH}_2$  and Diol that delivered the maximum theoretical efficiency, giving a plate height equal to two times the particle diameter at the optimal flow rate. In contrast, conventional bore columns prepared in this lab usually deliver only 70-80% of the theoretical maximum efficiency. These results support the claim that microbore columns are actually easier to pack than conventional bore columns, but of course with the proper technique both configurations yield the same efficiencies. A detailed description of the mode of column preparation and the packing procedure has been included to

emphasize those details that were found to be essential in preparing stable, high efficiency microbore columns.

Temperature programming was investigated for two reasons. First, a reduction in column diameter improves the ratio of the rates of liquid flow to thermal diffusion across the column bed, so that one fundamental restriction against the use of temperature programming (slow thermal equilibration) is relaxed using microbore columns. Second, the high cost of gradient micro LC systems may be avoided by the use of low cost temperature programming systems. While temperature does not provide the same dramatic solvent strength change as compositional changes, it may be useful in cases where a modest reduction in retention is needed. Three different temperature control systems are evaluated and their individual advantages and limitations are discussed.

## 2.0 HISTORICAL

### 2.1 MICROBORE LC

The term 'microbore' has been used to describe columns ranging in internal diameter (ID) from 0.19 mm (2) to 2.7 mm (3). It usually denotes a column with a reduced ID compared with currently popular or 'conventional' bore columns, which are 4.0-4.6 mm at this time. Scott and Kucera (1) specified microbore columns as 1 mm ID packed liquid chromatographic columns and their definition is used here.

The use of narrow bore columns is by no means a new idea. In 1962, Smith described reducing the column diameter in order to increase the eluting concentration of a fixed mass of sample from an LC column, calling it 'column amplification' (4). Narrow bore LC columns were in common use in the early 1970's (5). For example, Varian Aerograph marketed 10 foot long, 1 mm ID columns packed with 230-325 mesh (37-74  $\mu\text{m}$ ) ion exchange resin. During the 70's, smaller particles were developed (6) allowing shorter columns to be made with the same resolving power as these longer columns, but allowing much faster analyses. By 1980, the most common LC column dimensions were 4.6 mm ID x 25

cm long, packed with 5 or 10  $\mu\text{m}$  particles. With the recent development of 3  $\mu\text{m}$  particles, columns as short as 3 cm are now available for very high speed analysis (7).

The inner diameter of these columns (4.0-4.6 mm) reflects the minimum peak volumes current instrumentation is designed to handle. The connection volumes between the injector, column and detector and the volumes of the injector and detector contribute a fixed amount of band broadening to observed chromatographic peaks. Instrumentation has been designed so that the relative contribution of this extracolumn band broadening has a negligible effect on resolution, and cannot be reduced below current values without redesigning the instrumentation. If column diameters were reduced, the relative extracolumn band broadening would begin to seriously degrade observed column performance.

In 1979, R. P. W. Scott and Paul Kucera doing research at Hoffmann-La Roche Inc. (Nutley, NJ) were interested in developing sensitive, high resolution analytical techniques for drugs and metabolites. These are classic sample limited situations, for which reducing the column diameter can improve sensitivity by invoking Smith's column amplification principle. They assembled special, low extracolumn volume instrumentation

and examined the potential of microbore LC.

### 2.1.1 RESOLUTION AND COST

In their first paper (1), they compared 0.5, 0.75, 1.00 and 1.25 mm ID packed LC columns and found 1.00 mm ID columns offered the highest efficiency. They constructed a 14 meter long microbore column that developed over 500,000 theoretical plates, giving very impressive resolution. It should be noted that while a bank of conventional bore columns (i.e. fifty-six 25 cm x 4.6 mm ID columns) could have been constructed and would have delivered the same resolution, such a column would have cost between \$2,500 and \$15,000 and used 2 liters of solvent per analysis, while the microbore column could cost as little as \$120 and uses only 100 ml per analysis (where the final peak  $k'$  is 10). They therefore demonstrated that microbore columns provide a means of getting low cost, high resolution LC analyses.

### 2.1.2 SENSITIVITY

In their second paper (8), they used the term "mass sensitivity" (signal per unit mass) which on paper made microbore columns look more sensitive than conventional columns. Howev-

er, the term overstates this sensitivity advantage in most cases. While it is true that if the same mass of sample is injected onto both a conventional bore and a microbore column, the concentration from the microbore column will be greater because it elutes in a smaller volume and thus suffers less dilution, the conventional bore column is capable of handling much greater sample mass before column overload due to the larger sorbent bed than the microbore column. One can counter increased sample dilution on the conventional bore column by simply injecting more sample. In fact, these two factors cancel out each other so that if the same relative amount of sample (proportional to column overload mass) is placed on both columns, they will both deliver exactly the same concentration of sample to the detector. What is worse, in order to maintain resolution using microbore columns, the detector cell is commonly decreased in volume by either reducing the cell aperture or the pathlength. A smaller aperture allows less light through the cell and decreases the signal-to-noise level. A shorter pathlength reduces the observed absorbance due to Beer-Lambert law dependency ( $A = \epsilon bc$ ). In both cases, the sensitivity from the microbore column can then actually be less (9).

The only case where microbore columns provide a sensitivity

advantage is when the total available sample mass is both limited and also below the column overload mass. These are 'one-shot' situations, and while notable examples have been cited (10), they constitute a very low percentage of current LC applications. The sensitivity advantage of microbore columns has been grossly overstated.

### 2.1.3 SPEED

In their third paper (11), Scott, Kucera and Munroe demonstrated high speed analysis using microbore columns. They demonstrated baseline resolution of benzene and benzyl acetate in 2.5 seconds, and separated a seven component mixture in 30 seconds. A 25 cm column packed with 20  $\mu\text{m}$  particles was operated at 4.5 ml/min (60 times the optimal linear velocity) and developed only 4.6% of the maximum column efficiency. This was still very impressive. Knox, commenting on their work, said "Scott, Kucera and Munroe have recently emphasized the potential of short, small bore columns for very rapid separations, but in principle the reduction in the bore has no special influence on the speed of analysis" (12). Truly, the speed of analysis ultimately depends only on the diameter of the particles used to pack the column (13).

Perhaps in response to this, Kucera (14) compared high speed microbore to high speed conventional bore analysis. He showed the rate of decrease in resolution with increased linear velocity for 4.6 mm ID columns was greater than that for 1 mm ID columns (figure 1). This means microbore columns provide faster analysis than conventional columns packed with the same sorbent operated at the same linear velocity. This was probably the most revealing comparison made on microbore and conventional bore columns, yet he failed to ascertain correctly the cause or realize its implications at the time. Four years later, Scott (15) performed experiments on the heat generated by the mobile phase flowing through small particle column packings and its effect on column efficiency. He showed that the inability of a conventional bore column to dissipate the heat generated by the passage of the mobile phase caused the shape of the sample bands inside the column to distort, but the microbore column, with its narrower bed and its greater surface-to-volume ratio, was able to dissipate the heat, maintain a more constant temperature across the column and therefore not distort the shape of the sample bands as much at high flow rates. This can be used to explain the higher efficiency of microbore columns at higher flow rates. The faster thermal equilibration experienced by microbore columns has implications beyond more efficient high speed LC. Before dis-

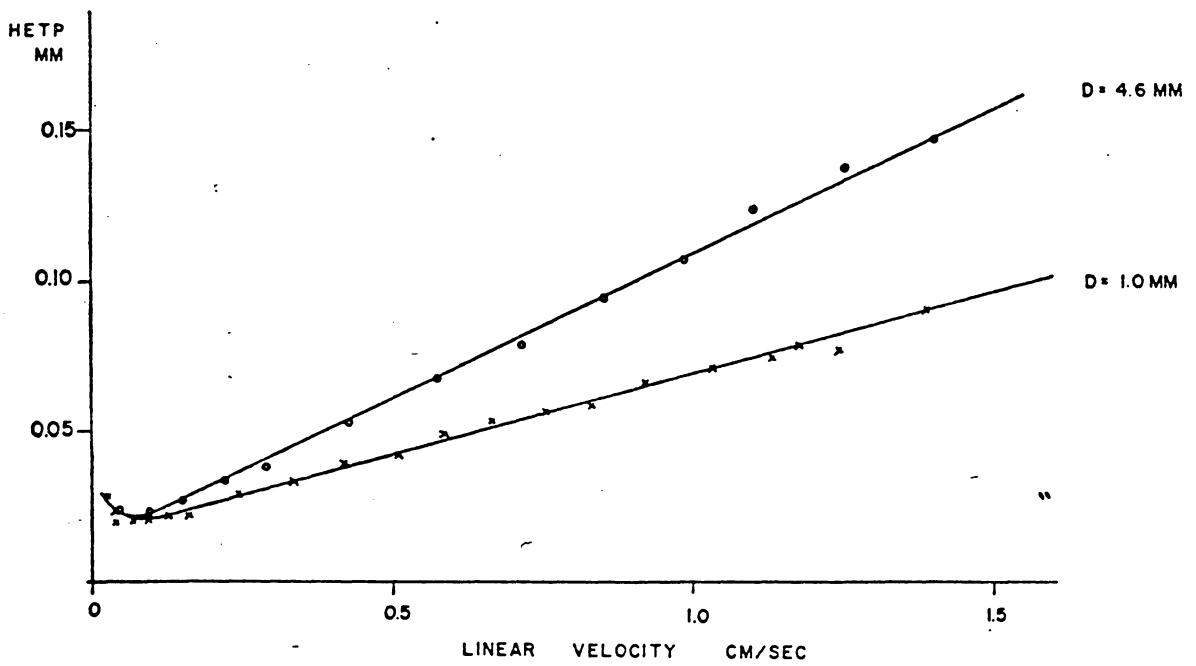


Figure 1. Speed for 1 mm and 4.6 mm ID columns (from ref. 14).

cussing these, the concept of gradient elution will be introduced.

#### 2.1.4 GRADIENT ELUTION

A problem common to both liquid and gas chromatography when using a fixed elution strength system (isothermal or isocratic) to analyse diverse, multicomponent mixtures is that early peaks elute too close together while later peaks elute too far apart and take too much time to come off the column. Snyder (16) called this the general elution problem (GEP). To overcome this, the system is altered to first provide more retention for the early peaks and then some retention property is gradually changed during the run to accelerate the migration rate of the later peaks. This is called gradient elution. Gradient elution in gas chromatography is limited to a programmed increase in column temperature, since changing the composition of the carrier gas has little effect on retention. However, gradient elution in liquid chromatography is usually produced by changing the composition of the mobile phase, and elaborate multiple fluid mixing systems are commercially available for use with conventional bore columns.

Two problems are encountered when one attempts to use micro-

bore columns with this gradient elution instrumentation. First, microbore columns use twenty times lower flow rates than conventional columns and this demands twenty times greater volumetric flow precision from the pump(s). Second, the delay volume from the point where the solvents mix to the injector (containing such elements as pulse dampeners, pressure transducers, static or dynamic mixers and connection tubing) is so large in comparison to the reduced microbore flow rate that unacceptable lag times are introduced. Both of these problems have been addressed (17) and a commercial microbore solvent gradient system has recently been introduced (Brownlee model MPLC pump, Brownlee Labs Inc., Santa Clara, CA.). The \$14,000 price tag is considerably more than twice the cost of two isocratic (constant composition) pumps (\$1,200-\$4,000 each). This higher cost reflects the addition of a custom programmed on-board computer to simultaneously control both pumps.

#### 2.1.5 TEMPERATURE GRADIENTS

With microbore columns showing faster thermal equilibration than conventional columns (see figure 43, p. 140), a viable alternative to the expense of a computer controlled dual pump system for gradient elution lies in temperature programming the microbore column. Temperature control systems similar to

those already developed for gas chromatography are available for less than \$1,000. Temperature programming conventional bore columns has never been successful, and the next section will examine the reasons behind this.

## 2.2 TEMPERATURE PROGRAMMED LC

The use of temperature gradients in liquid chromatography is virtually nonexistent. This is curious, since practically every commercial GC instrument has the provision for producing temperature gradients, while not a single commercial LC system allows temperature gradients. Most research LC systems provide some rudimentary form of temperature control, but these are nowhere near as sophisticated nor as well-conceived as their GC counterparts.

Since the discovery of liquid chromatography by Michael Tswett in 1906 (18) only a handful of papers have appeared which deal with changing the LC column temperature during the chromatographic run in order to improve separation performance. Most workers would prefer, for the sake of convenience, to operate their columns at room temperature and ignore the effects of temperature altogether. Still, some work has examined the effects of operating the LC column at fixed

temperatures (both higher and lower) than room temperature and looked at how this effects analysis time, resolution, relative peak position, as well as the column, sample and detector stability.

Assuming thermal equilibrium, it is possible to extrapolate temperature programmed performance in LC as some running average of the column performance at a number of closely spaced isothermal runs (19). Thus, temperature programming can be considered as a dynamic subset of temperature controlled LC. Even without a large body of research results using temperature programming, it is possible to predict results of temperature programming by extrapolation from fixed temperature results.

### 2.2.1 OBSERVED TEMPERATURE EFFECTS

The importance of temperature in controlling an LC separation was recognized in 1946 by Strain who noted that "the adsorption sequence of certain organic compounds is dependent to some extent on temperature." (20). Two years later, Le Rosen and Rivet (21) measured the retention, relative to the solvent front of three compounds at temperatures between 10° C and 70° C, showing a decrease in retention with an increase in temperature. They deduced that this effect should be

universal. "It is reasonable to assume that  $dT_a/dt$  ( $T_a$  = average time a compound is on the adsorbent,  $t$  = temperature) can never be positive, since with increasing temperature, the probability that any adsorbed molecule will have sufficient energy to leave the adsorbent becomes greater." (21). However, retention does not always decrease with increased temperature (22). In their argument, the tacit assumption was made that the activity of the adsorbent, the strength of the mobile phase and the conformation of the solute were invariant with temperature, which is not always the case.

Silica and alumina are commonly used polar adsorbents in column chromatography. Nonpolar mobile phases are usually used to elute sample species from these columns. This is referred to as "normal phase" LC. Retention times of sample species can be adjusted and optimized by mixing these nonpolar mobile phases with a more polar modifier, making binary mobile phases. Sometimes multiple modifiers are used but the effect is the same. In cases where mixed mobile phases are used, an equilibrium concentration of the more polar modifier is established on the polar adsorbent. This modified surface has a profound effect on the strength of adsorption experienced by a sample species. Upon raising the temperature, this adsorbed modifier is desorbed from the stationary phase into the mobile

phase. This has two effects. First, it raises the stationary phase polarity by uncovering the active surface groups to which these polar modifiers were attached. Second, it temporarily increases the mobile phase polarity by increasing the quantity of polar modifier it contains. The relative magnitudes of these two polarity changes dictate whether the retention of a solute will increase, decrease or remain the same (23). Thus, as early as 1953, Chang showed it was difficult to predict beforehand the direction and magnitude of the change in retention brought about by temperature in normal phase LC using binary solvents (22).

### 2.2.2 EQUILIBRATION TIME

A second inconvenience faced by early workers studying temperature effects in LC was the time it took their columns to equilibrate. Since the heat of adsorption of polar molecules in normal phase systems is high, they showed a slow response to any disturbance, such as temperature or solvent composition, which affects the equilibrium concentration of polar modifiers on their surface. For example, in raising the column temperature slightly, the fractional increase in the number of polar molecules possessing sufficient energy to leave the surface is small. Even in a state far from equilibrium, the rate at which

equilibration can occur is slow because so few molecules are participating in the equilibration process. In some normal phase systems, this response time was as "as long as 48 hours." (24). Scott, in 1969 stated that temperature programming has been "shown to be of little advantage due to the long time necessary for equilibration to occur between the phases." (25). Clearly, the advent of temperature programmed LC (TPLC) would have to wait at least until the development of a chromatographic system with much faster response time. Bonded phase LC, as developed by Aue and Hastings (26), Kirkland (27) and Majors (7) in the early 70's, fulfills this requirement but the common usage of reversed phase sorbents did not occur until the mid 70's.

### 2.2.3 COMPARISON OF PROGRAMMING TECHNIQUES

Meanwhile, in 1970, Snyder probably the foremost authority on LC at that time, published a comparison of the four available programming modes in LC: 1) Solvent Programming, 2) Flow Programming, 3) Temperature Programming and 4) Stationary Phase Programming (or column switching) (16). With analysis time and maximum column pressure held constant, the criteria for comparison was the number of effective plates generated in a fixed period of time,  $NQ^2$  (where  $Q = k'/k'+1$ , and  $k'$  is a fac-

tor proportional to the amount of retention experienced by a sample species). Snyder concluded that temperature programming was no better than normal, or isothermal elution. In his own words, "since this result is somewhat surprising, it deserves a rough analysis of the contributing factors." (16).

In his comparison, normal elution was assumed as using solvents of minimum viscosity (0.2-0.3 centapoise) while solvent viscosity in temperature programming was assumed to be minimal (0.2-0.3 centapoise) only at the end of the program (corresponding to the boiling point of the solvent). By assuming this, Snyder placed two unnecessary limitations on temperature programming. First, since the viscosity at the beginning of the temperature program was much higher than that for the normal elution case (it was estimated as 3 times higher) the flow rate would be 3 times lower given the restriction of a maximum column operating pressure. This handicapped temperature programming with a longer analysis time even though the column pressure would quickly decline below the maximum value shortly following the start of the program. Second, since the plate height,  $H$ , increases with viscosity due to a slower rate of mass transfer between phases, the number of plates  $N$  (where  $N = L/H$ , with  $L =$  column length) is lower at the start of the temperature program and only approaches the normal elution value

towards the end of the program. Given the severity of the limitations imposed by these two assumptions, it's surprising that Snyder predicted temperature programming was anywhere near normal elution in resolution per unit time.

For Snyder's temperature programming example, a 120° C span was needed to increase sufficiently the solvent strength. A common misconception (28) is that LC cannot operate above the solvent boiling point. To accommodate this, Snyder started his temperature program at -20° C. This, however, was unnecessary since operating the detector under pressure will prevent the mobile phase from boiling. The 120° C span required in his example could just as well have started at 20° C rather than -20° C. Clearly, a fair comparison of normal and temperature programmed elution should start with the same solvent at the same temperature for both systems.

The thrust of Snyder's paper was a strong support for solvent programming. As was correctly observed, its most important advantage over the other programming techniques is the greater scope of retention values it can handle during a single run. By scope is meant the ratio  $k'_z/k'_a$ , "where  $k'_a$  and  $k'_z$  refer to the  $k'$  values of the first and last eluted peaks a and z at the beginning of the separation, before these  $k'$  values

are changed by the solvent program" (16). The maximum  $k'_z/k'_a$  value for which temperature programming provides some practical benefit lies somewhere in the range of 10-100, while the value for solvent programming extends well into the 1000's. The change in solvent strength brought about using accessible temperatures is thus much less than that available by changing the solvent composition. However, most samples do not require the widest possible range of solvent strengths for their optimum elution. This merely divides samples into two types; those whose separation is improved by both solvent and temperature programming, and those which require the broader scope that is only available using solvent programming.

#### 2.2.4 USES OF TEMPERATURE PROGRAMMED LC

In spite of Snyder's paper, in 1974 Harvey et. al. (29) successfully employed linear temperature gradients to elute enzymes from affinity adsorbents.

"The adsorption of a solute from the mobile phase is generally exothermic and thus, according to the Le Chatlier principle, elevated temperatures will move the equilibrium in the direction that absorbs heat. Thus, a temperature rise will lead to a higher relative concentration in the mobile phase and thus a faster migration through the chromatographic bed. In general, the more exothermic the adsorption of a particular enzyme, the greater its sensitivity to temperature." (29)

The binding of enzymes to immobilized substrates was dramat-

ically affected by temperatures in the range of 0-40° C, even more than could be accounted for by considering the thermodynamics of the system. This was attributed to "temperature induced conformational changes in the enzyme protein" (29).

In the same year (1974), Kreji and Kourilova (30) published the first of three papers describing the use of a dynamic temperature gradient system in which an oven at 70° C moved down the column in the direction of solvent flow. Since they employed silica as their stationary phase, water was rigorously excluded to simplify the system and avoided any lengthy equilibration problems between runs. They showed a 50% reduction in analysis time and significantly improved peak shapes using this moving zone elution technique. In 1976 (31), they replaced the moving oven with moving electrical contacts on a heating coil surrounding the column, and in 1977 (32), they experimented with a binary solvent consisting of dry hexane with 0.2% di-n-butyl ether, a weak polar modifier. This binary solvent showed a greater temperature sensitivity than their first system, giving a four-fold reduction in analysis time when compared to isothermal operation. This greater temperature sensitivity was due predominantly to more strongly retained species in the isothermal run. Since a binary mobile phase was employed, the column required 20 minutes for

re-equilibration between runs.

The first mention of a bonded phase LC temperature programmed system was in 1977 by Kikta et. al. (33) who used an inexpensive water circulation bath and a Tygon tube enclosure surrounding the column to control the temperature. Regrettably, they chose a 2.5 gallon Pyrex reservoir with a 500 watt immersion heater which at full power could only provide a  $0.67^{\circ}$  C/min programming rate. For normal column flow rates, it will be shown that  $5^{\circ}$  C/min is the minimum rate required to provide any noticeable improvements in chromatographic performance. Understandably, the temperature programmed chromatogram they showed ( $40^{\circ}$  C to  $66.2^{\circ}$  C in 35 minutes) was little different from the isothermal run. More interestingly they showed that a trace component which appeared within the tail of a major peak at  $27^{\circ}$  C would elute before that peak at  $70^{\circ}$  C and thus enable better quantitation. Altering the selectivity of an LC system with temperature can be a powerful separation tool (34).

#### 2.2.5 COLUMN EFFICIENCY AND TEMPERATURE

There seemed to be a difference of opinion as to whether increasing the column temperature results in a reduction in the

plate height, H, and thus improved performance. Hesse and Engelhardt in 1966 (35) showed a reduction in plate height on alumina of approximately 30% going from 15° C to 65° C. Schmit, in 1971 (36) showed a 50% reduction in H using chemically bonded reversed phase Zipax® over the same temperature range. Hashimoto in 1979 (37) using a cation exchange resin reported that HETP "was improved about four-fold from 1.28 at 23° C to 0.29 at 60° C" (HETP in mm).

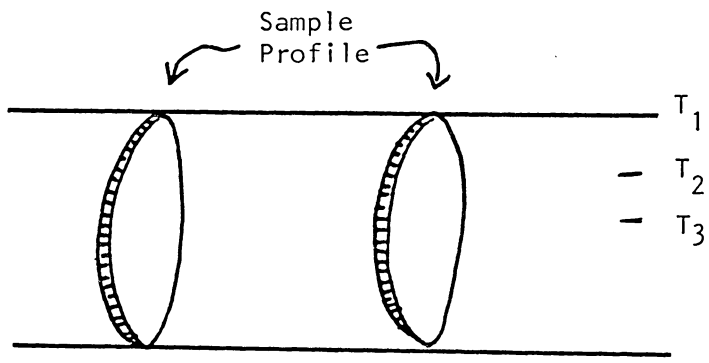
On the other hand, Saner et. al. in 1978 reported that

"Improvements in LC separations usually observed at elevated temperatures (60° C) were not observed for 5 µm RP-8 and RP-18 packed columns. In fact, a substantial loss occurred." (38)

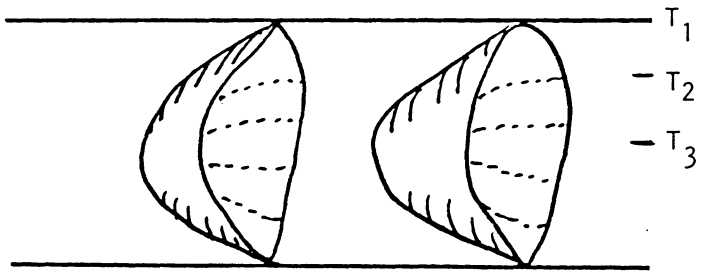
The next year, Perchalski and Wilder (39) reported peak splitting and low column performance using elevated temperatures when they failed to preheat the mobile phase, but good performance was obtained when they did. Since Saner (38) showed that high temperature performance was not as bad at lower flow rates, the reason for their observed reduced performance is consistent with a model given by Poppe and Kraak (40) and calculated by Abbott et. al. (41). With 4.6 mm ID columns, when the rate of temperature diffusion across the column bed is less than the velocity of the mobile phase through the column, sample front distortion occurs. The column ovens that were used

heated the walls of the column and that heat was then transferred to the entering mobile phase. This resulted in the formation of a radial temperature profile across the chromatographic bed. A sample component spread across these different temperature zones and moved at different rates, resulting in the formation of a three dimensional parabolic concentration profile of that species within the column (figure 2). Since the flow to the detector only contained an average of the concentration in two dimensions (across the column bed) the resulting detector signal showed peaks blurred and distorted even though the bands in the column were still sharply defined paraboloids. Operation at lower flow rates allows more time for thermal equilibration, reducing the radial temperature profile and improving detected peak shapes. Preheating the mobile phase eliminates the temperature profile altogether, and column performance in this case remains high.

A second source of intra-column temperature profiles in HPLC comes about through viscous heat dissipation of the mobile phase when it pushes through the stationary phase, especially when using small particle columns at high flow rates. With the column outlet at atmospheric pressure, almost all of the energy imparted to the solvent by the pump is dissipated as heat within the column. A column thermostated at the temperature of the



$$T_1 = T_2 = T_3$$



$$T_1 > T_2 > T_3$$

Figure 2. Formation of three dimensional concentration profiles with radial temperature gradients (after refs. 39 and 40).

entering mobile phase is thus hotter at the center than it is at the walls. Poppe et al. (42) made several suggestions to reduce this effect, the most practical being "use of temperature-controlled columns with smaller diameters." Katz et al. (15) used a temperature controlled microbore column (0.76 mm ID) and showed more than an order of magnitude greater temperature stability using this narrow bore column than obtained using a conventional bore column (4.6 mm ID). Thus, another problem with temperature programming conventional bore columns is that unless the column and the mobile phase are heated at the same rate, low separation efficiency is observed. While the solution to this problem may appear simple, considerable technical difficulties arise from the variety of thermal masses (and thus different heating rates) of the injector, column, sample loop and connection tubing. These result in temperature differences between the mobile phase entering the injector and the column. These simplify considerably if, as is the case with narrow bore columns, only the column need be heated.

#### 2.2.6 MICROCOLUMN TEMPERATURE PROGRAMMING

Recently, Hirata and Sumiya (43) demonstrated temperature programmed LC with a microcapillary column that was three times narrower than the microbore column used by Katz. It was men-

tioned that the narrow column bed was useful in eliminating radial temperature profiles. Given the limitations in sample capacity and detection limits using such narrow LC columns, a better approach would be to demonstrate temperature programming using columns of more practical dimensions (1 mm ID).

Bowermaster and McNair (44) studied the effects of heating a 1 mm ID microbore column by passing electrical current through the column, making the stainless steel column its own heater. A three-fold reduction in analysis time was demonstrated for a series of n-alkyl benzenes going from 25° C to 100° C. With this heating mode, a linear temperature gradient was imposed along the length of the column, reaching its maximum temperature only at the column outlet. This is not what an ideal heating system would be, and thus temperature controlled air and water baths were substituted for the electrical system in their next publication (45). In this, a detailed study of the effects of temperature on  $k'$  and  $\alpha$  at temperatures ranging from -60° C to 175° C were reported. While the rate of thermal transfer by temperature controlled liquids is superior to gases, providing virtually instantaneous column and mobile phase equilibration, the slow liquid heating rate (2.5°/min max.) using available wattage heaters and the difficulty in handling liquids above 100° C made the use of air circulating systems

more practical. Columns were shown to be reasonably stable at temperatures as high as 160° C but column lifetimes were reduced with high temperature operation as also seen by Hirata and Sumiya (43).

#### 2.2.7 COLUMN AND SAMPLE STABILITY

Column and sample stability are important considerations when programming LC columns to high temperatures. A commonly held belief is that LC columns should not be operated above 80° C (or the boiling point of the solvent, whichever comes first). Atwood et. al. (46) published a study which followed the dissolution of silica in packed LC columns by atomic absorption. They found bare silica was soluble in water in the range of 10-100 µg/ml between 20° and 70° C so that at a 1 ml/min flow rate, 1% of the column would dissolve in 7 hours at 70° C. It is fortunate few people operate bare silica columns using hot water as the mobile phase.

Stationary phases composed of chemically bound siloxanes (i.e. RP-18) "are stable towards water even at elevated temperatures in the absence of a catalyst" (acid/base) (47). Atwood found that:

"In contrast to experience with uncoated silica, it

appears that C<sub>18</sub> coating greatly reduces the amount of Si dissolved by the flowing mobile phase. However, after large volumes of mobile phase, especially at higher temperatures and high pH, the loss of silica from the C<sub>18</sub> packing is significant." (46)

While loss of column packing at even higher temperatures might be severe, use of a precolumn to saturate the mobile phase with silica was demonstrated (46) to extend the column life and fortunately, methanol and acetonitrile, common solvents in RPLC, have limited solubility for silica.

With reversed phase sorbents, dissolution of the silica backbone is not the only mode of column failure. Cleavage of the bound organic moiety may result "from the highly reactive conditions ... of the mobile phase used at high temperatures" (48). Also, while RP-18 material is usually rinsed at room temperature with THF (48), there may still be trace amounts of insoluble, unbound, low molecular weight silicone polymer left on the sorbent. When a column packed with sorbent is heated, this polymer melts and can fill the small flow channels between the particles and within the outlet frit, causing high back-pressure and column failure. This has been observed frequently in this research.

However, in the absence of a liquid mobile phase, silica derivatized with alkylsilanes has been shown to be thermolyti-

cally stable up to 200° C (49). In fact, one method of derivatizing silica for RP sorbents involves reaction of the monomer and silica at 350° C (50). This stresses that the specific chemical environment and not simply the high temperatures that lead to the possible removal of the bound organic moiety. Should this become a problem, it may be necessary to employ other types of stationary phases which might show greater stability towards high temperature mobile phases, such as pyrocarbons (51, 52) or PS-DVB based packings (53).

Reasons for choosing LC as an analytical technique over GC include sample nonvolatility, sample complexity and sample thermal instability. LC is characterized as a gentler separation technique than GC, since molecules need not be vaporized, excited or exposed heated surfaces which are potentially catalytic. High temperature programmed liquid chromatography would of course change all that. Certainly, hydrolysis and transesterification (in MeOH) would prevent the analysis of oligosaccharides and esters, and a great body of biological samples, proteins, peptides and the like, may be unstable at high temperatures. However, dismissing high temperature LC out-of-hand due to potential sample instability is not reasonable. Samples should be considered individually, and the upper temperature giving sufficient stability for

reliable determination should be established by experimentation. This is merely good analytical practice. Most researchers assume sample stability in LC, which has led to some problems in the past (54). Suffice it to say there are apt to be more sample stability problems when programming LC columns to high temperatures.

#### 2.2.8 SUMMARY

It was demonstrated that small bore columns are more likely candidates for temperature programmed LC. There were five main reasons given for the lack of popularity of temperature programming as a gradient technique using conventional bore LC columns. First, silica shows irreproducible chromatographic behavior due to a long equilibration time to environmental changes. Second, an authority on LC dismissed it early on as not being useful. Third, the range of capacity factors accessible by temperature programming a single mobile phase are not as wide as those obtained by changing the composition of the mobile phase. Fourth, the current popular dimensions of LC columns are too wide to obtain improved performance at high temperatures due to thermal gradients across the column bed. Fifth, the enormous cost of LC columns prevented most researchers from attempting unprecedented techniques which might

result in the destruction of their columns. It should be noted that this is a limitation of current sorbents, but not of the technique itself. Also, there is an increased potential for sample instability at high temperatures.

### 3.0 THEORY

#### 3.1 ISOTHERMAL MICROBORE INSTRUMENTATION REQUIREMENTS

Microbore columns (1 mm ID) represent a 21-fold reduction in the cross sectional area compared to conventional 4.6 mm ID columns. This results in 21 times smaller peak volumes from microbore columns compared to conventional bore columns operated under identical conditions except for flow rate (same sorbent, solvent, and linear velocity). A concern using microbore columns is whether available instrumentation is capable of handling these smaller volumes without compromising column efficiency. In initial microbore column development, it was not known whether poor column performance was caused by bad columns or if the instrumentation was at fault. Extracolumn contributions to band broadening can be evaluated by using plate theory.

##### 3.1.1 PLATE THEORY

Separation efficiency is defined as the number of theoretical plates,  $N$ , generated during a separation (55). Figure 3 shows a chromatogram in which several important variables for

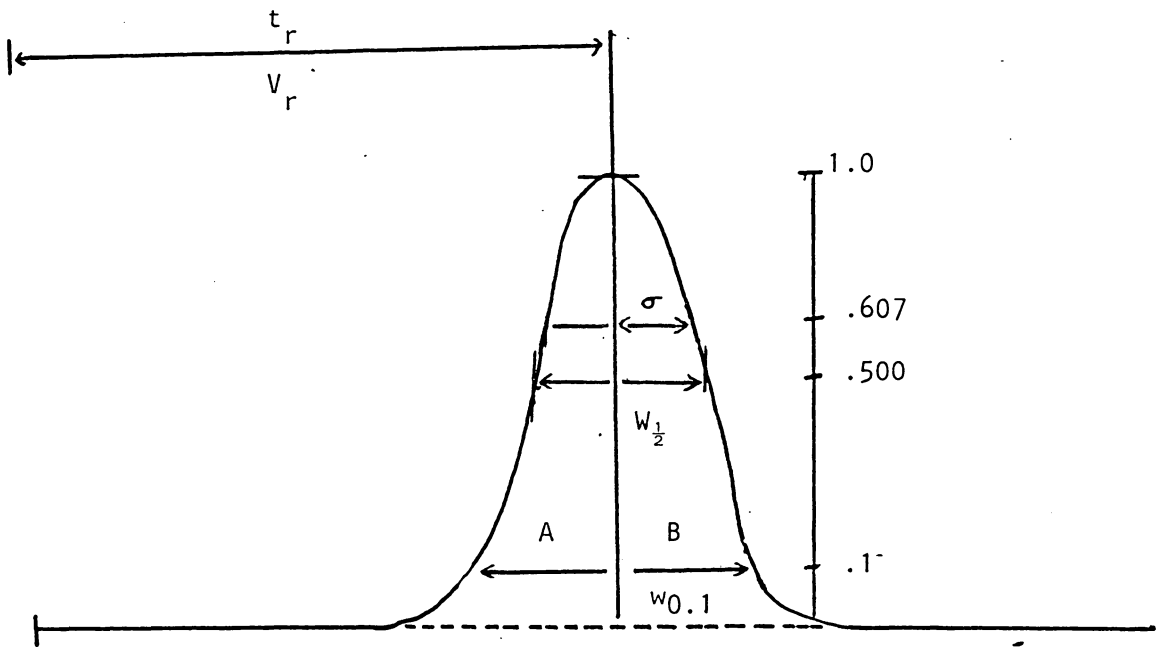


Figure 3. Variables used to calculate N.

theoretical plate calculations are included. The number of theoretical plates is defined as

$$N = (t_r/\sigma)^2 \quad (1)$$

where  $t_r$  is the retention time and  $\sigma$  is half the peak width at 0.607 of the peak height in time units. Use of volume units for both variables gives the same results. (i.e.  $V_r$  being the retention volume). For perfectly gaussian peaks, this is equivalent to

$$N = 5.54(t_r/w_{1/2})^2. \quad (2)$$

A reliable value for N from non-gaussian peaks is more difficult to obtain, usually requiring statistical moment analysis with a digital computer (56). Recently, a method using width at 10% of peak height and the values A and B in Figure 3 was shown to be a simple, reliable method for plate calculations from exponentially modified gaussian peaks (57) which does not require the use of an on-line computer. Peaks encountered in this study were evaluated by both the width at half height and the width at 10% height, A-B method (57) and plate counts were obtained that agreed to within 10%. Peaks were considered sufficiently gaussian to use width at half height for plate calculations.

### 3.1.2 EXTRACOLUMN VARIANCE

The observed variance ( $\sigma^2$ ) of a chromatographic peak is the sum of the variance contributions from each part of the chromatographic system

$$\sigma^2_{\text{obs}} = \sigma^2_{\text{inj}} + \sigma^2_{\text{col}} + \sigma^2_{\text{det}} + \sigma^2_{\text{conn}} \quad (3)$$

where obs = observed, inj = injector, col = column, det = detector and conn = connection volume. It is best to have column variance dominate while all other contributions are minimal, so that instrumentation does not seriously degrade column performance.

Various techniques have been used to quantitate the total extracolumn variance of a system (injector, detector and connection tubing) as well as to isolating individual component contributions to observed peak width. Scott and Simpson (58), Hupe et. al. (59) and Reese and Scott (60) took existing LC systems and placed different lengths of connection tubing or an additional detector cell inline between the injector and detector. The observed variance from the resulting system was the sum of the original system variance and the variance of the added component(s), since

$$\sigma^2_{\text{obs}} = \sigma^2_{\text{orig}} + \sigma^2_{\text{add}}. \quad (4)$$

The variance of the added component(s) are calculated as

$$\sigma^2_{\text{add}} = \sigma^2_{\text{obs}} - \sigma^2_{\text{orig.}} \quad (5)$$

If, for example, they doubled the length of the connection tubing in their system, the additional variance would then be equal to the variance of the original tubing in their system. In this way, both individual component band broadening and total system band broadening was determined.

Another method used by Kok et. al. (61) when evaluating the use of conventional instrumentation with microbore columns was based on the independence of plate count on retention. If  $N =$  constant, then  $\sigma$  is a linear function of retention volume. This was confirmed for a particular test mixture by running it on a conventional bore column where extracolumn band broadening was insignificant. The number of theoretical plates,  $N$ , from this conventional bore analysis was obtained. It can be shown that

$$V_r^2/N = \sigma^2_{\text{obs}} - \sigma^2_{\text{ec}} \quad (6)$$

A plot of  $V_r^2/N$  versus  $\sigma^2_{\text{obs}}$  will have an intercept equal to the extracolumn variance,  $\sigma^2_{\text{ec}}$ . If the system used in the microbore run was sufficiently good (low extracolumn volume), the plate count  $N$  may be obtained directly from the microbore column run from the more strongly retained peaks which are less sensitive to extracolumn band broadening (where  $\sigma^2_{\text{col}} \gg \sigma^2_{\text{ec}}$ ).

### 3.1.3 THEORETICAL EXTRACOLUMN VARIANCE EVALUATION

Purely theoretical calculations have also been made to calculate instrumental contributions to band broadening (62, 63). There are two main sources of extracolumn band broadening; radial dispersion by laminar flow and the static volume of injectors and detectors. The velocity profile of a fluid flowing through a tube is shown in Figure 4. The velocity of a fluid element at the center of the tube is twice the average linear velocity of the fluid and approaches zero near the walls. The effect this has on the width of an initially narrow solute band is shown as a function of time in Figure 5. While the thickness of the zone parallel to the flow remains constant, the profile seen from outside the tube continuously increases. Radial concentration profiles established by laminar flow are offset by diffusion, but diffusion in liquids is slow (the diffusion coefficient,  $D_m$ , for low molecular weight species in typical LC solvents is  $\approx 5.0 \times 10^{-6}$  cm<sup>2</sup>/sec). As a result of this slow diffusion, laminar dispersion increases with increasing flow rate. This effect was first studied by Taylor in 1953 (64) who published with Aris an equation in 1956 (65) relating band width as a function of diffusion coefficients, flow rate and tube diameter. Scott and Kucera (66) in 1971 evaluated connection tubing in LC systems and derived an equation giving the

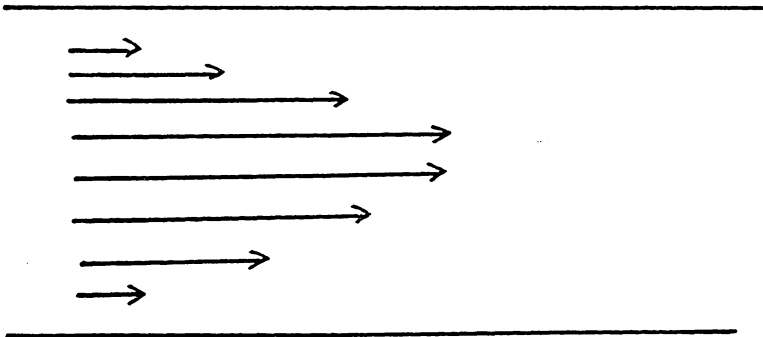


Figure 4. Velocity profile of laminar fluid flow through a tube. Arrowlength is proportional to fluid velocity.

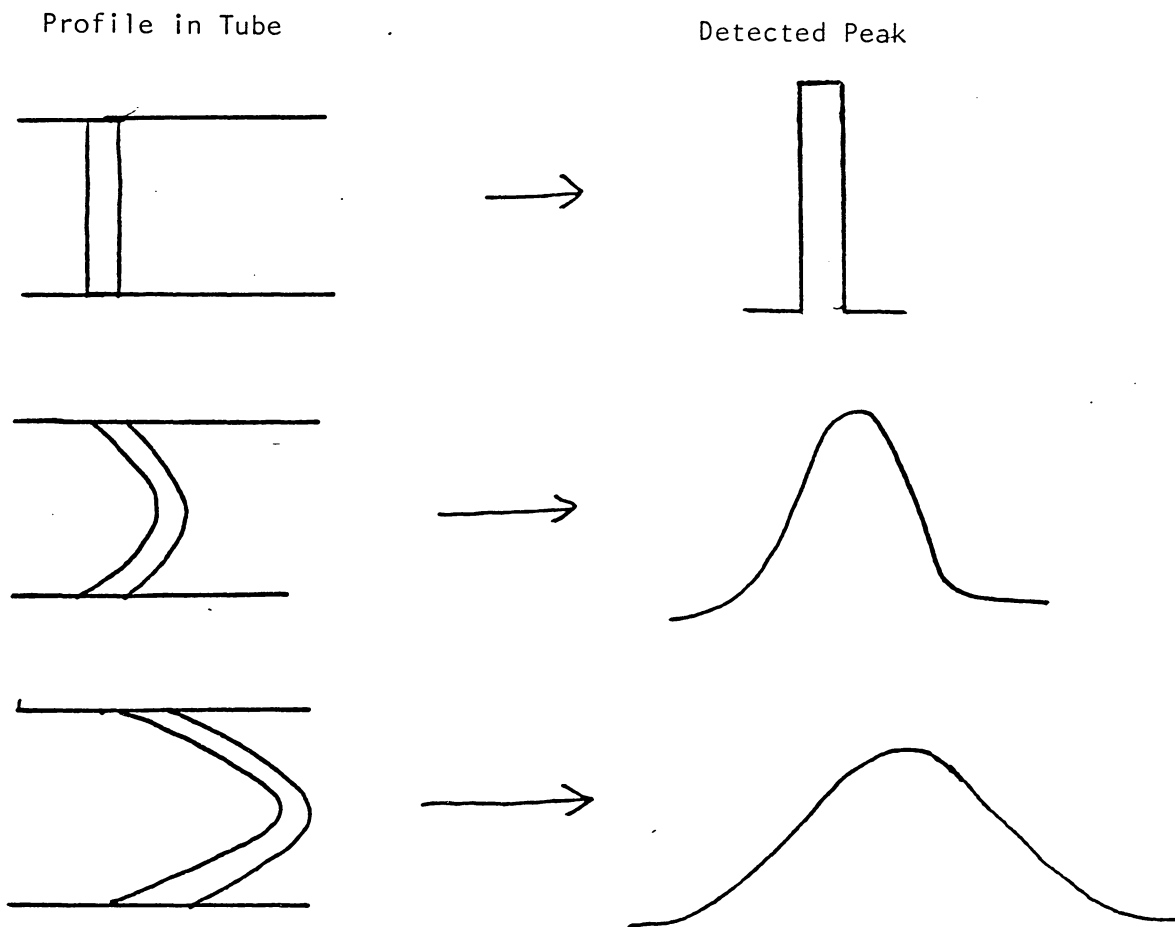


Figure 5. Effect of laminar flow on the width of an initially narrow sample zone.

maximum length of tubing that may be included which causes less than a 5% increase in the observed bandwidth of LC peaks, as

$$L = 40 V_r^2 D_m / \pi F d^4 N \quad (7)$$

where  $V_r$  is peak retention volume in ml,  $D_m$  is the diffusion coefficient in  $\text{cm}^2/\text{sec}$ ,  $F$  is the flow rate in ml/sec,  $d$  is the diameter of the connection tubing in cm, and  $N$  is the number of theoretical plates from the column. Table II lists maximum tube lengths for 0.010" and 0.007" ID tubing, the two most commonly used diameters in LC, as a function of retention on a 25 cm microbore column packed with 10  $\mu\text{m}$  particles operated at 50  $\mu\text{l}/\text{min}$  generating 12,500 theoretical plates. It is seen that while the 5% band broadening restriction severely limits connection tubing lengths for early eluting peaks (low  $k'$ 's), it quickly relaxes for later eluting peaks (large  $k'$ 's). ( $k' = V_r - V_0 / V_0$ , where  $k'$  is the dimensionless variable of retention which increases as sample interaction with the column packing increases.) Any volume between the inlet of the injector and the outlet of the detector that is not filled with either column packing or frits constitutes extracolumn volume and should be minimized when possible.

Table II

Maximum tubing length (cm.) producing less than a 5% increase in observed peak width (from equation 7).

Column: 25 cm x 1 mm ID  $V_0 = 150 \mu\text{l}$   
 $N = 12,500$

Tubing ID.		0.007"	0.010"
$k'$	0	2.7	0.7
	1	10.9	2.6
	5	98.1	23.6
	10	329.7	79.2

#### 3.1.4 INJECTOR VOLUME

An ideal injector would place the entire sample mass onto an infinitely thin section of sorbent at the head of the column, and in so doing not contribute any initial peak width to the sample band as it enters the column. Real injectors have finite volumes and the minimum variance contribution of this volume was shown by Sternberg (67) to be

$$\sigma^2_{inj} = V^2_{inj}/12. \quad (8)$$

Coq et. al. (68) demonstrated that this value can only be approached using a packed sample loop where laminar flow is eliminated. Illustration of laminar flow through a sample loop and its effect on the resulting injection profile are reproduced from that paper in Figure 6. Entering mobile phase from the pump moves the center of the loop out first and a slow wash out of the remaining sample in the loop makes the observed  $\sigma^2_{inj}$  value 1.3 to 1.8 times larger than the minimum value given by Sternberg. Temporary injection was shown (68) to be beneficial in reducing the width of injection profiles by switching off the wash out cycle.

#### 3.1.5 NON-ELUTING SAMPLE SOLVENT

The variance contribution of the injection volume can be

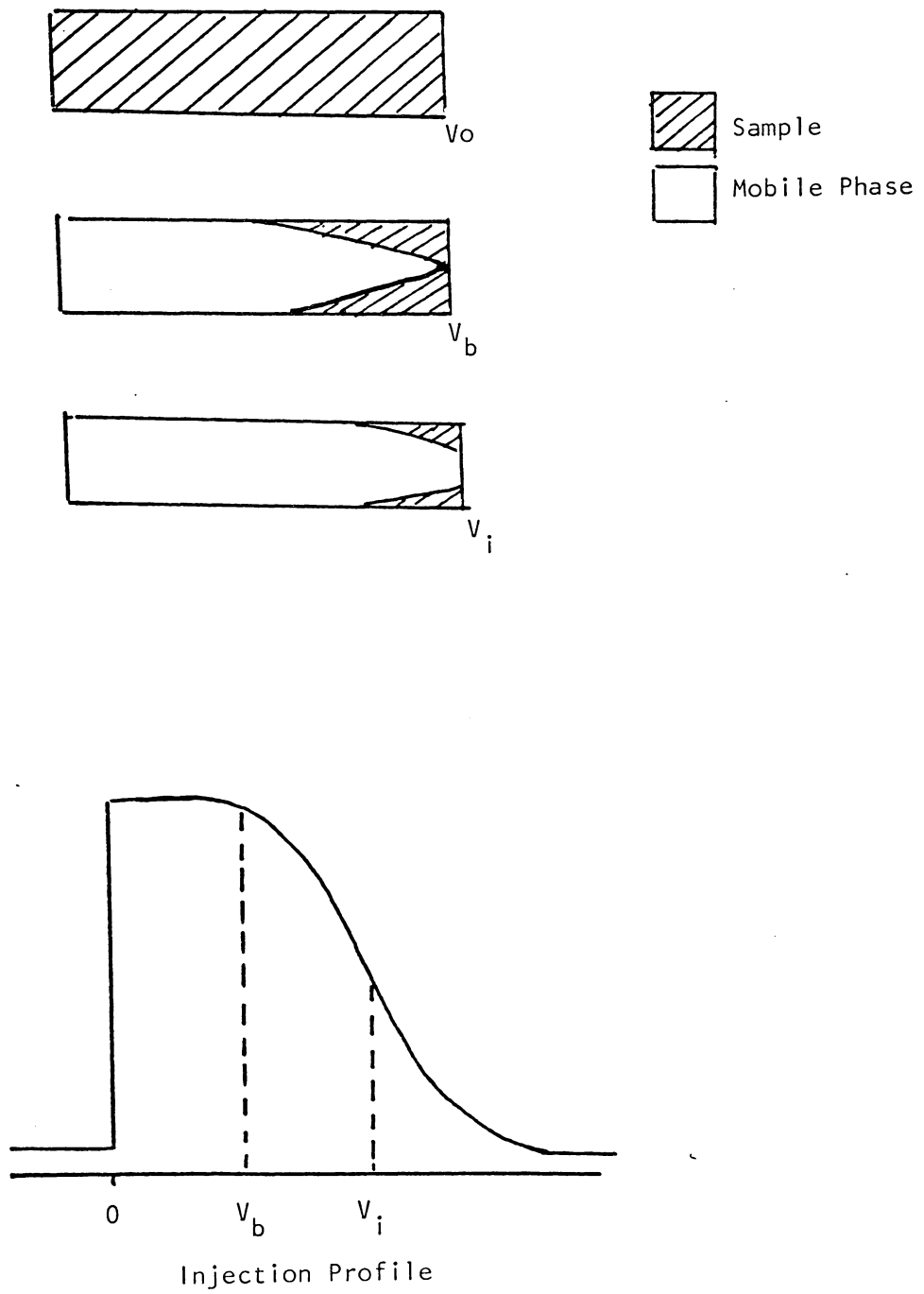


Figure 6. The effect of laminar flow on the injection profile from an open sample loop (from ref. 68).

essentially eliminated by dissolving the sample in a solvent which does not elute the sample from the column during the injection process. Broquaire and Guinebault (69, 70) studied bandwidths resulting from injection volumes up to several milliliters on conventional bore columns and found that

"Whatever the injection volume is, its contribution to band broadening is effectively zero. All the sample is concentrated at the top of the column during injection."  
(69)

Slais et. al. (71) used this peak compression technique on 0.7 mm ID microbore columns to inject up to 1 ml of aqueous samples on reversed phase sorbents. It should be noted that many reversed phase samples have a limited solubility in noneluting solvents so the technique is not without problems. However, dissolving samples in solvents weaker than the mobile phase is a useful technique for reducing injector band broadening. Yang (72) showed many examples of noneluting solvents using microbore columns.

### 3.1.6 DETECTOR VOLUME

Acceptable detector cell volume is bracketed by two mutually exclusive requirements; large detectors favor sensitivity while small detectors favor resolution. The greater the number of sample molecules that can be imposed between a UV source and

the photodetector, the larger the signal (Beer-Lambert Law). The smaller the volume of the detector cell, the less band broadening it will contribute to the sample. Constructing the longest possible pathlength cell with the smallest possible internal volume results in a vanishingly small optical aperture giving minimum optical throughput and spectacular refractive index effects making the system unstable. Optimal detector cell design considers pathlength, cell volume and aperture to arrive at a compromise between sensitivity and resolution.

Sternberg's evaluation of the static contribution of injector volume on variance applies to detector volume as well. The minimum variance of the detector volume is thus:

$$\sigma^2_{\text{det}} = V^2_{\text{det}}/12. \quad (9)$$

Similarly, detector variance usually exceeds this value due to laminar flow. A second term may be added to this equation to account for laminar dispersion, giving the total variance of the detector cell as:

$$\sigma^2_{\text{det}} = V^2_{\text{det}}/12 + F\pi r^4 L/24D_m \quad (10)$$

where  $F$  = flow rate,  $r$  = tube radius,  $L$  = length of tubing from the column outlet to the detector outlet and  $D_m$  = the diffusion coefficient. Table III lists calculated variance contributions for 0.5, 2.5 and 8.0  $\mu\text{l}$  cells used with  $10\mu\text{m}$  ( $N = 12,500$ )

Table III

Percent increase in the width of a microbore peak caused by a 0.5, 2.5 and 8.0  $\mu\text{l}$  detector cells as a function of capacity factor (from eq. 9).

Column: 25 cm x 1 mm ID

		Cell Volume ( $\mu\text{l}$ )			
		$k'$	0.5	2.5	8.0
N = 12,500	1	0.24	6.45	67.21	
	5	0.02	0.70	7.36	
	10	0.00	0.20	2.17	
N = 25,000	1	0.52	13.02	134.65	
	5	0.05	1.40	14.96	
	10	0.01	0.04	4.44	

and 5  $\mu\text{m}$  ( $N=25,000$ ) particles as a function of  $k'$  on a 25 cm microbore column, showing again that the major deterioration of resolution is suffered by early eluting peaks but becomes less important for the later ones.

### 3.2 RETENTION MECHANISM

The description of the retention mechanism in reversed phase liquid chromatography using binary aqueous-organic mobile phases has undergone many changes since its original formulation in the mid-70's (73,74). The original model depicted the nonpolar stationary phase as an inert support. The difference between the amount of energy required to form a cavity large enough to accommodate a solute molecule transferred from the gas phase into solution and the energy of the molecule adsorbed on the surface of the stationary phase was seen as the driving force in retention, and was labeled hydrophobic (73) or solvophobic (74) retention. The surface area (75) and molecular volume (76) of nonpolar solutes correlated well with their solubility in water. Interactions with other solvents were accounted for using extended solubility parameter theory (77, 78).

This solvent centered approach failed to account for chang-

es in retention with the surface coverage and chain length of the alkyl groups bound to the silica surface. Hemetsburger et. al. (79-81), Tanaka et. al. (82) and Hennion (83) studied these factors, showing an increase in both retention and selectivity with surface coverage and alkyl chain length. Slaats et. al. (84), McCormick and Karger (85) and Yonker et. al. (86) measured the adsorption isotherm of mixtures of water with THF, MeOH and MeCN on reversed phase sorbents showing the preferential adsorption of the organic component at the surface of the stationary phase. This leads to two different environments for the sample to inhabit. They may either exist in the bulk mobile phase (with its higher water content) or in the layer of organic rich solvent adsorbed on the stationary phase. The difference in the chemical potential of the sample in these two environments governs retention. This leads to a partition retention mechanism.

The simplicity of this model is reduced by the need to include the effect of residual silanol groups on the retention of polar sample components. Colin et. al. (87) compared hexadecane/water partition coefficients to retention on reversed phase sorbents for a variety of polar and non-polar solutes. He demonstrated that at a single temperature, surface silanols add a fixed  $\Delta G$  component to the overall retention energy. With

$\Delta G = \Delta H - T\Delta S$ , and the likelihood that  $\Delta H$  and  $\Delta S$  components of adsorption will be different from those of partition (88), changes in temperature are apt to affect the retention of polar and non-polar solutes differently. Temperature changes can be useful in resolving complex mixtures containing polar and non-polar species (89).

### 3.2.1 THERMODYNAMICS

Solute retention is expressed in terms of a capacity factor,  $k'$ , which is related to the solution equilibrium coefficient,  $K$ , by

$$k' = \phi K \quad (11)$$

where  $\phi = V_s/V_m$ , the ratio of the stationary phase volume to the mobile phase volume, or simply the phase ratio. Gibbs free energy is given by

$$\Delta G^\circ = -RT \ln K = \Delta H^\circ - T\Delta S^\circ. \quad (12)$$

Combining these two relationships gives

$$\ln k' = -\Delta H^\circ/RT + \Delta S^\circ/R + \ln \phi. \quad (13)$$

If  $\Delta S^\circ$  and  $\Delta H^\circ$  and  $\phi$  are independent of  $T$ , a plot of  $\ln k'$  vs  $1/T$  (Van't Hoff plot) will be linear. The slope gives the standard enthalpy of transfer between phases while the intercept gives the entropy of transfer when the phase ratio is known. The thermodynamic model predicts that increasing the temperature

will decrease retention. While exceptions have been noted for normal phase LC (22), reversed phase LC follows this rule in most cases reported so far. The magnitude of the change in  $\ln k'$  with temperature depends only on  $\Delta H$  of transfer going from the mobile to the stationary phase. In general, the greater the retention experienced by a solute, the greater the effect temperature will have on retention.

Chmielowiec and Sawatzky (34) were able to isolate the  $\Delta H$  and  $\Delta S$  contributions for various polynuclear aromatic hydrocarbons, and found that when  $\Delta S$  was different for a pair of closely eluting solutes, changes in temperature was effective in increasing their resolution. Retention in these cases was termed "entropy dominated".

### 3.2.2 MEASUREMENT OF THE TEMPERATURE EFFECT

The effect of temperature on retention may be performed on a compound-by-compound basis, like that done for mobile phase composition (90). However, reduction in the number of different modes of chemical interactions available to a set of sample species can lead to less cluttered models describing how temperature affects retention. Homologous series have been used extensively as model compounds in retention investigations

(91-101). The simplest homologous series is composed of n-alkanes and other series are constructed by adding alkyl side chains to some base functional group. Examples of homologous series include aromatics, alcohols, acids, aldehydes, ketones, amides, alkenes, halides, nitroalkanes, esters, and so on. The methylene selectivity,  $\alpha$  (97), is defined as the ratio of the capacity factors of any two consecutive members of a homologous series,  $(k'_n/k'_{n-1})$ , and has been shown to be a constant independent of the series that is used (102). This consistency enables the isolation of specific (base group dependent) and non-specific (methylene group dependent) interactions which define retention (95).

Another advantage using homologous series to study retention is that they have been shown to offer a means of estimating the void volume of the column with the least number of assumptions (101,102). Before describing how this is done, the importance of an accurate value for void volume and the shortcomings of available methods will be discussed.

### 3.2.3 VOID VOLUME

The capacity factor  $k'$  of a solute is defined as  $k' = \frac{V_r - V_0}{V_0}$  where  $V_r$  is the observed retention volume and  $V_0$  is the

void volume of the column. In order to exploit the thermodynamic information contained in  $k'$ , the void volume must be accurately known.

The void volume is difficult to define and even more difficult to measure. Melander (103) used the term "mobile phase space", and in very simple terms, the  $V_0$  is the volume of the mobile phase that moves through the column. The remainder of the column is taken up by sorbent surrounded by its adsorbed layer of solvent. Depending on the model used to define adsorption on the surface, a number of possible  $V_0$ 's can exist (101,103).

Several methods have been used to determine  $V_0$ ; including static methods (weighing the column filled with two solvents of different densities) (104); dynamic methods injecting components of the mobile phase (85); as well as radiolabeled mobile phase components (84); injection of inorganic salts (105); or "unretained" organic compounds (such as acetone (106), uracil (73) and phloroglucinol (107)); measurement of the retention at different temperatures (108) and mathematical methods based on the linearization of retention data for homologous series (92 102,109). These methods were evaluated by Krstulovic et. al. (101) and none of them was shown to be completely satisfac-

tory. Static methods measure total column porosity and result in negative values for  $k'$  when the mobile phase is preferentially adsorbed over the sample species. Injection of a single mobile phase component results in two peaks which describe the adsorption isotherm of the mobile phase rather than the void volume (110). Injection of inorganic ionic salts underestimates  $V_0$  because these salts are excluded from the pore volume. Non-retained samples like acetone and uracil are only non-retained over limited range of solvent strengths. Linearization of retention data for homologous series only works for the later members of the series since pendant group effects (close proximity of the base group to the alkyl side chain) distorts the linearity for the earlier members (93). Krstulovic et. al. concluded that "since  $V_0$  depends on the thermodynamic model chosen to describe the adsorption of the mobile phase components on the stationary phase, one cannot define a single  $V_0$  value " (101). Melander et.al. (103) came to essentially the same conclusion. Of all these, however, they found that convergence of homologous series are in very close agreement with those obtained using injections of radiolabeled mobile phase components, a method with very few assumptions. Berensen et.al. concludes "in our opinion, the most accurate hold-up time in methanol/water is derived from the linearization of the logarithmic net retention times of a homologous

series" (102). Based on these conclusions, homologous series were used in this study to provide an estimation of the void volume needed to calculate capacity factors and thermodynamic variables, as well as to provide a large data base to describe the effects of temperature on retention.

#### 3.2.4 VOID VOLUME VIA LINEARIZATION OF HOMOLOGOUS SERIES

Void volume estimation from homologous series is based on the linear relationship observed between the logarithm of the capacity factor and the number of methylene carbons,  $n_c$ , in the alkyl side chain (95)

$$\ln k' = n_c \ln \alpha + \ln \beta \quad (14)$$

where  $\alpha$  is the methylene selectivity for two consecutive homologs ( $k'_{n_c} / k'_{n_c-1}$ ) and  $\beta$  is the capacity factor of the functional group of a given homologous series. There is no rigorous thermodynamic basis for this linearity, but it may be thought of as the addition of a constant incremental  $\Delta G$  to solute retention with each additional methylene unit added to the side chain on the homolog. In fact, this  $\Delta(\Delta G)$  is not constant for the first few members of the series and only approaches linearity for  $n_c$  above 3 to 5 (93).

Three mathematically equivalent methods exist which extract

void volume from this relationship, and are given in detail in Appendix A. Simply stated, Berendsen's method (102) plots the retention of the  $n^{\text{th}}$  homolog versus the  $n-1^{\text{th}}$  homolog. The intercept divided by the slope minus 1 equals the void volume. Grobler's method (109) views the observed retention as a constant term (the void volume) plus another constant raised to an exponent. Plotting the logarithm of the difference in retention volumes between two consecutive homologs versus the carbon number gives a line whose slope is the exponent, and then plotting the retention volume versus exp raised to that exponent times the carbon number gives another line whose intercept is the void volume. Mockel's method (92) assumes that if the correct value for the void volume is picked, a straight line will result; but if the wrong value is chosen, a curved line will result. One starts with a reasonable range of values for  $V_0$ , and calculates sets of  $k'$  values using values in that range. Performing a linear regression on  $\ln k'$  versus  $nc$  will give the greatest correlation coefficient for the straightest line indicating when the best choice of  $V_0$  has been made.

### 3.2.5 COLUMN EFFICIENCY VS TEMPERATURE

A complete equation describing all the factors influencing

plate height in LC was derived by Huber (111) in 1969. He broke down the observed plate height,  $H$ , into four terms, which took into consideration four independent processes: mixing by diffusion  $H_{md}$ , mixing by convection  $H_{mc}$ , mass transfer in the moving phase  $H_{em}$  and mass transfer in the stationary phase  $H_{es}$ .

$$H = H_{md} + H_{mc} + H_{em} + H_{es} \quad (15)$$

The complete expression he derived is complex and is simplified here to eliminate those terms invariant with temperature.

$$H = 2D_m/c_1u + c_2/(1-c_3\sqrt{D_m/ud_p}) + c_4(k^2/(k^2 + 1))\sqrt{u/D_m} + c_5(k/(k + 1))u/D_m \quad (16)$$

where  $u$  is the linear velocity,  $D_m$  is the diffusion coefficient,  $k$  is the capacity factor,  $d_p$  is the particle diameter and  $c_1$ - $c_5$  are all temperature independent constants. An increase in temperature will decrease  $k$  and increase  $D_m$ . In all but the first term of equation 16, these two effects reduce the plate height contribution and improve column efficiency.

Values for  $k/(k + 1)$  and  $k^2/(k + 1)^2$  versus  $k$  appear in Table IV. Reducing  $k$  from 10 to 2 would decrease the last two terms in equation 16 by a factor of 1.36 and 1.86 respectively.

The effect of temperature on the diffusion coefficient  $D_m$  was derived empirically by Wilke and Chang (112) in 1955 as

$$D_m = 7.4 \times 10^{-10} T \sqrt{(\chi M)}/\eta V^{0.6} \quad (17)$$

Table IV

Calculated Values of  $k/(k + 1)$   
and  $k^2/(k + 1)^2$  as a  
function of capacity factor  $k$ .

$k$	$k/(k + 1)$	$k^2/(k + 1)^2$
0	0.000	0.000
1	0.500	0.250
2	0.667	0.444
3	0.750	0.563
4	0.800	0.640
5	0.833	0.694
6	0.867	0.735
7	0.875	0.766
8	0.889	0.790
9	0.900	0.810
10	0.909	0.826

where  $T$  is the temperature ( $^{\circ}\text{K}$ ),  $\alpha$  is an associative factor, (which for water is 2.6, for methanol is 1.9 and for unassociated liquids is 1.0),  $M$  is the molecular weight of the solvent,  $\eta$  is the solvent viscosity, and  $V$  is the molar volume of the solute, in cc/g Mol. Viscosity as a function of temperature for common LC solvents is available in the literature (113). The viscosity versus temperature for methanol is shown in Table V. Increasing the temperature from  $20^{\circ}\text{C}$  to  $150^{\circ}\text{C}$  results in a four-fold reduction in the viscosity.

So, as an example, the diffusion coefficient of benzene in methanol as a function of temperature was calculated, and is shown in Figure 7. Increasing the temperature from  $20^{\circ}\text{C}$  to  $150^{\circ}\text{C}$  increases the diffusion coefficient by a factor of 6.

Knox (114) showed that plots of the reduced plate height  $h$ , ( $h = H/d_p$ ) versus the reduced linear velocity  $v$  ( $v = u D_m/d_p$ ) were independent of both the particle diameter and the diffusion coefficient of the solute. Column efficiency plotted as either  $H$  versus  $u$  or  $\log h$  versus  $\log v$  is shown in Figure 8. This shows that an increase in the diffusion coefficient with temperature should linearly translate to a higher optimum linear velocity, leading to faster analyses. Decreased solvent viscosity with temperature (Table V) allows the LC pump to

Table V

Viscosity of methanol as a function of temperature (from 113).

Temperature (° C)	Viscosity (centapoise)
0	.809
10	.619
20	.594
30	.515
40	.450
50	.395
60	.349
70	.310
80	.277
90	.248
100	.223
110	.201
120	.183
130	.166
140	.151
150	.138

Figure 7

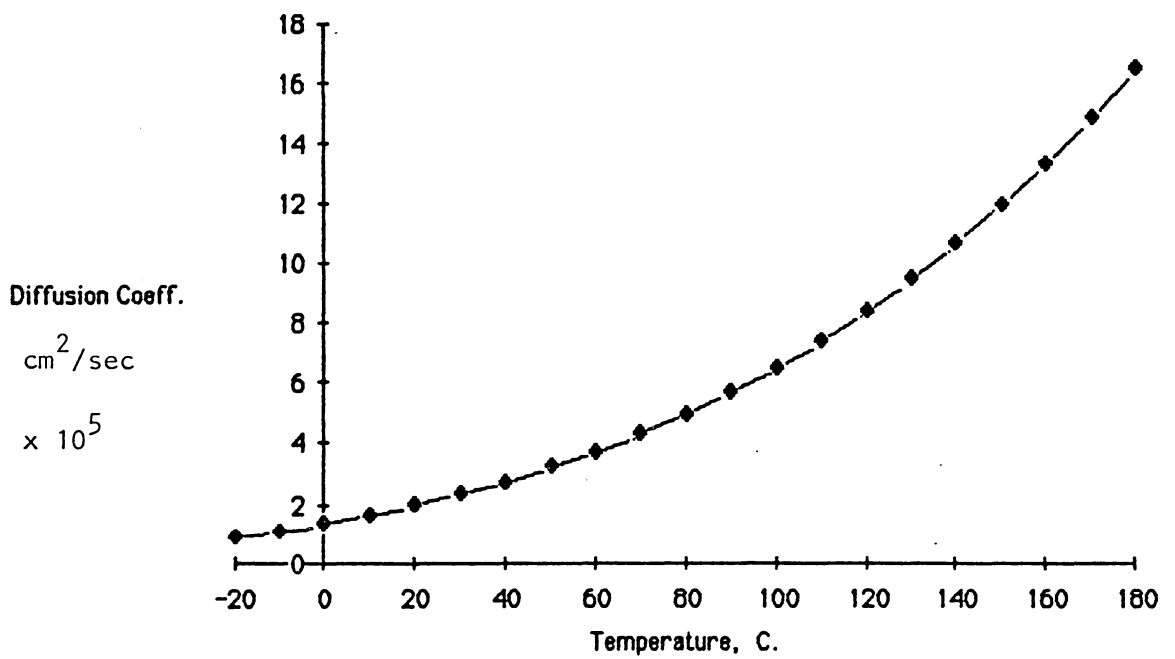
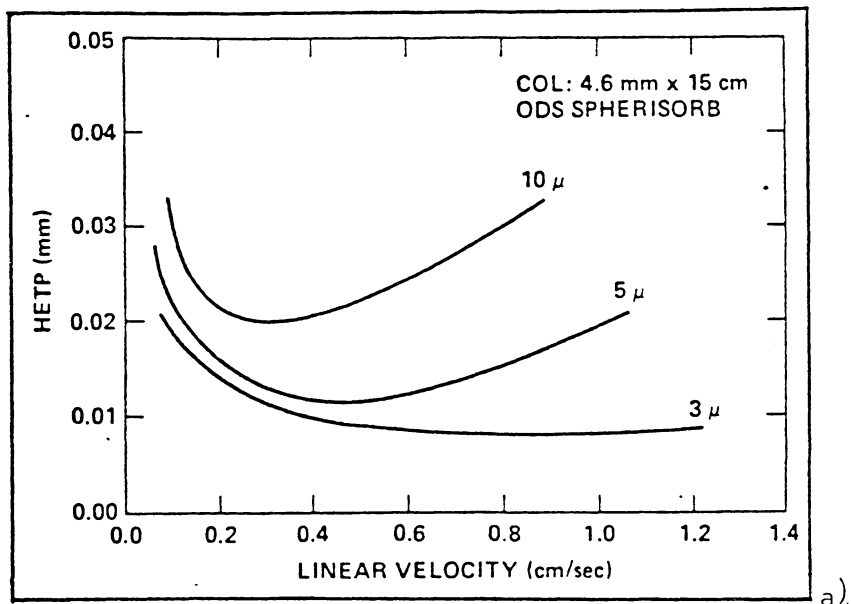
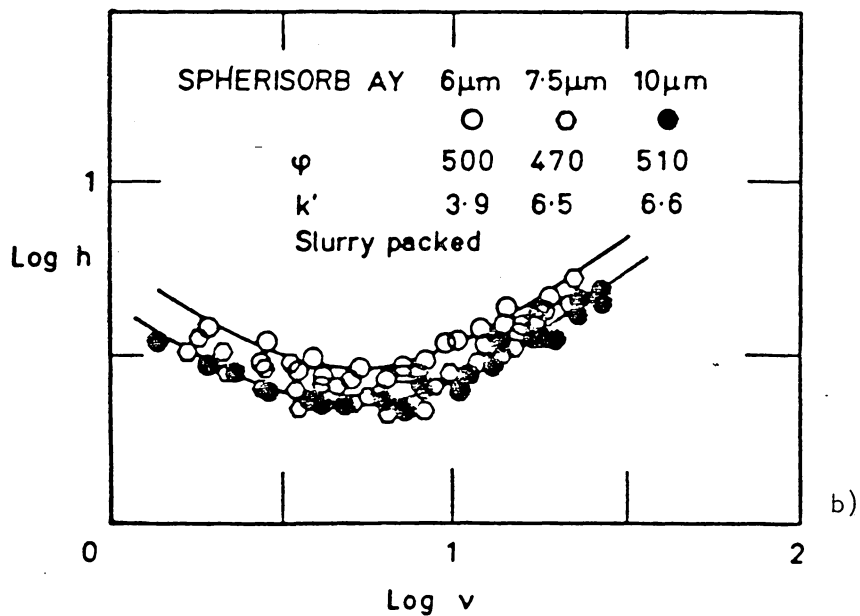


Figure 7. Calculated diffusion coefficients of benzene in methanol as a function of temperature. (from eq. 17 and ref. 113)



a)



b)

Figure 8. a) Plot of plate height versus linear velocity (from ref. 115) and b) reduced plate height versus reduced linear velocity (from ref. 114)

operate at higher flow rates without generating excessive pressures.

### 3.3 CONCLUSIONS

A theoretical evaluation of the injector, detector and connection volume has shown that the use of conventional instrumentation will cause a reduction in resolution for the very earliest eluted peaks, but has a minor influence on the later peaks. Use of the proper combination of sample solvent and mobile phase will permit conventional volume injections on microbore columns with no loss in resolution. The loss in resolution caused by using conventional 8  $\mu$ l detector cells with microbore columns is by no means prohibitive and furthermore enhances sensitivity compared to 0.5  $\mu$ l cells which use shorter pathlengths. Experimental comparisons will be made using microbore columns with both micro LC instrumentation and conventional LC instrumentation to highlight the sensitivity and resolution compromises achieved using both systems.

An experimental evaluation examining the influence of temperature on retention for members of homologous series will provide information on how it effects solvent strength, as well as its influence on the void volume of the column. The increase

in the diffusion coefficient of sample species with temperature is expected to produce an increase in the optimal linear velocity and thus improve the speed of analysis. Measurement of the change in column efficiency with temperature at different flow rates will provide experimental evidence for the applicability of this theory.

## 4.0 EXPERIMENTAL

### 4.1 INSTRUMENTATION

This section will describe in detail the instrumentation used in temperature programmed microbore HPLC, emphasizing its differences from conventional 4.6 mm bore isothermal LC instrumentation. It will briefly describe some performance criteria for various types of instruments to give some insight into why particular designs were chosen.

A sizable amount of literature exists in which the authors briefly describe the instrumentation used. Few of them go into sufficient detail so that someone unfamiliar with microbore LC could use it without running into problems. The goal of this instrumentation section is to include all the little hints and tricks that are usually omitted from technical journals for the sake of brevity. Most of these are merely common sense and attention to details.

#### 4.1.1 SOLVENT RESERVOIR

The small volumetric flow rates of microbore columns

allowed the use of very small (50 ml) glass bottles for solvent reservoirs. The bottle caps were fitted with 1/8" OD Teflon tubes to transfer the liquids to the pump, and a pinhole was used to equilibrate pressure inside the bottle while providing a low evaporation rate and negligible compositional changes of binary mobile phases. A filter (frit) inside the bottle doubled as both a solvent inlet filter to protect the pump from debris and as an initial solvent degassing inlet for helium.

For UV detection below 200 nm where O<sub>2</sub> absorbs, the solvent reservoir was maintained at a slight positive pressure with helium. Diffusion of O<sub>2</sub> through Teflon, giving an increasing baseline, was observed due to the long residence time of solvent in the lines at low flow rates. For this reason, Teflon was replaced with stainless steel tubing for low UV detection.

#### 4.1.2 PUMP

Three pumping systems were used to deliver low flow rates for this study. As originally proposed by Scott and Kucera (1), a Waters model 6000A reciprocating piston pump (Waters Associates, Milford, Ma) was slowed down by placing a Hewlett-Packard 3311A Frequency Generator (Hewlett-Packard, Palo Alto, CA.) before the power transistors which drove the

stepper motor. This motor rotated a cam which moved two 90  $\mu$ l solvent delivery pistons 180° out of phase from each other. A digital frequency counter attached to the frequency generator allowed accurate monitoring of the pump speed and permitted very repeatable flows to be set.

The second system was the Gilson 302 pump (Gilson Medical Electronics, Middleton, WI.; sold by E. M. Science, Gibbstown, NJ, including the pressure transducer and low volume pulse damper) which used a single 39.7  $\mu$ l piston with a stroke similar to the Waters pump. This sapphire piston had a smaller diameter than the Waters piston, and greater care was needed not to break this small piston when removing the pump head and changing the piston seal. It was driven by a similar stepper motor and cam, with onboard electronics permitting flow rates as low as 5  $\mu$ l/min. It showed better flow stability than the Waters pump during the elution of microbore peaks since it used a smaller volume piston operating at a higher frequency.

The third system was a modification of a system used by Yang (116) involving a Varian 5000 conventional LC single piston pump (Varian Associates, Walnut Creek, CA.) operating at 1 ml/min and a splitter which directed 95% of this output to waste (Figure 9). The splitter was constructed by attaching a

## SPLITTER 1:20

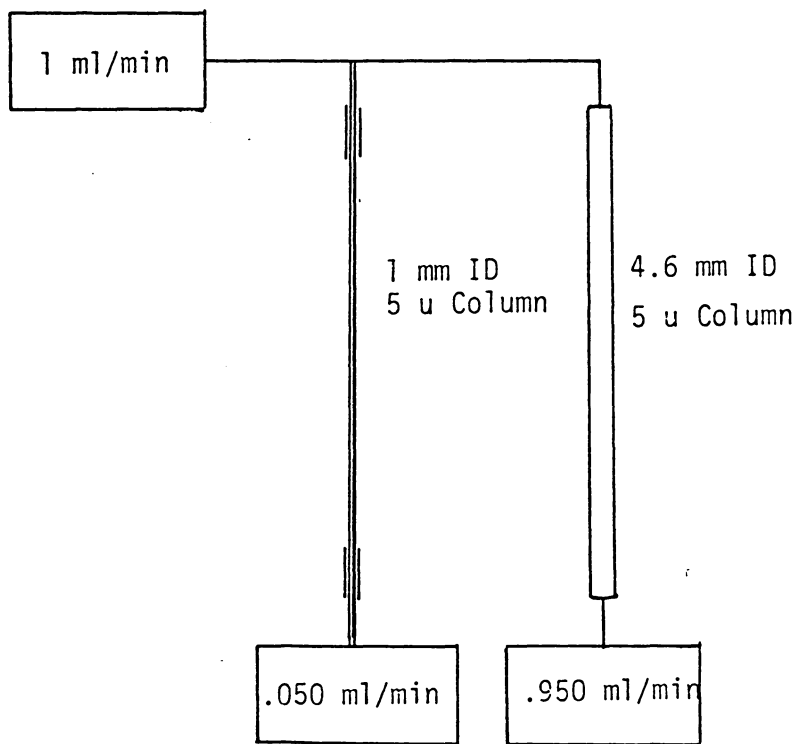


Figure 9. Solvent splitter system used to form microbore compatible gradients.

4.6 mm ID conventional column into the pump outlet packed with the same size sorbent as the microbore column. With this sorbent, the same pressure applied to both columns produces the same linear velocities, so the split was simply the ratio of their cross sectional areas ( $4.6^2$  to  $1^2$ , or 21.16 to 1), as verified by flow measurement.

#### 4.1.3 PULSE DAMPENER

For stable, pulseless flow, the Gilson pump required the addition of a Gilson model 802 manometric module containing a pressure transducer and an 11.7 ml helical pulse dampener of the bourdon tube type. Analysis showed that up to 50 ml of solvent were required to remove 99% of the previous solvent from this pulse dampener during solvent changeovers (Figure 10), severely decreasing the advantage of low solvent consumption when using this dampener in a microbore system.

Therefore, this large pulse dampener was replaced by a 0.75 ml volume pulse dampener with a diaphragm that separated this volume from a 10 ml passive reservoir. This reservoir acted as a dynamic ballast to stabilize the pressure in the system. It provided the same performance as the first pulse dampener, but since the majority of this pulse dampeners volume was phys-

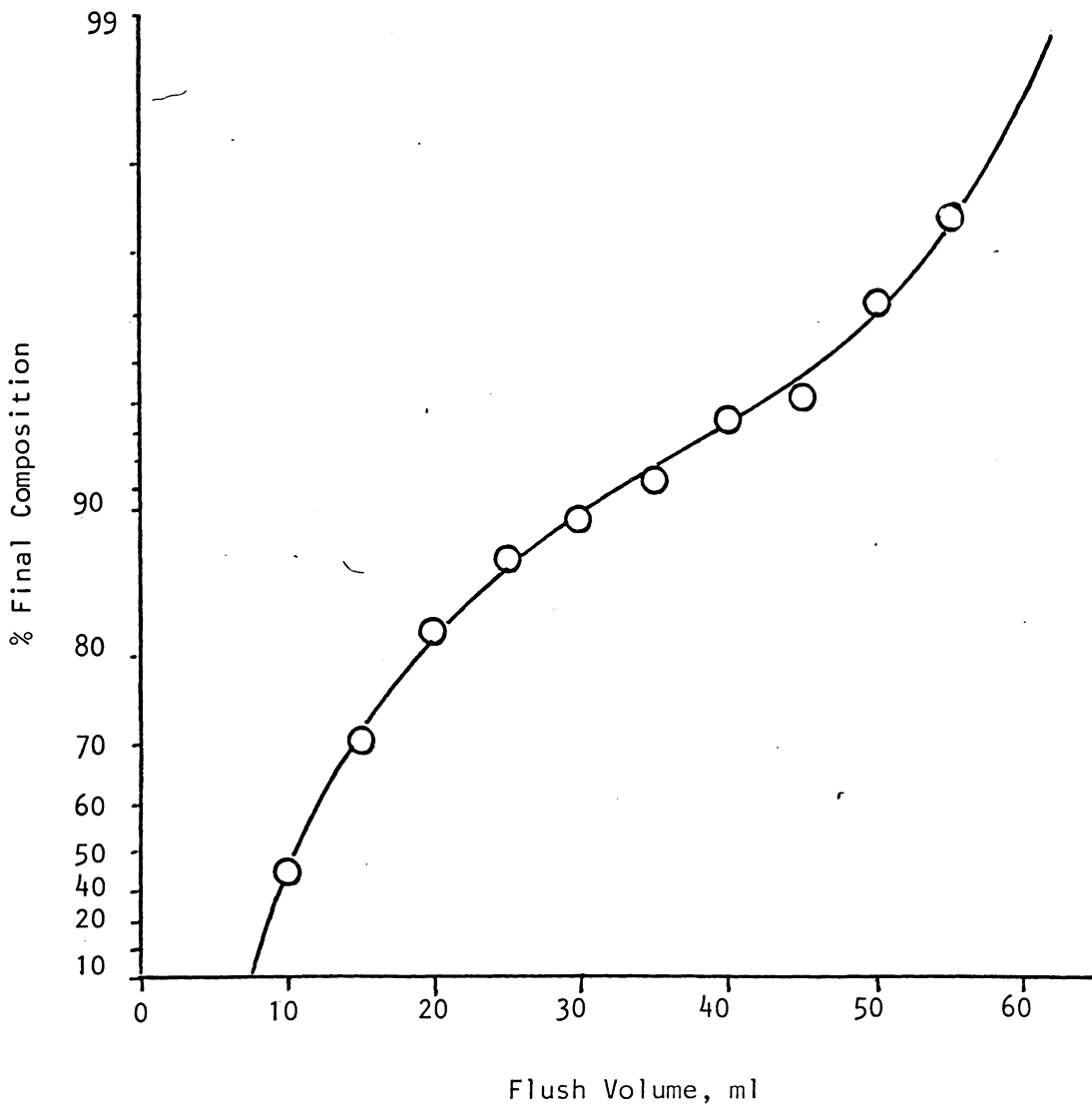


Figure 10. Flush volume requirements of a 11.7 ml pulse dampener.

ically isolated from the flow path, it did not require a large volume of solvent to flush it when changing solvents.

#### 4.1.4 INJECTOR

Two styles of sample injectors were used; external loop and internal loop. A type PX injector from Valco (Valco Instrument Company Inc., Houston, TX) and a model 7120 injector from Rheodyne (Rheodyne Inc., Cotati, CA). require an external loop to bridge the distance between two ports on the valve. Even with the minimum length and ID of tubing, the minimum practical volume was still 10  $\mu$ l. Typical microbore injection volumes are 0.5  $\mu$ l, so to provide acceptably narrow microbore injection profiles, either momentary partial loop transfers or noneluting sample solvents were required.

Internal loop injectors from Valco (type P, 2  $\mu$ l) and Rheodyne model 7410 (0.5 and 5.0  $\mu$ l) were also used and provide very reproducible small injection volumes.

#### 4.1.5 FRITS

An initial design for connecting the column and injector given by Scott and Kucera (3) showed the column screwed direct-

ly into the injector port, with the valve body containing a filter (frit) which kept the column packing (sorberent) within the column (Figure 11). In the absence of this frit, the sorberent in the column may back flow into the injector whenever pressure to the column from the pump is removed. This abrasive sorberent can score the valve seat, causing leaks and injector failure. This made including a column inlet frit essential.

Frits are 1/16" diameter filters composed of sintered (partially fused) small particle stainless steel powder having a porous structure composed of approximately 40% air. A nut and a ferrule were used to grip and seal the column to the injection valve body (Figure 12). During the tightening process, once the ferrule grips the column, the column end moves forward a fraction of an inch. This movement was sufficient to crush the edges of the frit inside the injector port and seal it permanently to the injector. After a short time of operation, this partially crushed frit became clogged with miscellaneous debris and had to be removed. This could only be accomplished by sending the injector back to the manufacturer, drilling out the frit and resurfacing the valve seat (a costly and time consuming procedure).

The frit was therefore placed in the next nearest available

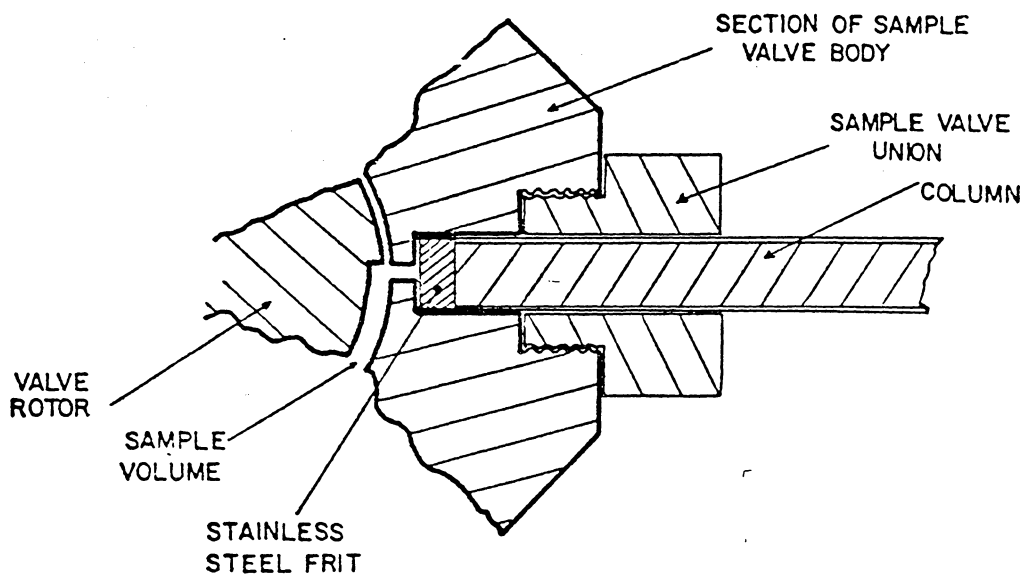


Figure 11. Direct column attachment to a sample valve according to Scott and Kucera (ref. 1).

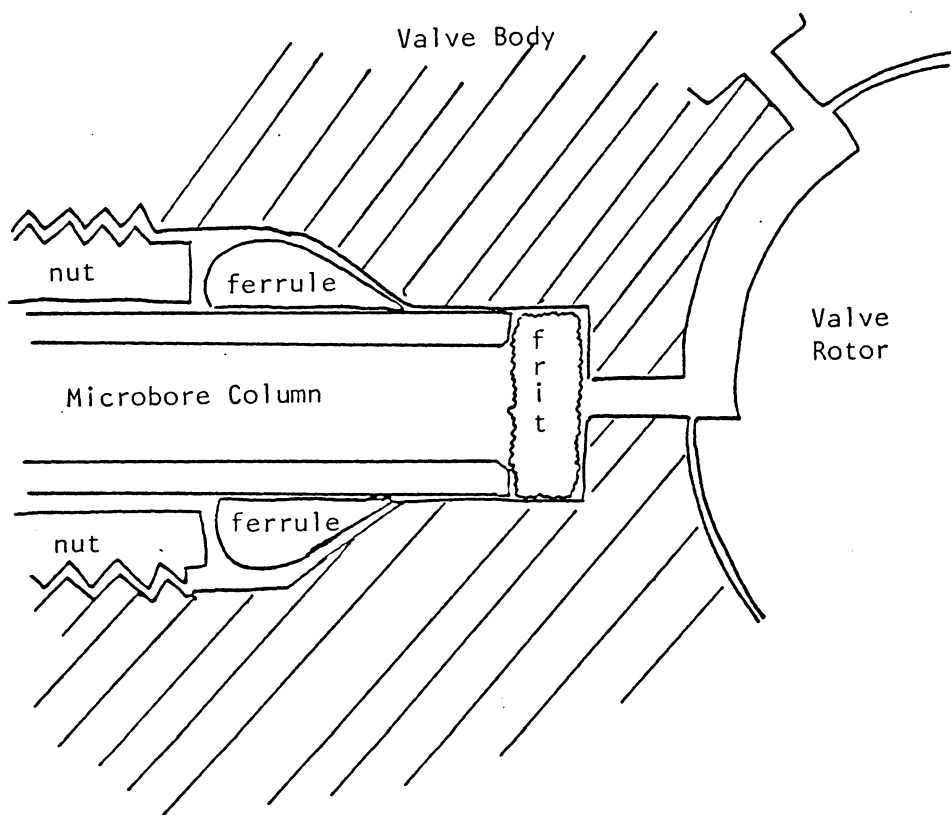


Figure 12. Nut and Ferrule used to seal the column to the valve

spot. The microbore column was partially drilled out before packing, and enough of a lip was left to allow a frit to be inserted directly into the column itself (Figure 13). While this lip prevents the frit from adhering to the valve body, the in-column frit was still somewhat compressed when the column was secured to the injector. Frit replacement is a common cure for columns which develop high backpressure after extended operation but it was difficult to replace this frit without column bed damage. The inability to replace this frit reduced the available column lifetime. Other researchers (114) and a commercial vendor (Alltech Associates, Deerfield, IL) use this in-column frit design.

A recent column design by ISCO (ISCO Inc, Lincoln, NE.) uses a variation of this in-column frit design (118), where the replacement problem was eliminated (Figure 14). Rather than 1/16" stainless steel tubing, the column was 1/8" glass lined tubing (GLT) which due to the larger column diameter can be threaded at the ends to accommodate a threaded column terminator containing a press fitted frit. A custom built injector valve with a 1/8" port, the bottom of which was equipped with a Teflon gasket, provided the tightest possible design to date for connecting the column to the injector.

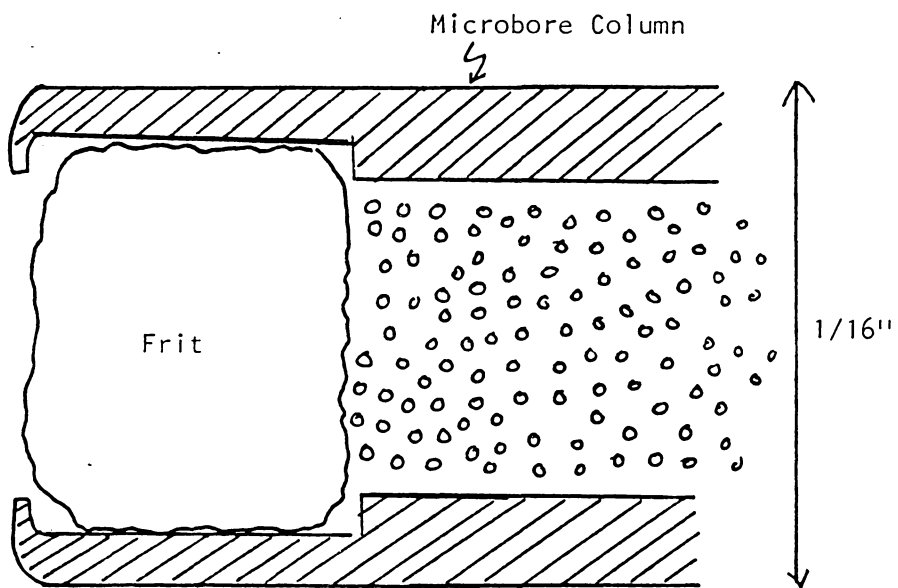


Figure 13. Inside column end frit.

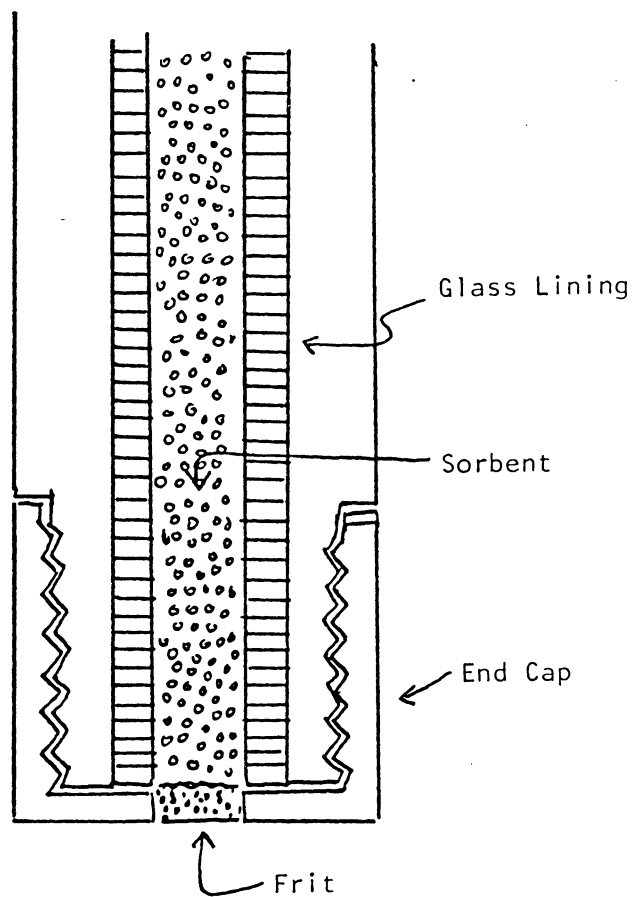


Figure 14. ISCO's threaded in-column frit design.

Since 1/16" column walls are too thin to be threaded to allow the removable inclusion of a frit between the injector and column, a zero dead volume (ZDV) union was inserted between the injector and the column in all 1/16" columns as the final design solution to both terminate the column and safely contain the frit (Figure 15). This required a minimum of 3.65 mm of tubing be inserted between the injector and column. For .010" ID tubing, this results in 1.85  $\mu$ l of connection volume. Smaller diameter tubing was available but it easily (and in fact routinely) plugged unless extreme measures were taken to remove offending particles from the samples and the mobile phase. Tubing smaller than 0.010" ID was seldom used since the debilitating effect of this extracolumn volume was removed using noneluting sample solvents (see section 3.1.5, p. 45, NON-ELUTING SAMPLE SOLVENT).

#### 4.1.5.1 KEL-F® SURROUNDED FRITS

Frits which are 1/16" in diameter comprised solely of stainless steel show the same tendency to become permanently fixed inside ZDV unions as they do to injection valve ports. An examination of the frit before insertion (Figure 16) and after insertion (Figure 17) shows the degree of compression the frit suffers when the column was tightened into the ZDV union. The

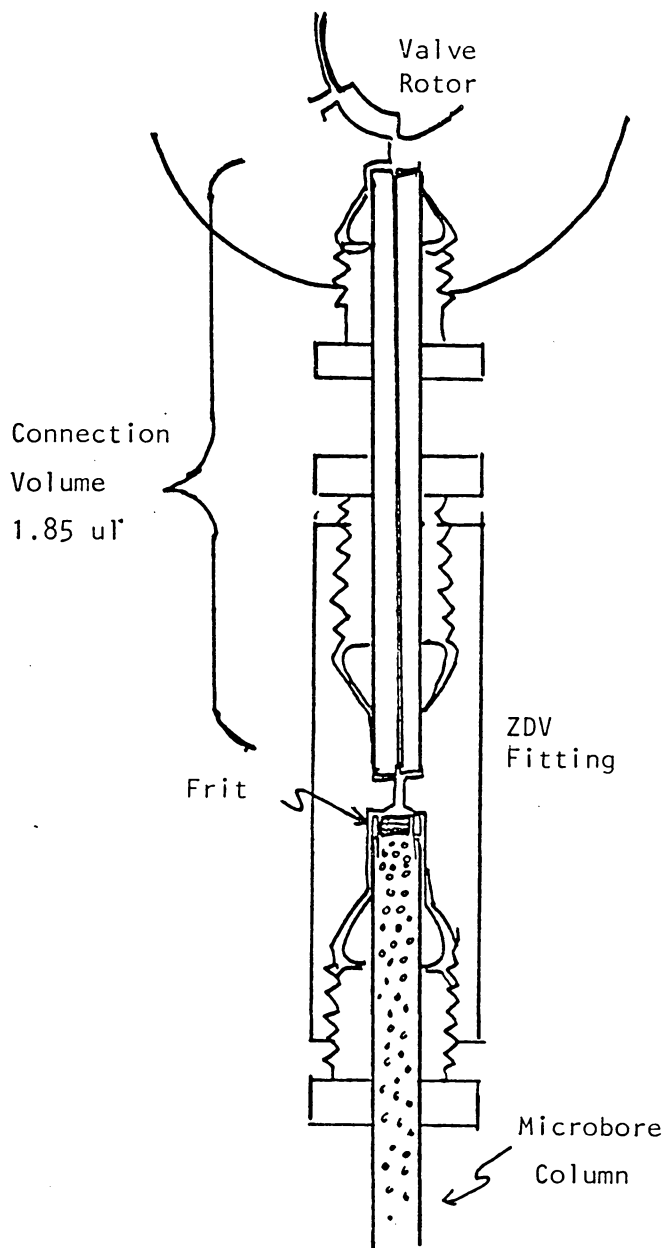


Figure 15. Safe top-column connection of a microbore column to a sample valve.

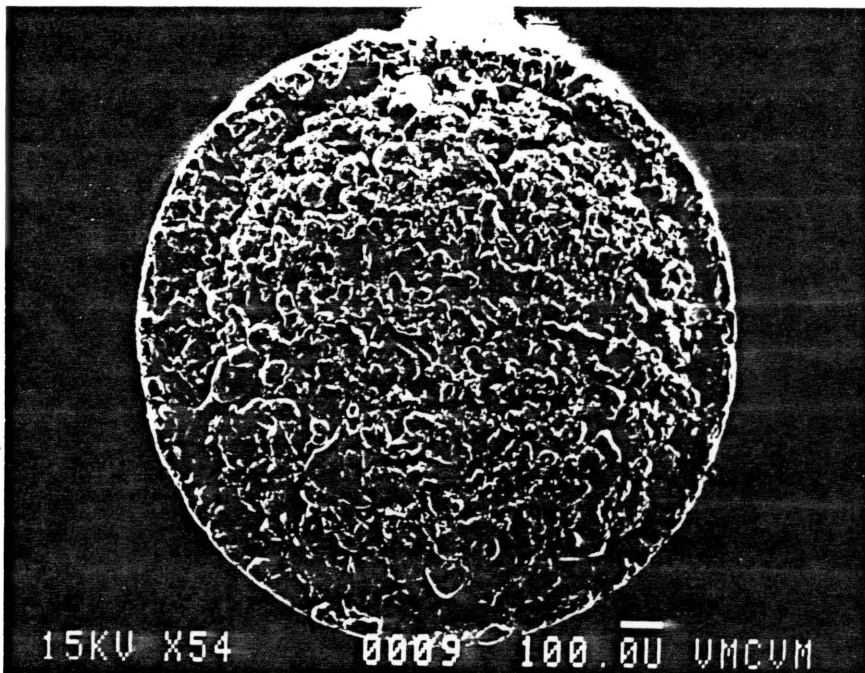
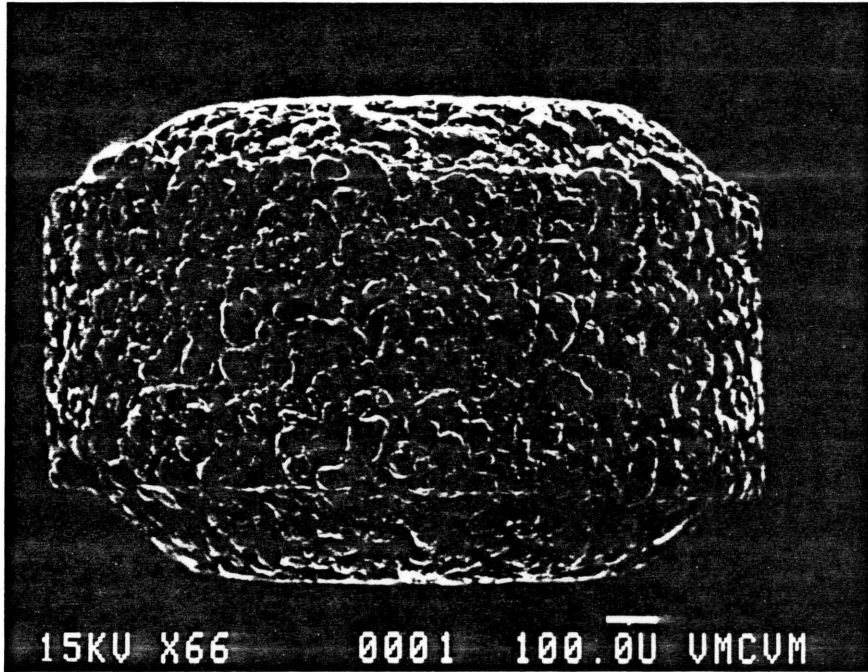


Figure 16. Frit before insertion into a column end-fitting.

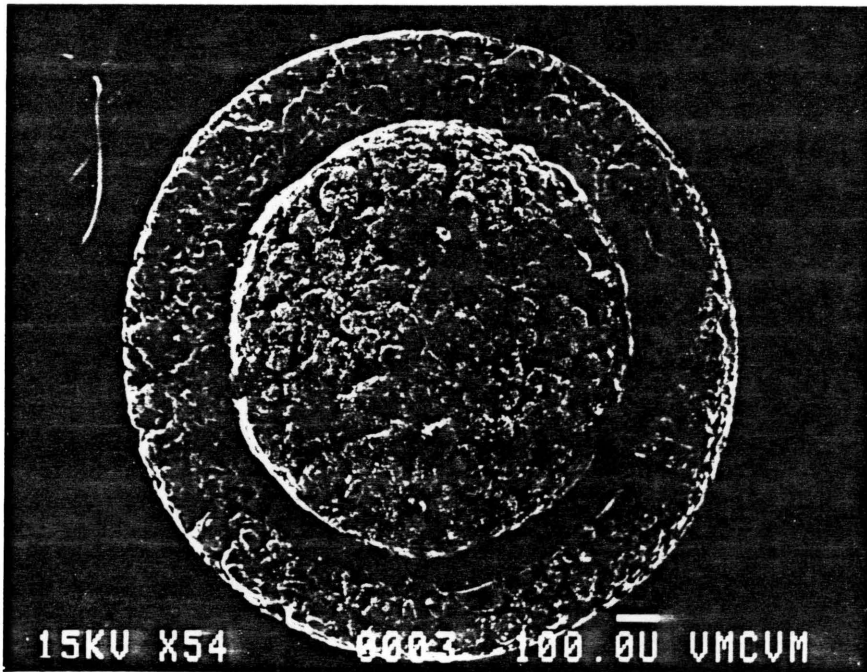
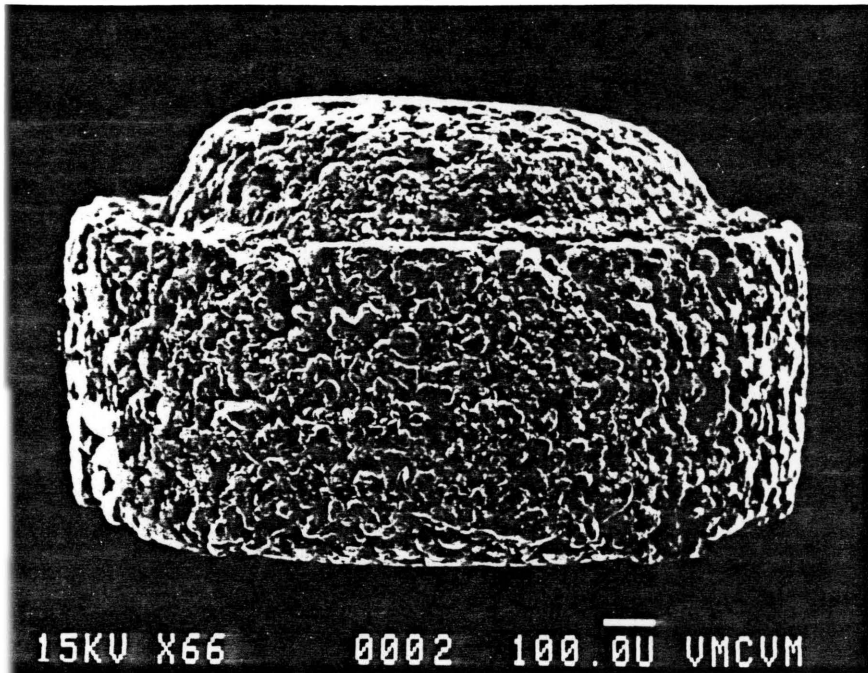


Figure 17. Frit after insertion into a column end-fitting.

shape of the frit was distorted, and columns using these frits developed high back pressure after only 2 hours operation at 100  $\mu$ l/min. It was assumed therefore that the total porosity of the frit was also reduced by this compression. since columns using non-crushed frits have been used for several weeks at 100  $\mu$ l/min with no increase in back pressure.

Frit crushing was prevented by surrounding a smaller frit with a Kel-F® plastic ring. The column presses against the plastic instead of the frit (see Figure 19, p. 88). A 0.95 mm diameter, 0.5 mm thick 2  $\mu$ m frit (Figure 18 a) (Mott Metallurgical, Cransford, MA.) was placed into a 0.5 mm piece of 1/16" Kel-F® rod that had been drilled out with a 0.95 mm drill bit (Figure 18 b). Insertion of the frit into the ring was made with tweezers, the flat edge of a razor blade.

#### 4.1.6 COLUMNS

Microbore columns are made with two different types of tubing, either 1/16" OD x 1 mm ID stainless steel tubing (SST) or 1/8" OD x 1 mm ID glass lined tubing (GLT). In terms of which tubing is best, for isothermal work it is largely a matter of personal preference. Both types of tubing packed in the same manner should perform the same under typical operating condi-

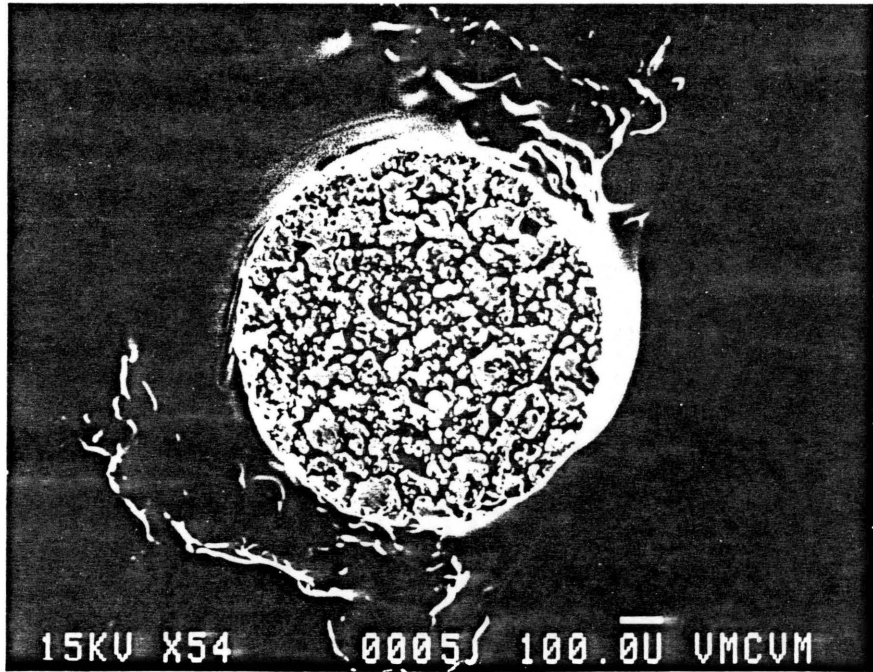
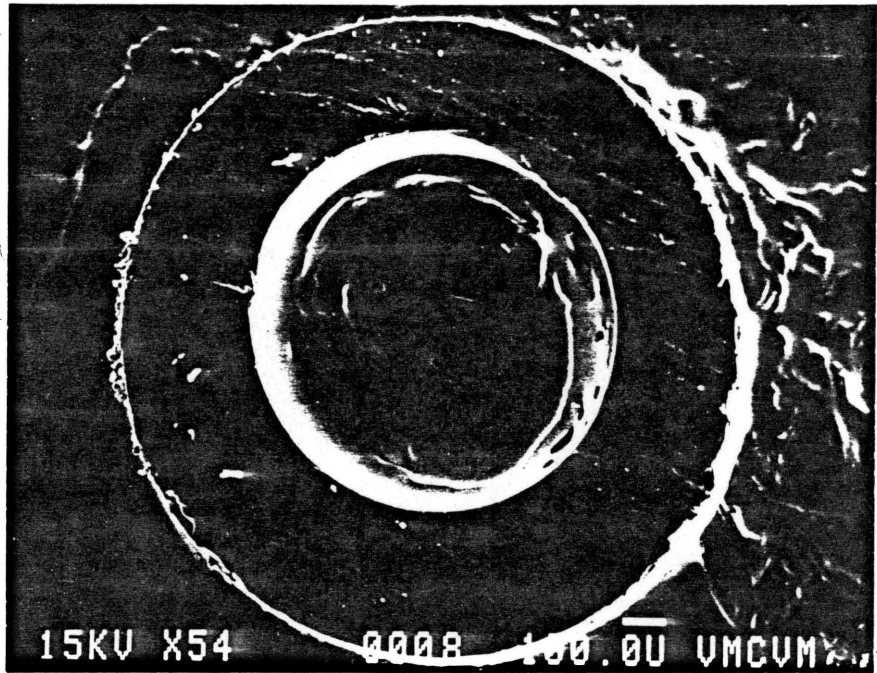


Figure 18. Kel-F surrounded frit.

tions. For temperature programming work, however, 1/16" SST responds faster to temperature changes than 1/8" GLT, and therefore 1/16" SST was used exclusively in temperature programmed studies.

Glass lined tubing has a very smooth internal surface while commercial 1/16" stainless steel tubing has a very rough inside surface. During column packing, indentations in the walls of rough tubing will not pack with sorbent, since the force on the sorbent particles is parallel with the walls rather than perpendicular to it. These unpacked pockets in the walls provide a space for the column bed to flow into. Assuming a 20  $\mu\text{m}$  amplitude random undulations, this constitutes a 3.9  $\mu\text{l}$  volume capable of producing a 5 cm void at the head of the column. This reduces the column efficiency. Therefore, 1/16" SST was polished on the inside before packing (see section 4.4.1, page 117, COLUMN POLISHING).

GLT initially costs more and is harder to cut than SST, but polishing SST is time consuming and therefore costly. Initial cost, however, is not a major factor since both column types may be packed over and over again. The limit to the number of times a column can be packed comes from ferrule distortion during column attachment (117). Stainless steel ferrules preman-

ently seal to the outside of a column. After repeated use, the end of the ferrule eventually distorts to the point where it no longer provides an adequate seal at high pressures. However, plastic vespel ferrules were used and sealed at surprisingly high pressures. When worn, these were easily removed from the column. The use of vespel ferrules gave practically an unlimited column tubing lifetime. Since vespel does not actually bite into the tubing, care was taken to adequately tighten the nut pressing against this ferrule to prevent the column from suddenly flying apart under high pressure.

#### 4.1.7 TUBING CUTTER

While a triangular file and patience was initially used to cut 1/16" tubing, an SSI model TC-10 tube cut-off machine (Scientific Systems Inc., State College, PA.) having a motorized carborundum disk and a right-angle securing arm was required to reproducibly provide clean, square column ends. The small dimensions of the tubing coupled to the small size of the sorbents used demanded high precision. Since the polishing process on 1/16" SST distorted the column ends, a tube 5 cm longer than required was cut before polishing and only after polishing was it cut to the desired length. A tool on the TC-10 was used to remove burrs and provide an inside bevel (Figure 19 a),

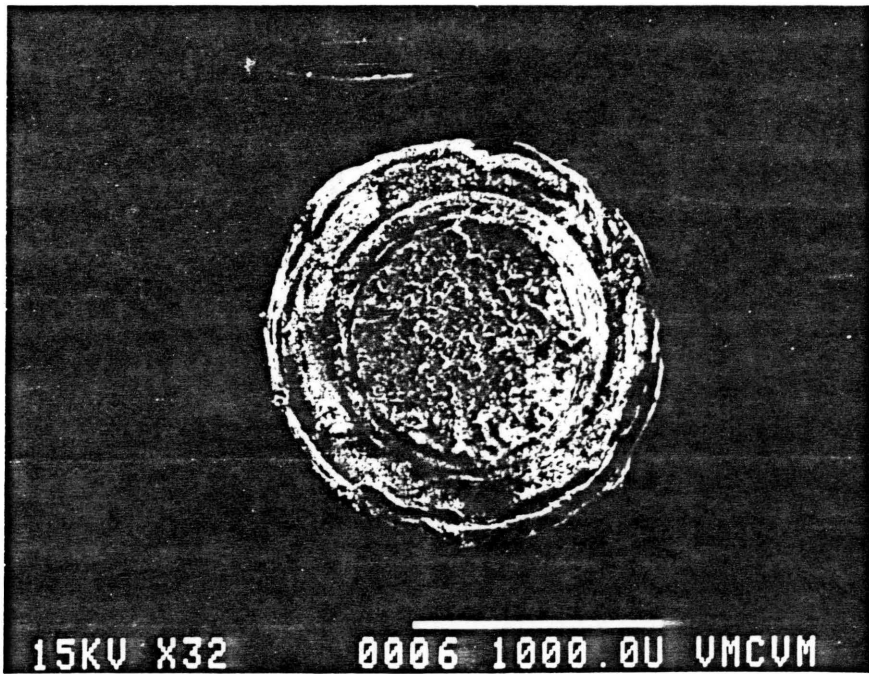
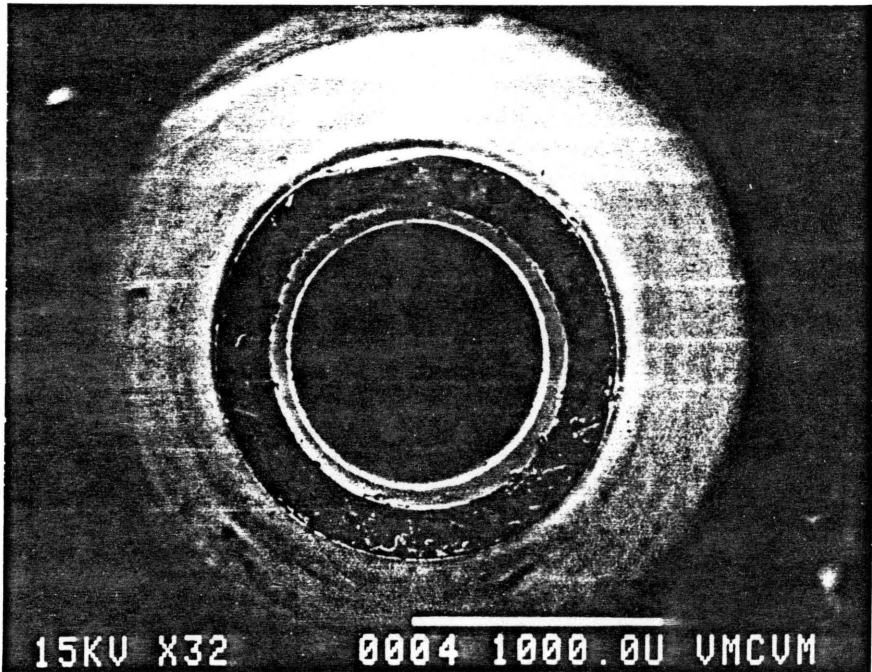


Figure 19. Beveled microbore column end and the seal made with the Kel-F® surrounded frit.

which can be seen impressed on the Kel-F® plastic surrounding the frit (Figure 19 b). This provides a tight plastic seal between the frit and the end of the column.

#### 4.1.8 COLUMN PACKER

A diagram of the column packing equipment is shown in Figure 20. A Haskel DST-122 pump (maximum pressure - 15,000 psi) or a Haskel DSXHP-602 (maximum pressure - 60,000 psi) (Haskel Eng. and Supply Co., Burbank, CA) were used to drive solvents into a slurry reservoir at high pressures. These reservoirs were either empty conventional bore columns or very long, thick walled high pressure tubes. A SSI 15,000 psi two-way valve (model # 02-0180) was included between the pump and slurry reservoir. Fluid filled 25,000 and 60,000 psi pressure gauges (United Instruments, Chicago, IL.) were used to indicate the pressures during packing. A description of the packing procedure is given in the procedures section.

#### 4.1.9 DETECTOR

A Kratos model 769 variable wavelength UV detector (Kratos Analytical Instruments, Ramsey, NJ.; sold by E. M. Science, Gibbstown, NJ) was used to detect sample species eluting from

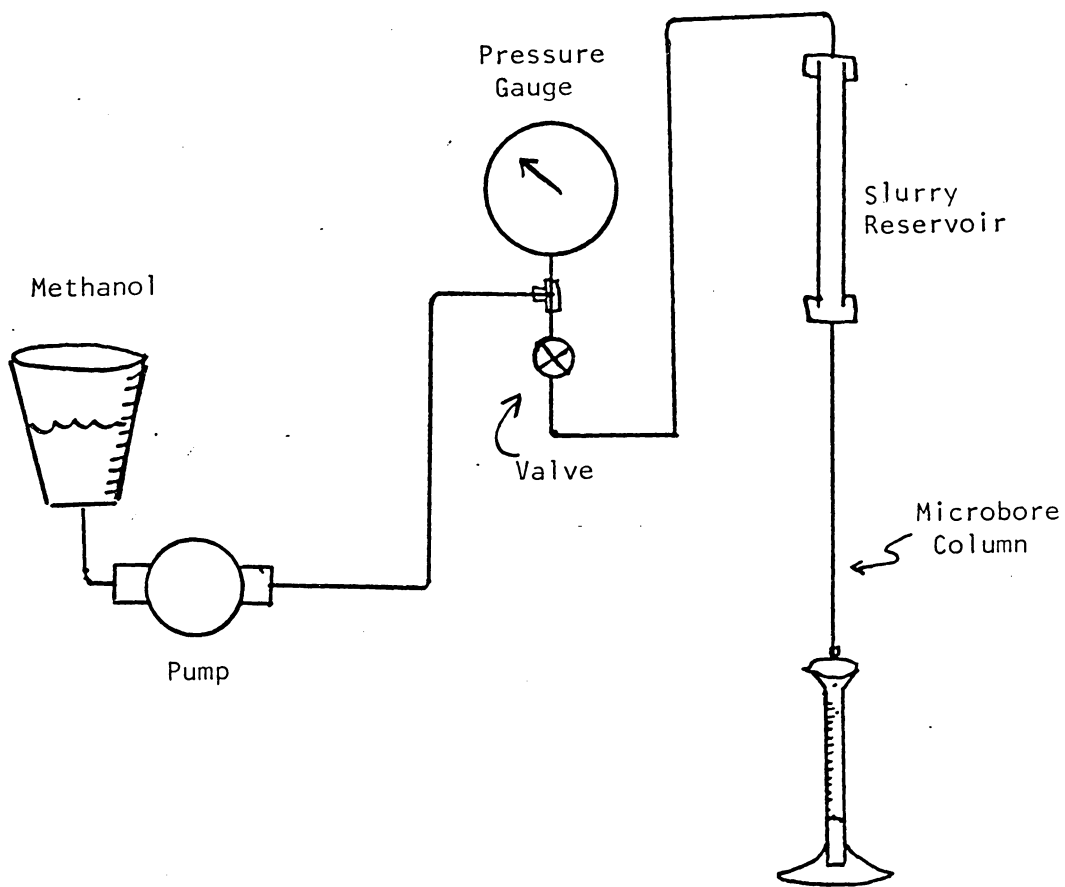
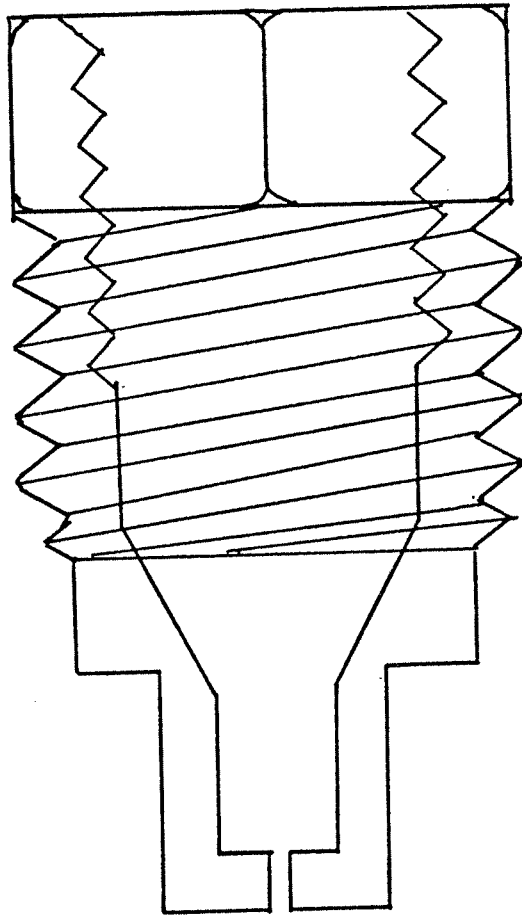


Figure 20. Column packing equipment.

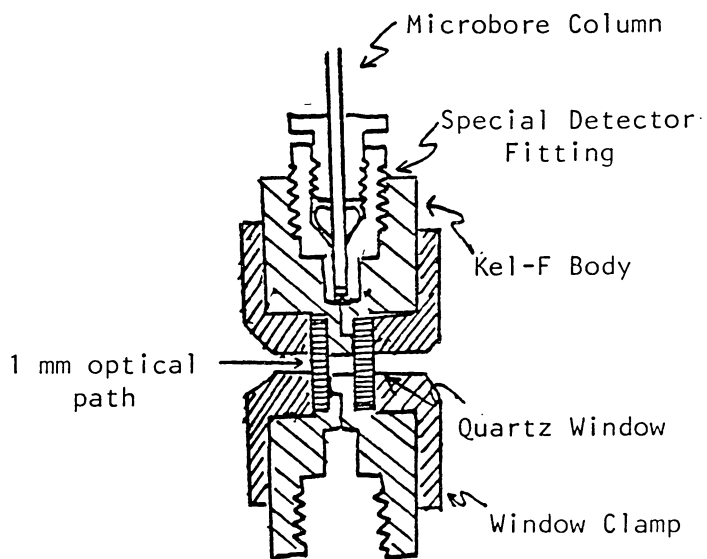
microbore columns. Columns manufactured with special end fittings (Figure 21) permitted direct connection of the column end to the detector cell. Temperature programmed columns terminated within a heated zone with a ZDV fitting and a transfer tube with thermal isolation was placed between the column outlet and detector cell inlet.

Two different sizes of detector cells were used; the 0.5  $\mu$ l microbore column cell and the 8.0  $\mu$ l conventional bore column cell. The 0.5  $\mu$ l cell (Figure 22 a) contained a 0.25 mm ID x 2 mm long channel (0.10  $\mu$ l volume) which directed the column effluent to an end-on, cylindrical, 0.8 mm ID, 1 mm pathlength optical path where the ultraviolet absorbance of the column effluent was measured. The 8  $\mu$ l cell had a similar design (Figure 22 b). It had a 0.75 mm ID x 7 mm channel within the cell body before the 1 mm ID x 10 mm optical cell. For microbore use, this channel was reduced in volume from 7.2  $\mu$ l to 0.22  $\mu$ l by inserting a 0.75 mm OD x 0.20 mm ID tube. The detector cell used depended on the sensitivity and resolution required for a particular analysis. Minimization of both the column-to-detector connection volume and the volume of the optical path was required to maintain high resolution for the low volume, early eluting microbore peaks. The larger volume of later eluting peaks made the choice between these two cells

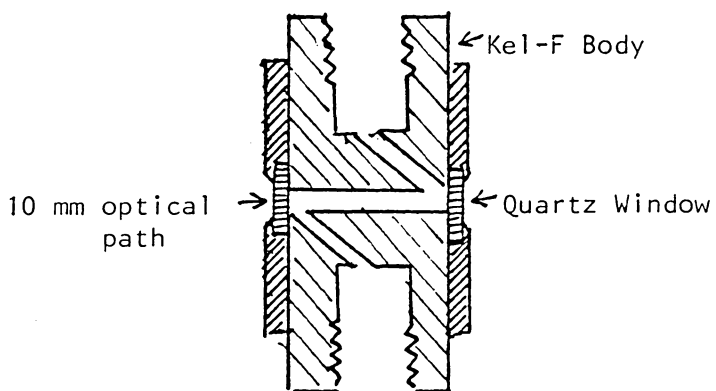


1/16"

Figure 21. Special column end-fitting for direct column-to-detector cell connection.



0.5  $\mu$ l cell



8.0  $\mu$ l cell

Figure 22. The 0.5 and 8.0  $\mu$ l UV detector cells.

less critical. Sensitivity was naturally greater for the longer pathlength cell (Beer-Lambert law).

#### 4.1.10 THERMAL ISOLATION

At elevated column temperatures, the detector cell must be thermally isolated from the column. The column terminated inside an oven with a ZDV union in order that the entire column be in a temperature controlled region. A 7 cm long, 1/16" OD x 0.010" ID tube (3.55  $\mu$ l volume) transferred the column effluent from the controlled zone to the detector cell. A copper heat sink was attached to this transfer line to isolate the the detector cell from high column temperatures. For intermittent temperature programmed operation, a 190 g uncooled copper block absorbed sufficient heat for stable detector operation. However, at steady high temperatures, active cooling of this block was necessary. This was provided by flowing cold water through a hole drilled through the block.

The cross-sectional area of the stainless steel in the transfer line was reduced by 92% by switching from 1/16" (0.062") OD tubing to 0.020" OD capillary tubing of the same 0.010" ID. This eliminated the need for a thermal sink at temperatures up to 75° C. At higher temperatures, the cooled cop-

per heat sink had to be bolted to this tube as well.

#### 4.1.11 BACK PRESSURE REGULATOR

Liquids have higher boiling points at higher pressures, and typical inlet pressures in LC systems (> 400 psi) are sufficient to keep all common LC solvents liquid at high temperatures (i.e. 150°C). However, the outlet of the column is at atmospheric pressure and unless the outlet pressure is raised above the vapor pressure of the mobile phase, some combination of LC and GC near the end of the column will result. Vapor pressure vs temperature data (119) for methanol and water are shown in Figure 23.

One means of maintaining a detector cell pressure above atmospheric is to install a pressure relief valve on the detector outlet tube. An adjustable spring keeps this valve closed, but when the pressure from the detector cell exceeds the spring pressure, the valve temporarily opens, passing solvent until the pressure falls below the spring pressure. While this works well at conventional LC flow rates, its intermittent operation (open-and-close) causes severe pressure fluctuations at typical microbore flow rates, resulting in baseline disturbances (Figure 24). A better means to stabilize the detector cell

Figure 23

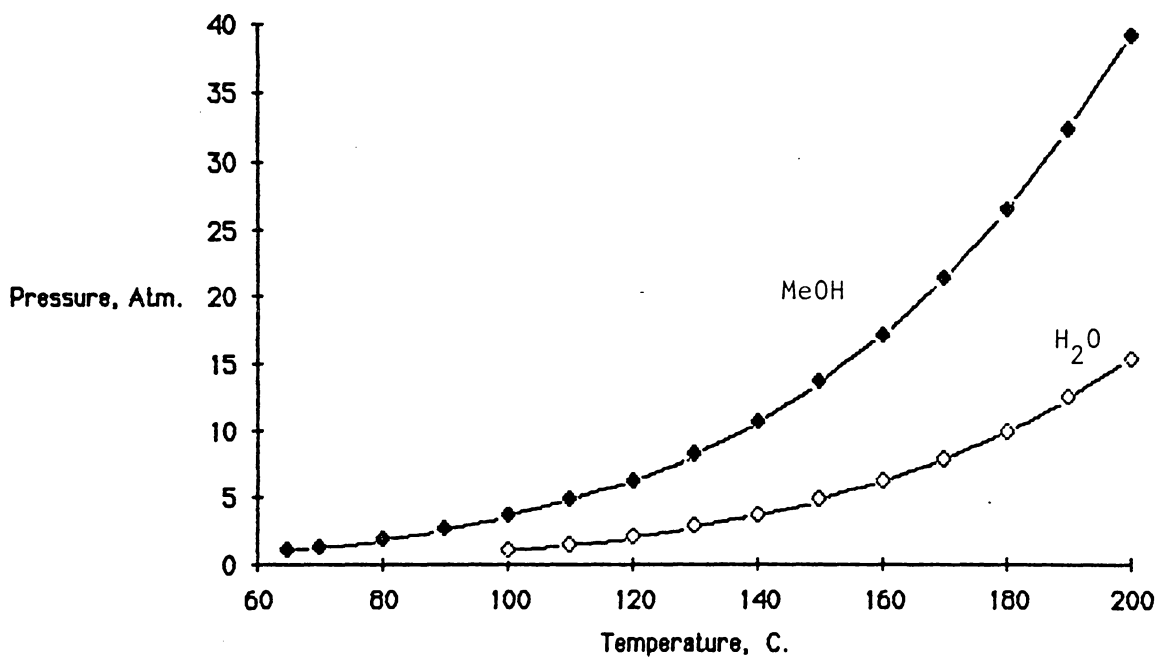


Figure 23. Vapor pressures versus temperatures for methanol and water (from ref. 119).

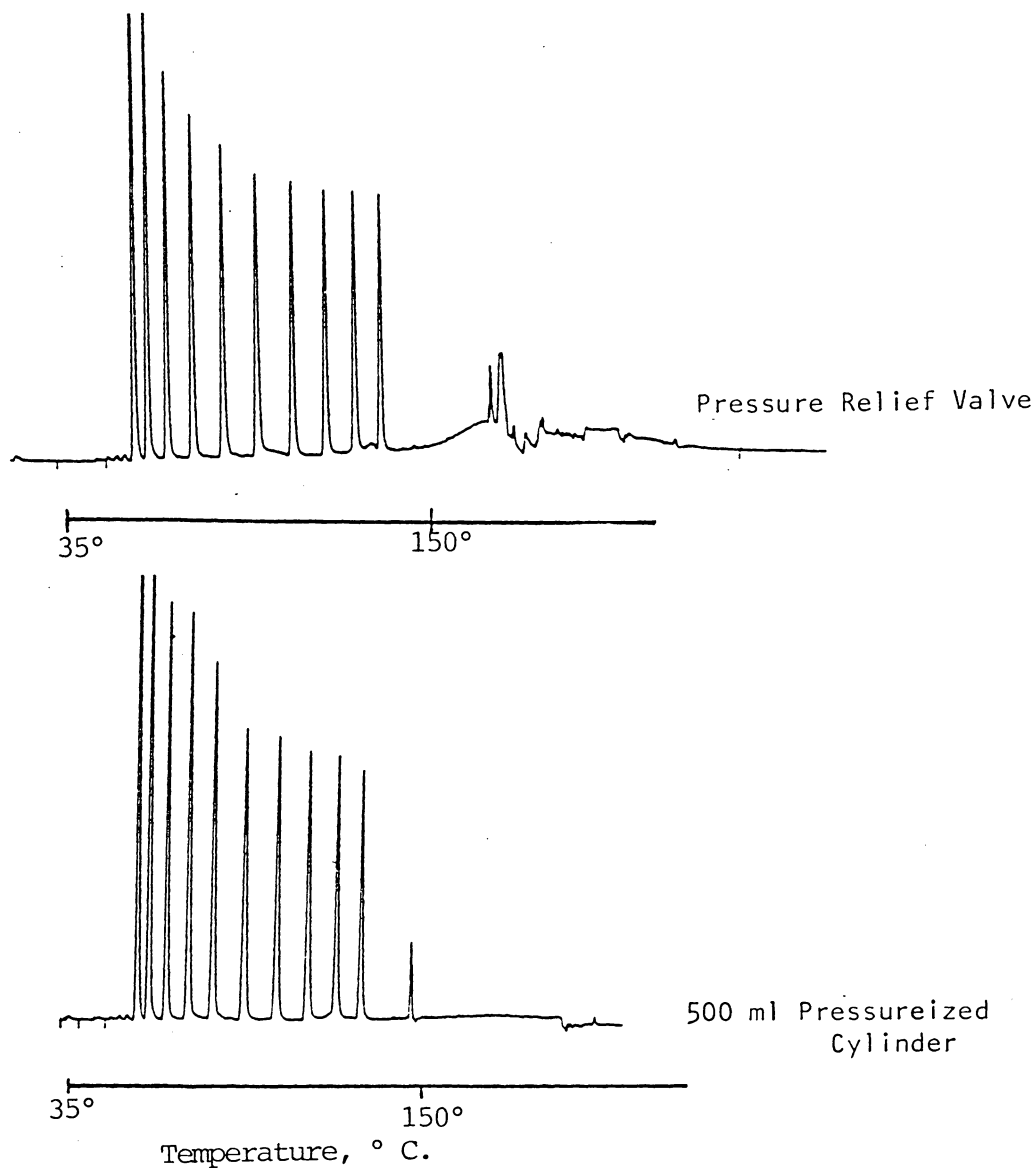


Figure 24. Temperature programmed chromatograms using two different types of back pressure regulators. Baseline disturbances after 150° C in the top chromatogram are due to pressure fluctuations inside the detector cell.

pressure for microbore columns was devised. A dual port, 500 ml sealed stainless steel cylinder was assembled with a pressure gauge which accepted the column effluent at one port and could be pressurized with CO<sub>2</sub> gas at the other (Figure 25). Since the typical column effluent over an entire day amounted to only 10% of this volume, the pressure to the cell was stable to better than 10% over this period. With solvents containing water, the CO<sub>2</sub> was in reality a pressure buffer, since when the pressure increased as the cylinder filled, more CO<sub>2</sub> dissolved in the mobile phase. This effect helped maintain a constant column outlet pressure.

## 4.2 COLUMN TEMPERATURE CONTROL

Three systems were used to control the temperature of the column. They were: 1) resistive electrical heating of the column itself; 2) a water bath circulation system; and 3) an air oven using a temperature regulated heat gun. Each method had its advantages and limitations which will be briefly discussed.

### 4.2.1 ELECTRICAL HEATING

The electrical heating scheme is shown in Figure 26. It

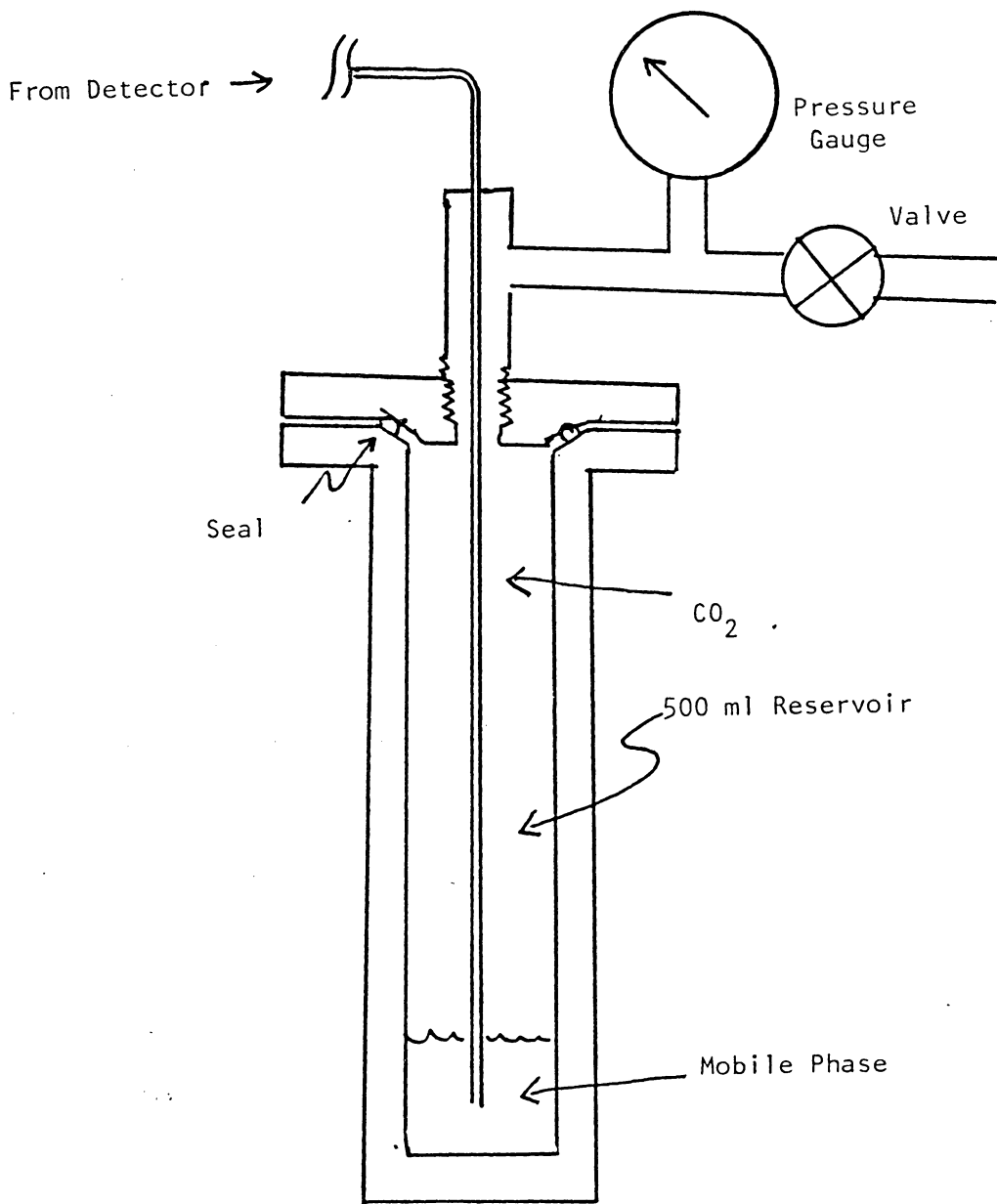


Figure 25. Stable microbore back pressure regulator.

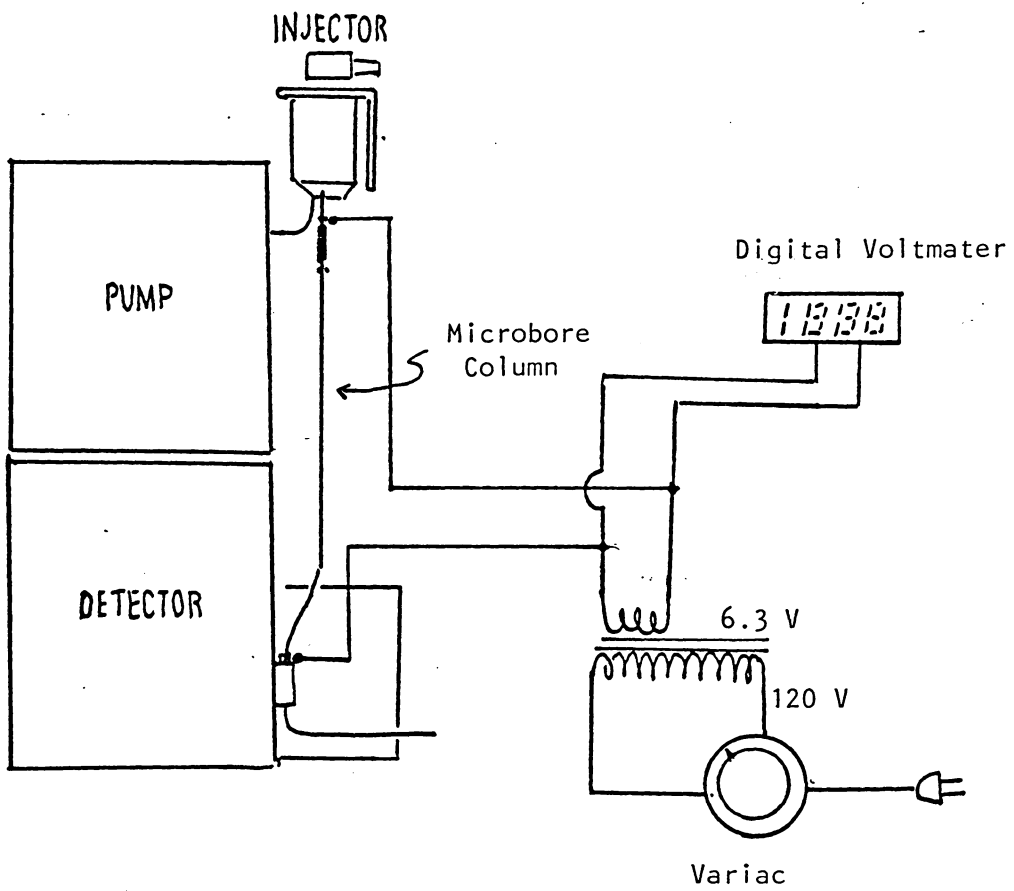


Figure 26. Electrical column heating system.

owed its inception to the fact that the detector cell was a non-conductive plastic, making the end of the column electrically insulated from the rest of the instrument. This made it possible to connect the outputs of a low voltage transformer directly across the metal column heat it by its own electrical resistance. A 0-140 VAC Powerstat type 116 variable transformer (Superior Electric Co., Bristol, CT.) provided primary voltage to a F-16X Filament transformer (Triad-Utrad, Huntington, IN.) with a 6.3 VAC secondary output. The resistance of the column was approximately  $0.5 \Omega$ . This was very close to the dynamic (AC) resistance of the transformer, meaning that both the column and the transformer heated during programming. Imposing 3 volts across the column caused its temperature to rise  $75^\circ$  above ambient. It was important to wrap the column with insulation since convective cooling by the surrounding air caused a nonlinearity in the temperature/power response curve. Surface temperature was measured by placing n-alkanes ( $C_{18}$ - $C_{36}$ ) on the column and noting at what input voltage the alkane melted. The calibration curve of voltage vs temperature is shown in Figure 27. Note the voltage squared axis (Watts =  $V^2/R$ ). Linear temperature programs were generated by selecting a program time and final temperature, relating that to voltage, and then calculating a Table of voltage vs time that gave a linear increase in power per unit time ending at the desired

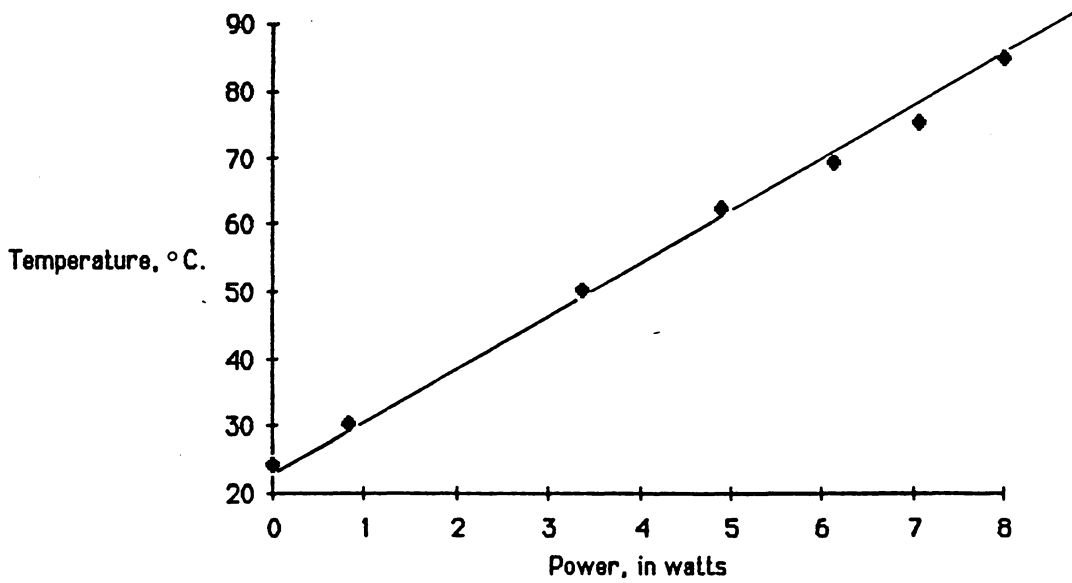


Figure 27. Power (watts) versus temperature for an electrically heated microbore column.

temperature. A digital voltmeter (Heathkit model SM-1210, Heathkit, USA) with  $\pm 0.001$  Vac resolution was attached across the column and voltages from the Table were dialed in manually with the Powerstat at the proper times using a stopwatch. No automation was attempted.

The advantages of this system were that it was quiet and simple. The disadvantages was that the actual temperature of the column bed was difficult to measure and depended both on the flow rate and the position along the column. Based on theoretical considerations, the mobile phase picks up an equal increment of energy from every incremental portion of the column from the inlet to the outlet. Therefore, the temperature of the mobile phase was a linear function of the distance down the column. If there had to be a temperature gradient on the column, it would be better to have the column inlet hotter than the outlet, thereby encouraging the movement of strongly retained components at the inlet of the column. However, in the current situation, these species remain in the coolest portion of the column and do not benefit from temperature programming. Schemes have been developed (30) whereby unequally spaced multiple contacts are made to a column heater to offset this effect (Figure 28), but the extremely low electrical resistance of short sections of microbore tubing would be

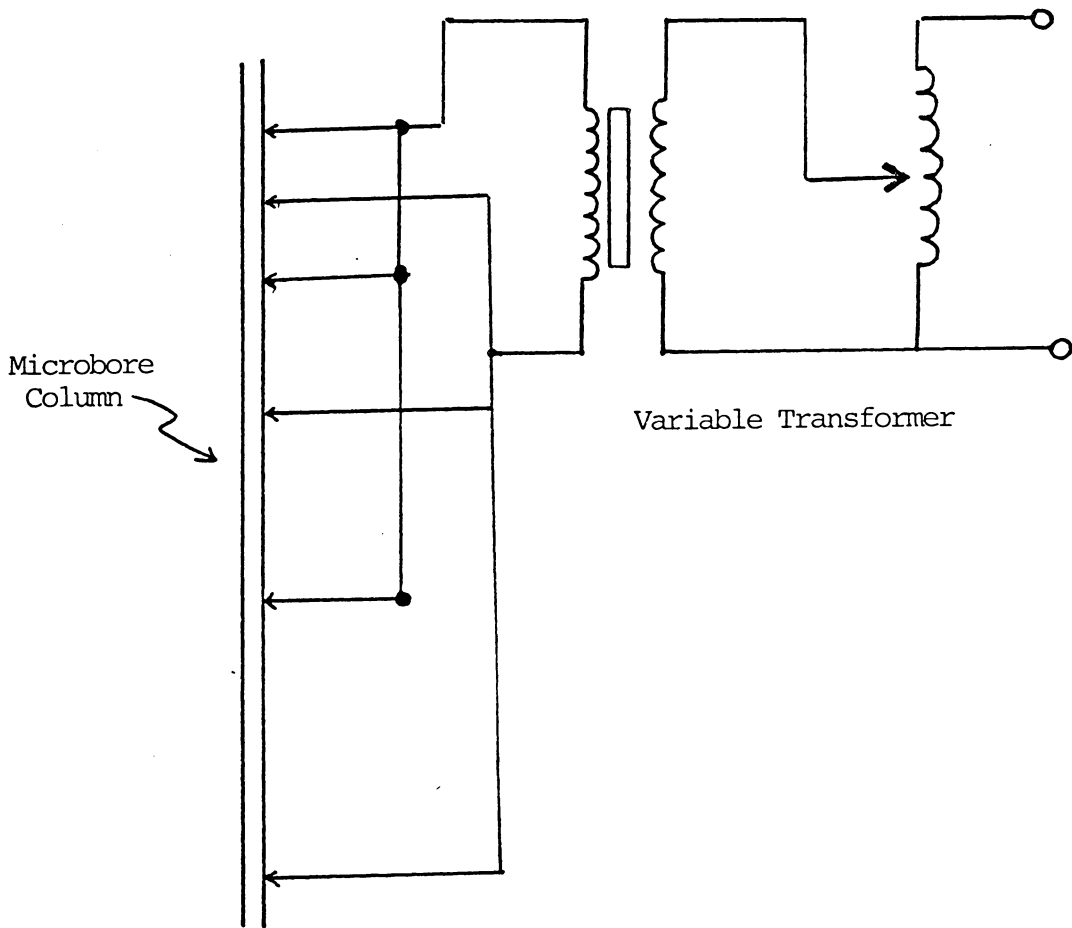


Figure 28. Multiple electrical contact system for offsetting longitudinal temperature gradients with electrical heating (after 30).

insufficient to couple significant power from the transformer to heat the column. An outer wrapping of thin nichrome wire could in this case replace the column as the heating element, but the actual column temperature would still be extremely difficult to measure or calculate. A more easily characterized temperature control system was sought.

#### 4.2.2 WATER BATH CIRCULATION

A Neslab RTE-5B refrigerated circulating bath (Neslab, Portsmouth, NH) was used to provide a temperature controlled liquid environment to surround a microbore column contained in a water jacket (Figure 29). This jacket was constructed from a 10 mm OD x 34 cm long glass tube with two 1/4" OD x 3 cm long side arms, 2 cm from each end through which the temperature controlled liquid would enter and exit. Both ends of the 10 mm tube were plugged with #2 rubber stoppers pierced with 1/16" OD x 0.010" ID column inlet and outlet tubes 12 cm long. The water tight fit these tubes made through the stoppers sealed the system, but once ferrules were attached to these tubes, they could not be removed from the stoppers. They were therefore cut long enough to permit the assembly and disassembly of the column within the water jacket, but short enough not to seriously degrade the resolution of the column. A total immersion -20°

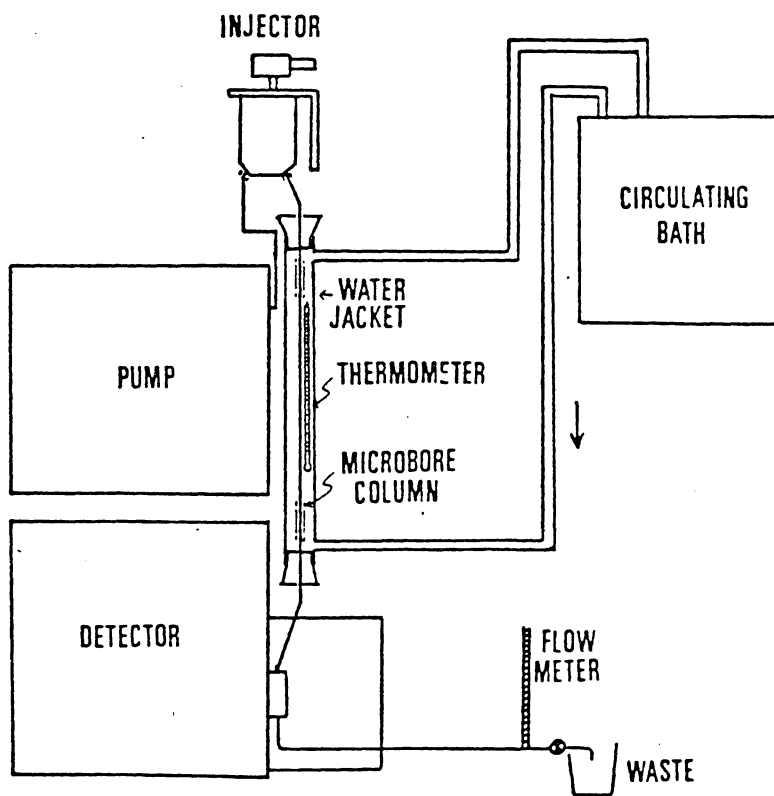


Figure 29. Circulating water microbore column temperature control system.

to 150° C thermometer (Fisher Scientific, Fair Lawn, NJ) was inserted through the top stopper. Swagelok fittings with rubber o-rings were used to attach the glass side arms to 1/4" polyethylene tubing. Stainless steel tubing was too stiff to attach to the glass side arms without breaking them off. Thin brass sleeves were inserted into the ends of the polyethylene tubing (Figure 30) since without them plastic tubing tends to relax away from ferrules at high temperatures and leak. For subambient operation, the entire liquid circuit was wrapped in fiberglass tape to cut down on condensation.

This system has several advantages. It provided extremely stable temperature control ( $\pm 0.1^\circ \text{C}$ ). The higher density of liquids compared to gases makes the rate of heat transfer using liquids faster than that obtained using gases (i.e. air circulating ovens), meaning that the temperature of the mobile phase in the column was more rapidly raised to the temperature of the control bath than it would have been in an oven. Liquid circulation helped keep the entire column at the same temperature. With the built-in refrigerator, subambient operation to  $-20^\circ \text{C}$  was possible, and with MeOH/Acetone/Dry Ice,  $-60^\circ \text{C}$  was obtained. It was the best system to evaluate the performance of a microbore column at fixed temperatures.

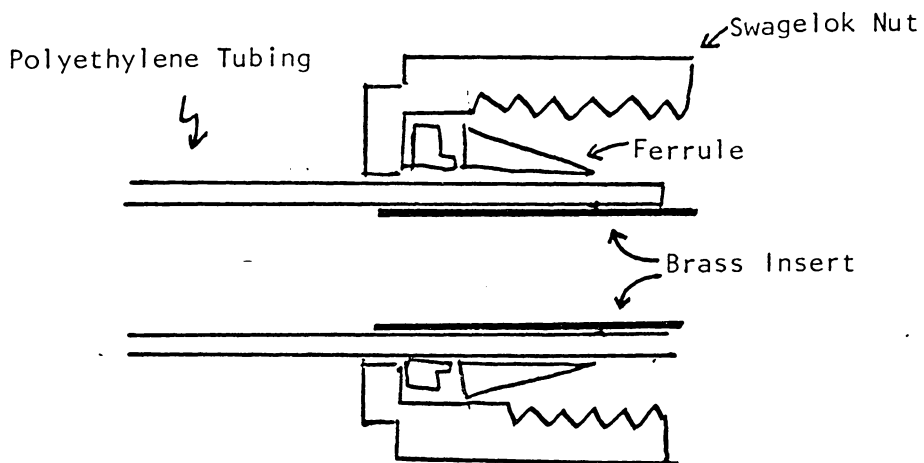


Figure 30. Brass insert allowing polyethylene tubing to be used with swagelock fittings leak free at 100 ° C.

Its disadvantage was that the maximum program rate for the bath was only 2.5° C/min, due to the volume of the bath, the mass of stainless steel in its construction and the limited power of the heater (800 W). The bath was after all designed to provide stable temperatures. At the upper temperature limit of 105° C, the odor of antifreeze becomes overpowering. Higher temperatures were prohibited by the styrofoam used as insulation.

With these considerations in mind, a liquid circulation temperature control system could undoubtedly be assembled with some manageable circulating fluid and with sufficient response time to be of practical use in temperature programmed LC. However, because of the limitations of the current system, it was used exclusively to examine the effect of fixed temperature on retention and to relate solvent strength from temperature to solvent strength from mobile phase composition.

#### 4.2.3 HOT AIR BLOWER SYSTEM

With response time considerations in mind, a heated air column temperature control system was assembled (Figure 31) using a heat gun (model HG-751, 20 amps, Master Appliance Co., Racine WI.), a conduit to contain the air around the column and a feed-

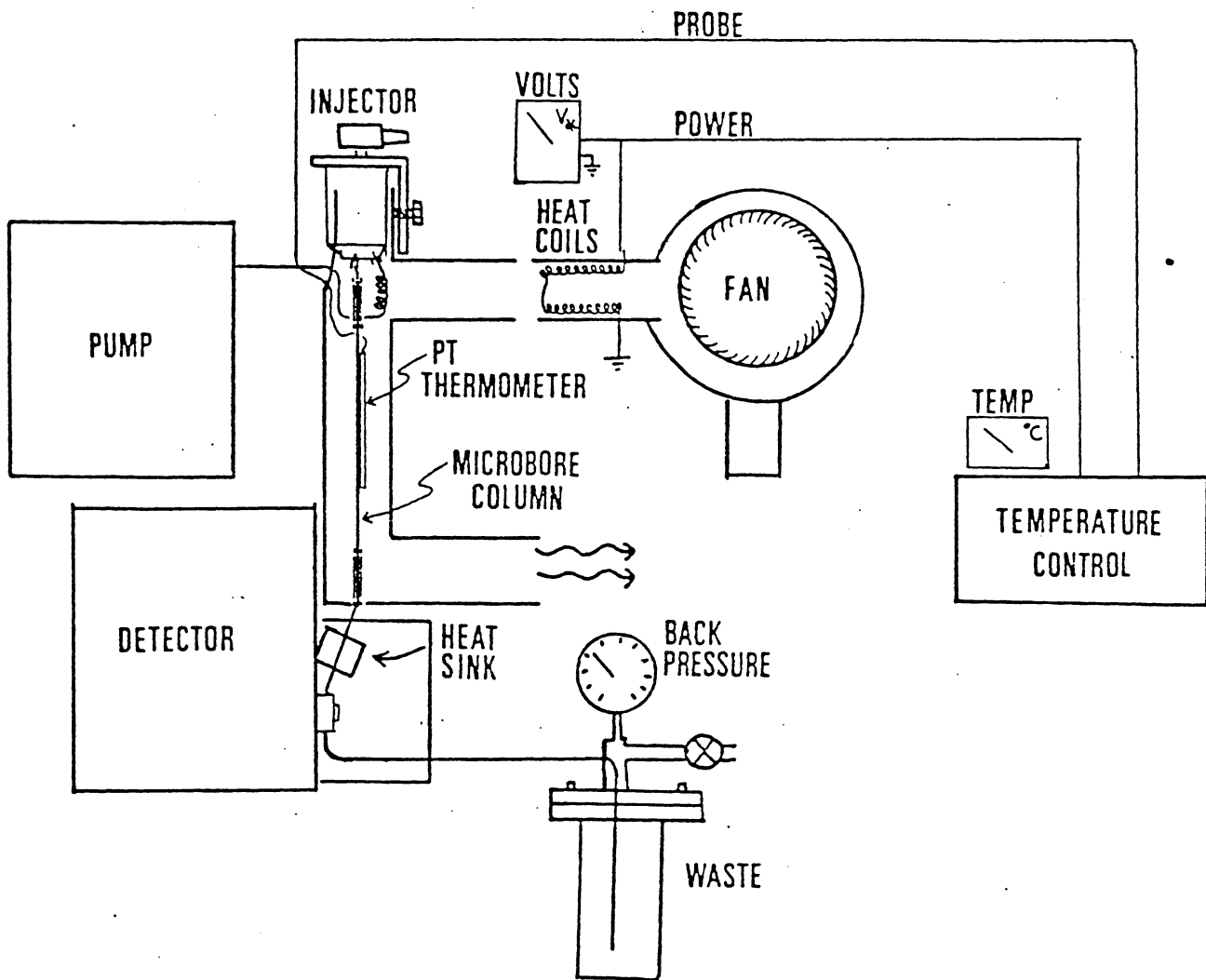


Figure 31. Heated air column temperature control system.

back controlled automatic temperature controller (Bendix Corp., Lewisburg, W.Va.). The conduit was 36 mm ID corresponding to both the hot air nozzle of the heat gun and the diameter of the injector. A 19 cm transfer tube separated the heat gun from the head of the column, avoiding a concentrated hot spot were the column placed too close to the heat gun. A right angle bend of the conduit allowed the injector to be placed inside the top of a 33 cm long oven with the column and a platinum resistance thermometer. This thermometer delivered the temperature signal to the electronics in the automatic temperature controller which then directs the appropriate power to the coils of the heat gun. Another right angle bend at the bottom of the column directed the hot air away from the detector and out into the lab. A 1 ml volume coil preheated the mobile phase prior to entering the injector. Sample and waste were directed to the injector ports by 3 cm transfer tubes inserted through a slot on the side of the conduit. A voltmeter and thermocouple temperature gage indicated the power to the coils of the heat gun and the temperature environment of the column respectively.

The advantage of this system was that it allowed unattended, fully automated temperature programmed operation from ambient to 200° C. at rates from 0.1° C/min to 50° C/min. It provided

rapid heating rates and no handling problems were encountered with the heating medium. A disadvantage was that the poor heat transfer properties of gases compared to liquids resulted in the entering mobile phase being slightly cooler than the column at any given time during the program. Even with the loop preheating the mobile phase, the bulk of stainless steel in the injector with its small surface area exposed to the hot air could not respond as quickly as the thin microbore column. While this effect was slight, it was sufficient to hide any anticipated improvements in resolution at elevated temperatures (see section 3.2.5, p. 58, COLUMN EFFICIENCY VS TEMPERATURE). The system also tended to be noisy.

### 4.3 REAGENTS AND MATERIALS

#### 4.3.1 HOMOLOGOUS SERIES

A collection of homologous series was assembled from a variety of sources. Table VI lists the six series that were used, the members of those series and their source. Members of three series were synthesized. Acetates and benzoates were prepared by reaction of the acid chlorides with the alcohols, and were heated to expel the HCl produced during the reaction. Pyridine was not used as a scavenger for HCl in order to eliminate a purification step. Pyridine would produce an extra peak in the chromatograms. Excess alcohol was used in the reaction, which in all cases boiled at a lower temperature than the product and could be removed by distillation. Analysis of the product by GC was used to monitor the reaction mixture and indicate completion. While good product purity (> 90%) of acetates were obtained for the short chain alcohols, purity of the longer chain acetates was less (the C<sub>8</sub> alcohol only gave a 50% yield of the acetate, the remainder was alcohol). Since the alcohol gives no LC signal, alcohol in the product did not interfere with the LC study. Benzoates analysed by LC showed only benzoic acid and the desired benzoate, and during the homologous series study the benzoic acid peak was ignored. Parabens were

Table VI

## Homologous Series Used

Alkyl Benzenes <sup>1</sup>	Benzoates <sup>4</sup>	Phenones <sup>3</sup>
Toluene	Methyl Benzoate	Acetophenone
Ethyl Benzene	Ethyl Benzoate	Propiophenone
n-Propyl Benzene	Propyl Benzoate	Butyrophenone
n-Butyl Benzene	Butyl Benzoate	Valerophenone
Phenyl Pentane <sup>2</sup>	Pentyl Benzoate	Hexanophenone
Phenyl Hexane	Hexyl Benzoate	Octanophenone
Phenyl Heptane <sup>2</sup>	Heptyl Benzoate	Decanophenone
Phenyl Octane	Octyl Benzoate	Laurophenone
Phenyl Nonane <sup>2</sup>		
Phenyl Decane		
Parabens <sup>1</sup>	Acetates <sup>6</sup>	Ketones <sup>2</sup>
Methyl Paraben	Methyl Acetate	Acetone
Ethyl Paraben	Ethyl Acetate	MEK
Propyl Paraben	Propyl Acetate	2-Pentanone
Butyl Paraben	Butyl Acetate	2-Hexanone
Pentyl Paraben <sup>5</sup>	Pentyl Acetate	2-Heptanone
Hexyl Paraben <sup>5</sup>	Hexyl Acetate	2-Octanone
Heptyl Paraben	Heptyl Acetate	2-Nonanone
Octyl Paraben <sup>5</sup>	Octyl Acetate	2-Decanone
		2-Undecanone

## Sources:

- 1) Polyscience Corp, Niles, Il.
- 2) Aldrich Chemical Co., Milwaukee, Wi.
- 3) Pierce Chemical Co., Rockford, Il.

## Synthesized:

- 4)  $\text{ROH} + \phi\text{COCl} \rightarrow \phi\text{COOR} + \text{HCl}$
- 5)  $\text{ROH}(\text{excess}) + \text{HO}\phi\text{COOCH}_3 \rightarrow \text{HO}\phi\text{COOR} + \text{CH}_3\text{OH}$
- 6)  $\text{ROH} + \text{CH}_3\text{COCl} \rightarrow \text{CH}_3\text{COOR} + \text{HCl}$

Synthetic starting materials from (2).

prepared through transesterification using  $\text{BF}_3$  as a catalyst. Several UV active products were formed, so the desired paraben was purified by preparative LC.

Ultraviolet absorbance detection was used throughout this study and limited the choice of base group functionality to those with good UV chromophores. While the aromatic group is an excellent chromophore, its bulk interferes with the linearity of  $\Delta G$  contributions by each additional methylene unit via a pendant group effect. Acetates and ketones have smaller functional groups but unfortunately also exhibit lower molar absorptivity ( $\epsilon$ ). Maximum absorption wavelengths ( $\lambda_{\text{max}}$ ),  $\epsilon$  values and sample concentrations are listed in Table VII. Samples were prepared with the goal of providing a 0.1 absorbance for the first member of the homologous series. Acetates and ketones only gave 0.08 and 0.04 absorbance for the maximum sample concentration possible without column overload (20  $\mu\text{g}/\text{ml}.$ ) due to their low  $\epsilon$  values.

Table VII

UV absorbance and sample concentrations  
for homologous series samples  
( $\lambda_{\max}$  and  $\epsilon$  from (120)).

	$\lambda_{\max}$	$\epsilon$	Concentration (mg/ml)
Alkyl Benzenes	208	7900	0.1
Benzoates	225	8100	0.1
Phenones	242	12600	0.1
Parabens	254	9000	0.1
Acetates	207	38	20.0
Ketones	277	17	20.0

#### 4.3.2 LC SOLVENTS

HPLC grade methanol, acetonitrile and water were obtained from Fisher (Fair Lawn, NJ), Ashland Chemical Co. (Columbus, OH), MC/B (Cincinnati, OH) Burdick and Jackson (Muskegon, WI) and J. T. Baker (Phillipsburg, NJ) and were used as received. Solvent mixtures were degased with helium before use and analysed by GC.

#### 4.3.3 SORBENTS

LiChrosorb® RP-18 (Merck, Darmstadt, Ger.), an irregular particle silica derivatized with triethoxyoctadecyl silane was used throughout this study. Particle diameters of 5, 7 and 10  $\mu\text{m}$  were used.

#### 4.4 PROCEDURES

##### 4.4.1 COLUMN POLISHING

Internal surface irregularities in commercial 1/16" OD SST result from the way the tubing is manufactured. This tubing is typically drawn from 1.500" OD x 0.250" ID stock which was successively reduced in diameter and wall thickness until the

proper dimensions were achieved (121). During some of the draws, both the inside and the outside of the tube were squeezed using a tethered plug and a die. The final draw with commercial off-the-shelf 1/16" OD x 1 mm ID tubing used only an outside die, making the inside surface wrinkled and irregular. Figure 32 shows the inside of this tubing under low and high magnification. The deviations in the surface height amount to as much as 20  $\mu\text{m}$ . This corresponded to an RMS value of 400. "RMS (Root Mean Squared) is a means of describing the average height of random peaks and valleys of the surface finish. A surface roughness of 20 RMS would be the equivalent of 0.5 microns" (122).

Considerable efforts were required to remove these irregularities. Conventional techniques, such as drilling, boring (123), sandblasting and slurry polishing (124) work well with tubes having larger ID's but could not be adapted for use on 1 mm ID tubing.

In 1981, Kok et. al. (61) published a description of a polishing procedure where an abrasive coated string was drawn back and forth through the tubing to scrape off irregularities. Ishii (125) and Poppe (126) have also reported similar procedures. Apffel (127) described using string smaller than 1 mm

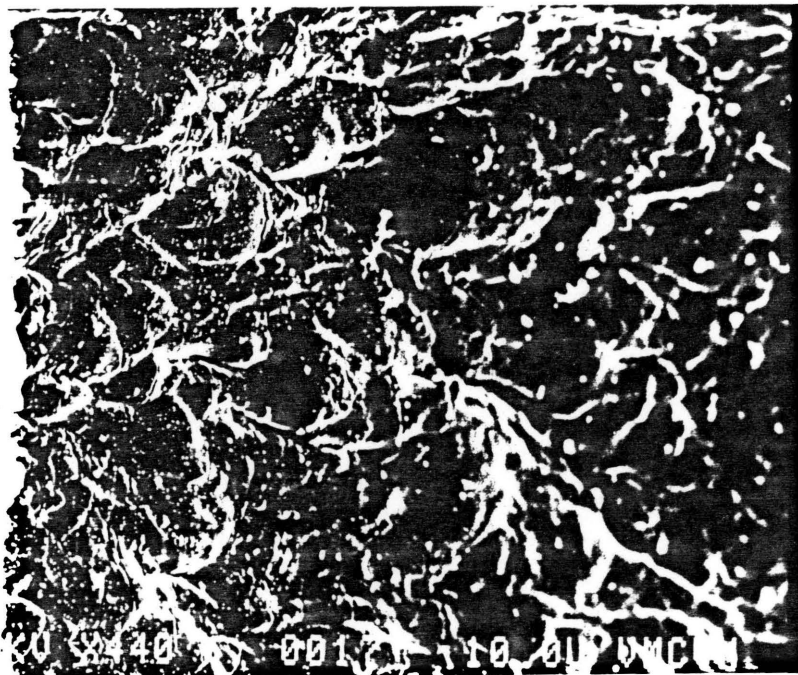
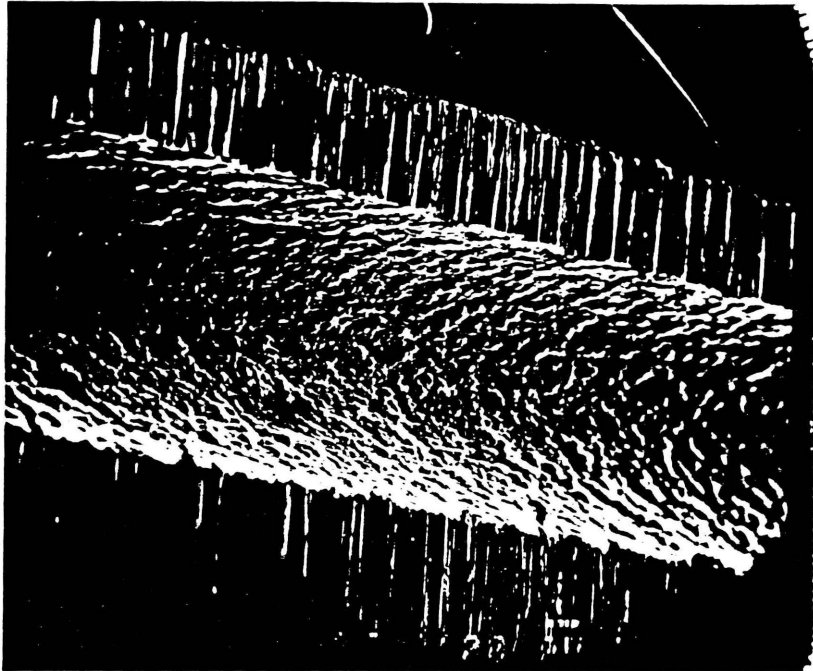


Figure 32. Inside surface of commercial 1/16" ID stainless steel tubing.

in diameter with knots tied in it. It should be noted that a great deal of pressure must be exerted at right angles to the motion of the string in order to remove metal from the walls of the tubing.

The procedure first used in our lab was to thread a tube with a 2 meter length of knotted string, tie it securely between two stable objects in the lab, coat the string with abrasive and pull the tube back and forth along the string for several minutes. Many problems arose using this method. It was difficult to produce a smooth motion with the tube since it would snag on the knots; the tube quickly became too slippery to hold, and in trying to hold it, the tube became bent and kinked; the knots would quickly wear down and no longer press tightly against the tube walls; and since even with the knots tied in it, the string was still only a single strand, it kept breaking.

An alternate method of polishing was developed. First, two 4" jaw vices were used to hold an extended section of the column ends. To prevent the vices from crushing the tubing, thick walled rubber tubing surrounded the 1/16" tubing so that when the vices were closed, the pressure was evenly distributed through a soft rubber buffer. This provided an extremely tight, non-slip grip on the tubes. Second, the single thread

was replaced with between 4 and 7 lengths of strong thread (such as button and carpet thread available from various sources) that were pulled through the tubing by an initial loop of thread which was drawn through the column using a vacuum pump. This loop was made from a length of thread which was 3.5 times longer than the tube to be polished. One end was spliced back through the center thread, making a loop without a knot in it capable of being drawn through the tubing. This loop was strong enough to tug a tight bundle of threads through the tube. This bundle was made by taking long lengths of thread (2-3 meters), inserting and pulling them halfway through the loop to even up the ends, providing in two strands through the column for each thread used. (Three 3 meter strands would result in six 1.5 meter polishing threads inside the column.) To get an odd number of strands, as was occasionally needed to achieve a tight fit, half the usual length was cut and its end was barely inserted into the loop, which held it in place when the loop was pulled back through the column.

This thread bundle was not only strong but provided a very tight fit inside the tube. Once abrasive was applied to the threads, a very tight fit resulted requiring up to 50 lbs of pull to move it. The ends of the threads were knotted together to manage them, and the threads were pulled back and forth a few

times before applying the abrasive in order to break them in.

The threads were coated with an abrasive polishing compound. Two brands of polishing compound were used. Both were a suspension of small particle (0.5-10  $\mu\text{m}$ ) alumina in a silicone oil base. They were sold commercially to remove oxidized paint from automotive finishes. DuPont white polishing compound (E.I. DuPont de Nemours Co. Inc., Wilmington, DE.) seemed to dry out faster than the Ditzler DRX-25 polishing compound (PPG Industries, Detroit, MI.) but both provided a good interior surface.

If hand polishing was performed, the threads were looped around the hands and the string were tugged back and forth through the column. As this abrasive coated thread was sufficient to remove stainless steel metal from the column, it was easily capable of removing several layers of skin from the hands of the polisher. Any object (wrench, screwdriver, pen, ruler, etc.) can be made into a handle to which the threads can be tied to protect the skin of the polisher. Approximately 10 minutes of hard labor were required per column to get a smooth interior surface. Towards the end of the polishing process, the threads mat together into a black, perfectly cylindrical rod whose force against the walls at any point was evenly dis-

tributed. For best results two changes of thread were used with abrasive. The final set of threads consisted of one strong thread (doubled over) and one piece of an absorbent cotton string. These were not coated with abrasive but were used to remove residual polishing compound and smooth off the rough edges. Figure 33 shows the column after the polishing process. Compare this to Figure 32.

As was mentioned, considerable effort was needed to adequately polish the column. The state of fatigue of the polisher made the smoothness of the final surface difficult to estimate without cutting open and destroying the column, and so to improve the reproducibility of the final inside surface, a machine was constructed which automatically pulled the threads through the tubing (Figure 34). Two 2-way solenoid actuated air valves connected in ying-yang configuration provide pressure and vent to both sides of a 24" throw double action pneumatic piston (model 120 DRE 24", Advance Automation, Chicago, IL.). Pulleys and cables direct the motion to clamps which grip the polishing threads running through the tubing so that the piston only saw forces acting on it parallel to its motion. A piston power multiple of 1.23 meant that for an inlet pressure of 50 psi, the piston delivered 61.5 lbs of pulling force. End-of-travel electrical switches reversed the state of the

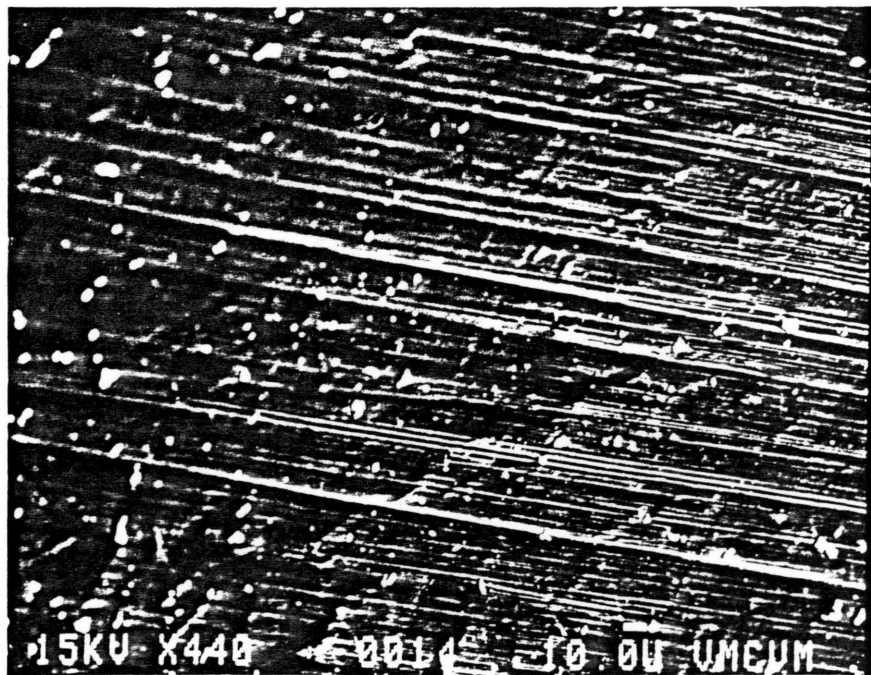
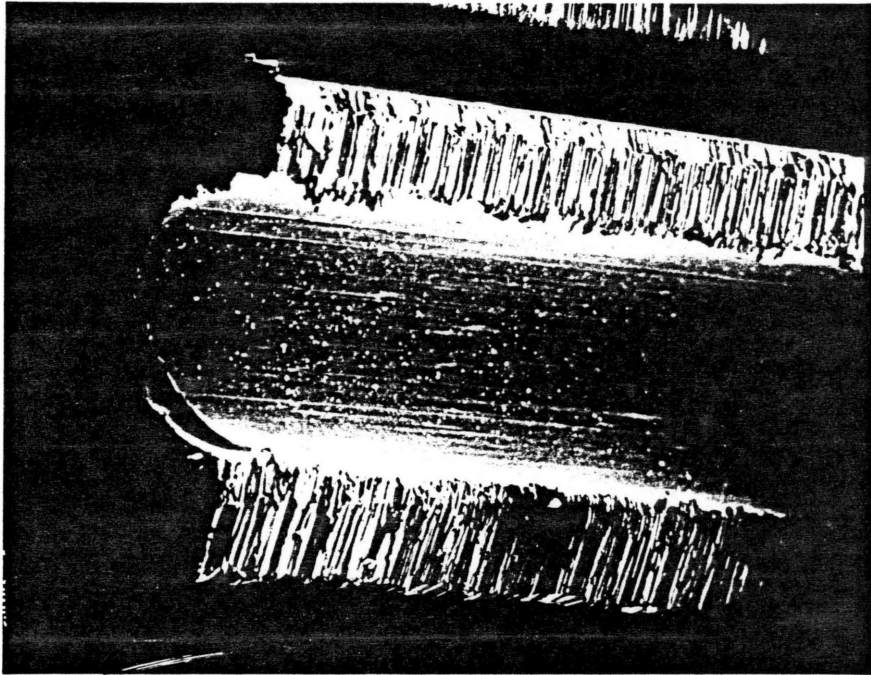


Figure 33. Inside tubing finish after polishing.

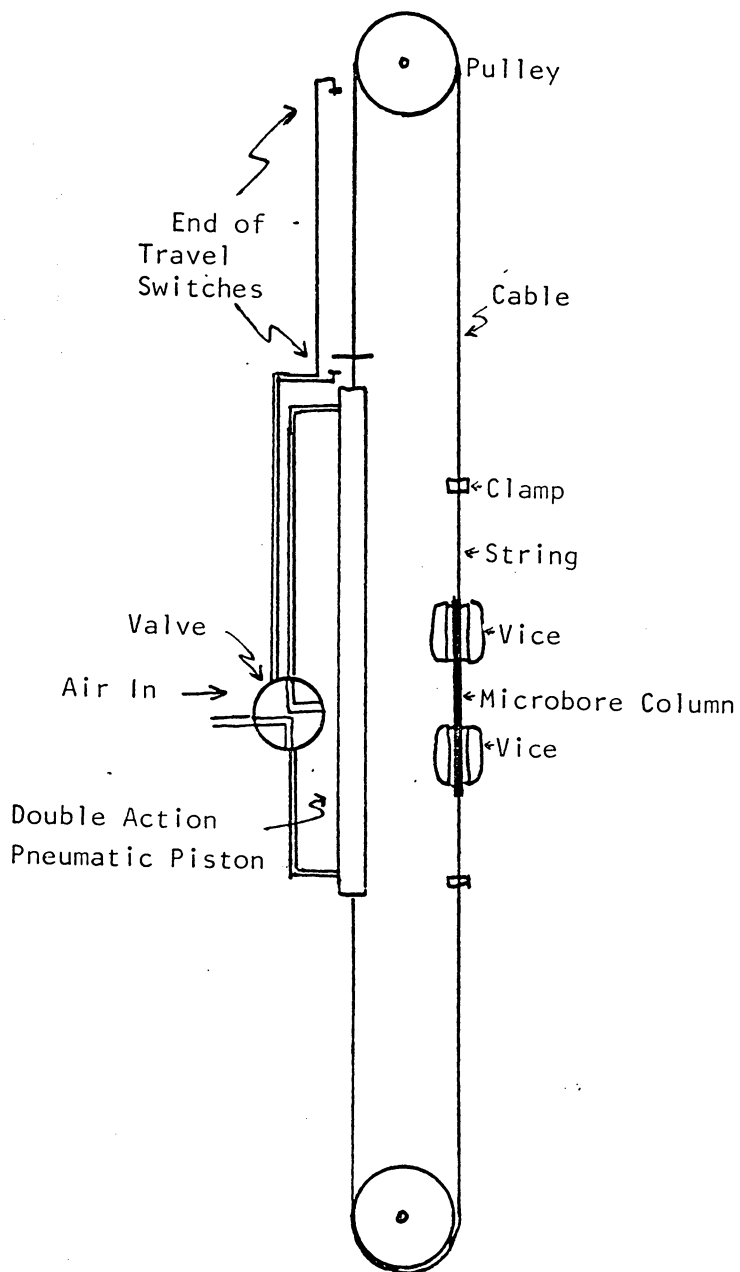


Figure 34. Automatic column polisher.

air directing valves which automatically reversed the direction of the polisher at the end of each stroke. The polishing speed was set by the incoming air pressure and the resistance the thread felt within the column, usually running around 2-4 seconds per stroke. Since a single column polishing consumed 1/4 of a tank of bottled air, an air compressor, a ballast tank and a pressure regulator replaced the bottled air following the initial automated polisher development.

#### 4.4.2 COLUMN PACKING

Microbore columns were packed using a slurry method (128-131) in a manner identical to conventional bore column packing procedures. Figure 35 shows the apparatus used to pack microbore columns. An empty 1/4" OD standard LC column with the frits removed and the flow passages drilled out to 1/16" (Figure 35, inset a) was used as the slurry reservoir. Columns with stainless steel ferrules were preassembled with their final fittings in order to set the ferrules in their proper positions before connecting the columns to the slurry reservoir.

For 25 cm long microbore columns, 0.18 g of RP-18 sorbent was required. This material was first slightly wetted with

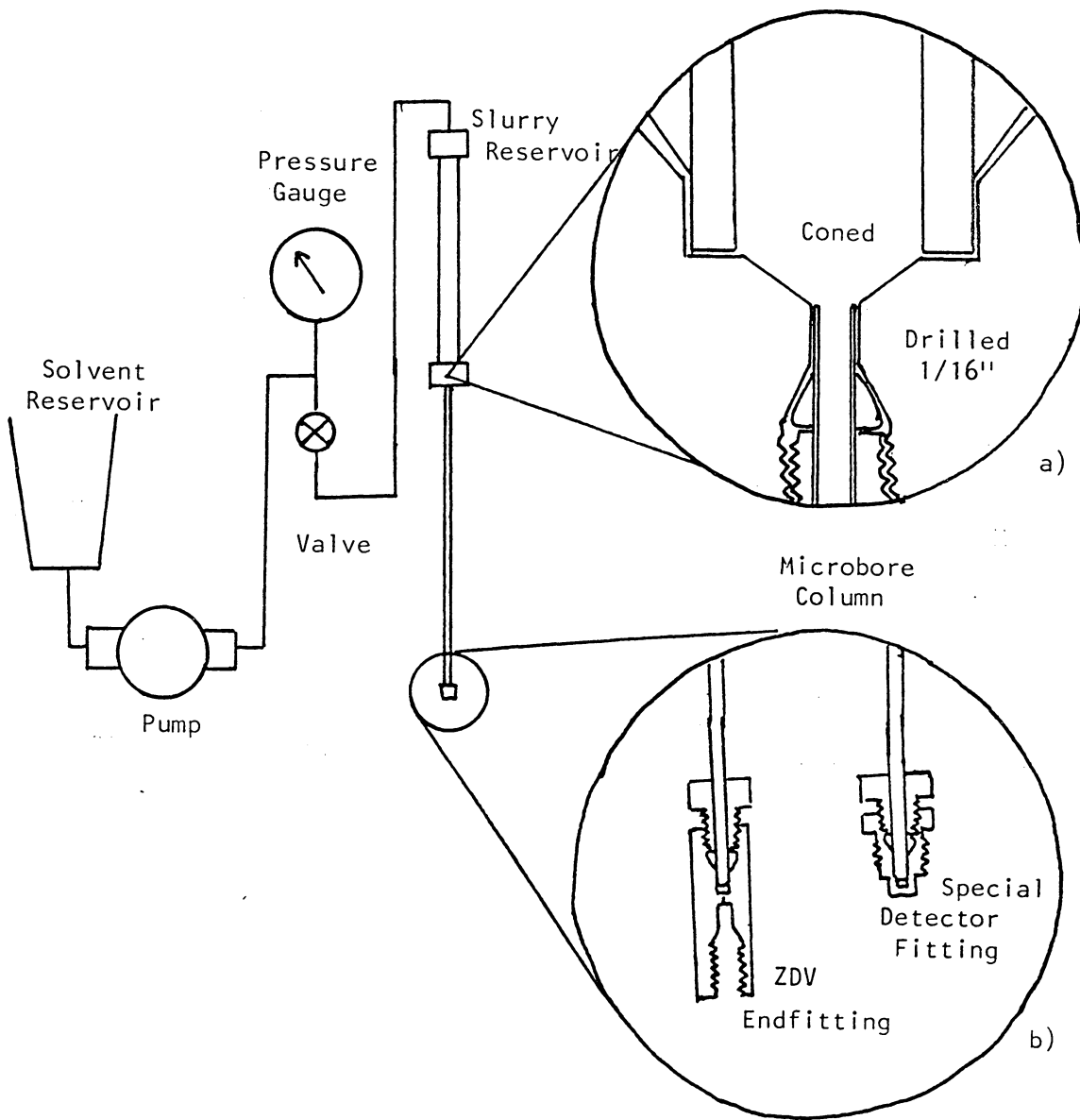


Figure 35. Column packing instrumentation.

Inserts: a) Bottom of slurry reservoir showing internal coned surface and 1/16" bored out passages; b) two types of microbore column end fittings.

methanol to solvate any surface water to permit wetting by 4 ml of  $\text{CCl}_4$ . In a stoppered 10 ml sample vial, the mixture was agitated in an ultrasonic bath for 10 minutes. A syringe was used to transfer this slurry into both the column and the slurry reservoir (Fig 36) so that no air was left trapped anywhere in the system. Air would suddenly compress under the force of the high pressure packing pump and result in a sudden jolt during the packing process. Any sudden movements of the slurry solvent during column packing are to be avoided, since rapid accelerations may fracture the porous silica structure of the sorbent. A ZDV union or a special column endfitting (fig 35, inset b) which allowed direct column connection to the detector cell were used to terminate the column. A Kel-F® surrounded frit, the same as at the head of the column, was placed inside these fittings to contain the column packing.

A Haskel model DST-122 pneumatic amplifier pump was used to pump methanol to the top of the slurry reservoir at a pressure of 10,000 psi. Its piston volume of 6 ml made it possible to completely pack the microbore column in a single piston stroke. The pump did not need to refill while the 4 ml slurry was transferred from the reservoir to the column, resulting in a continuous, smooth column packing process without hesitations or interruptions which might result in a disturbance of the column

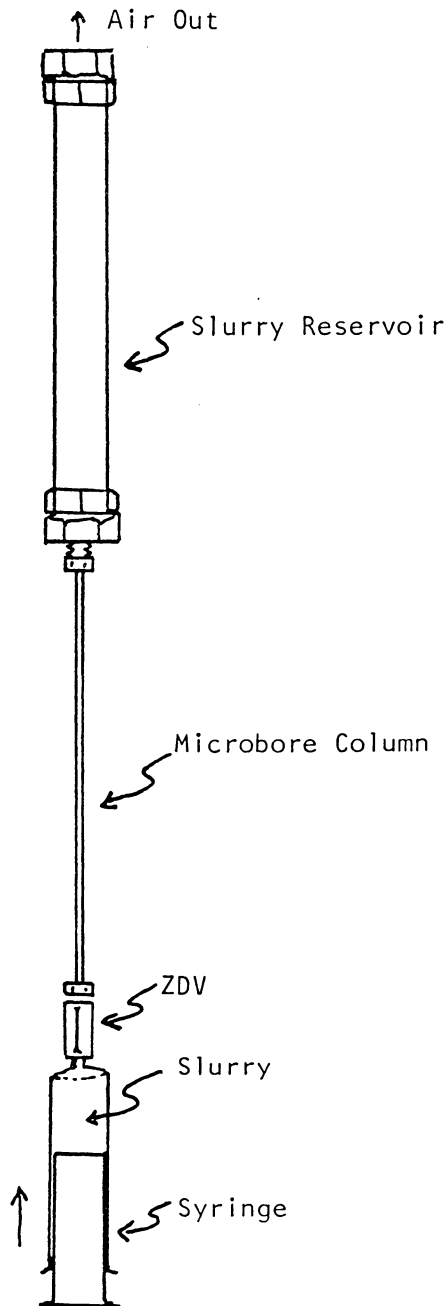


Figure 36. Means of loading the slurry into the column and reservoir excluding air.

bed (131). It was necessary to start the pump at the beginning of its delivery stroke to insure this smooth operation. The Haskel pump, initially with the flow valve closed pressurized the system with MeOH to 1000 psi. This valve was slowly opened to smoothly start slurry flow into the column. The initial solvent drip rate was then maintained by continuously increasing the pressure up to 10,000 psi over approximately 1 minute for 10  $\mu\text{m}$  particles and over a 2 minute period for 5  $\mu\text{m}$  particles. This caused the impact velocities of all the particles onto the bed to be the same regardless of the particles position within the column (constant flow mode). Once 4 ml of solvent has dripped from the column, a sharp refractive index change was observed in the collection graduated cylinder, indicating that no appreciable mixing of the incoming MeOH with the  $\text{CCl}_4$  slurry occurred during the displacement process. In the downward packing mode, the density difference between MeOH and  $\text{CCl}_4$  was responsible for this segregation. This gave a constant concentration of slurry during the packing process. These two solvents are miscible and the  $\text{CCl}_4$  was washed from the column with 25 ml of MeOH. The pressure was then slowly relieved from the column by bleeding off the driving air pressure to the Haskel pump. This was done immediately following a piston refill stroke to prevent the sudden loss of pressure if the piston were to attempt to refill during column depressuri-

zation. After the pressure gauge read 0 psi, 5 minutes elapsed before the column was removed from the slurry reservoir allowing any residual pressure to dissipate since even a small amount of flow during disconnection would disturb the bed at the head of the column. The flow valve was also closed to prevent MeOH syphoning.

For longer columns (50 cm or more) packed with small particles (3-5  $\mu\text{m}$ ) the gradual increase in pressure was not sufficient to insure constant particle impact velocity during the packing process, since in these cases only a fraction of the column was packed once the pressure reached 10,000 psi. While short columns may be packed individually and then concatenated to form an efficient column of any length desired (132), this adds to the complexity, time and cost needed to pack a long column. The Haskel model DST-122 pump was used at 15,000 psi without any noticeable gains in column efficiency. A Haskel model DSXHT-602 pump, capable of 60,000 psi was also used. While packing microbore columns, two separate slurry reservoirs made from 1/4" OD x 4.6 mm ID conventional LC columns ruptured somewhat spectacularly at 18,000 and 19,000 psi. They were replaced by a reservoir of the same volume but with thicker walls to withstand higher pressures. In two separate experiments, microbore columns were packed using programmed pres-

tures for constant flow up to 22,500 and 23,000 psi. In both cases, the flow at these pressures abruptly stopped and did not resume even when the retaining frit at the end of the column was removed. It was assumed that near 23,000 psi, the highly porous silica backbone of LiChrosorb® RP-18 collapses to form an impervious blockage within the column. It may have simply been good luck that allowed Scott and Kucera (1) to pack micro-bore columns at 25,000 psi.

Viewing the need for high packing pressure objectively, it was seen that this need was a result of the viscous drag of the slurry solvent in the lower portion of the column which had already been packed. This pressure drop serves no useful purpose, since the relative arrangement of the particles was fixed once each particle was blocked from movement by the particles surrounding it. A means of eliminating this useless pressure drop was to reduce the solvents viscosity by increasing its temperature.

A 50 cm, 5  $\mu$ m LiChrosorb® RP-18 column was packed using the slurry packing system, with the lower 25 cm of the column surrounded by a cylindrical temperature controlled oven (see section 4.2.3, p. 109, HOT AIR BLOWER SYSTEM). Temperature programming the lower portion of the column proceeded after the

pressure had been increased to 10,000 psi and the lower portion of the column had been packed. The temperature program was made from 25° C to 135° C at 20° C/min. This produced both a constant flow rate and greatly reduced the column packing time. Column performance (theoretical plate counts) for temperature programmed packed columns was quite high (fig 37).

#### 4.4.3 RETENTION VERSUS TEMPERATURE STUDY

The effect of temperature and mobile phase composition was measured for 52 compounds grouped as members of six different homologous series. Temperature control was provided using the fluid circulating constant temperature control system. The column was a preconditioned 25 cm x 1 mm ID microbore column packed with 10 µm LiChrosorb® RP-18 (E. Merck, Darmstadt, Ger.). Flow rates were 250 µl nominal and were measured in duplicate with the pipette side arm device both before and after the six different homologous series had been run at each temperature and mobile phase composition. Three different mobile phases were used; 90/10, 70/30 and 50/50 methanol/water, mixed by volume at 20° C. Mobile phases were degassed by helium sparging before use. Six different column temperatures were used; -20°, 0°, 25°, 50°, 75° and 100° C. They were set with the dial on the Neslab RTE-5B constant tem-

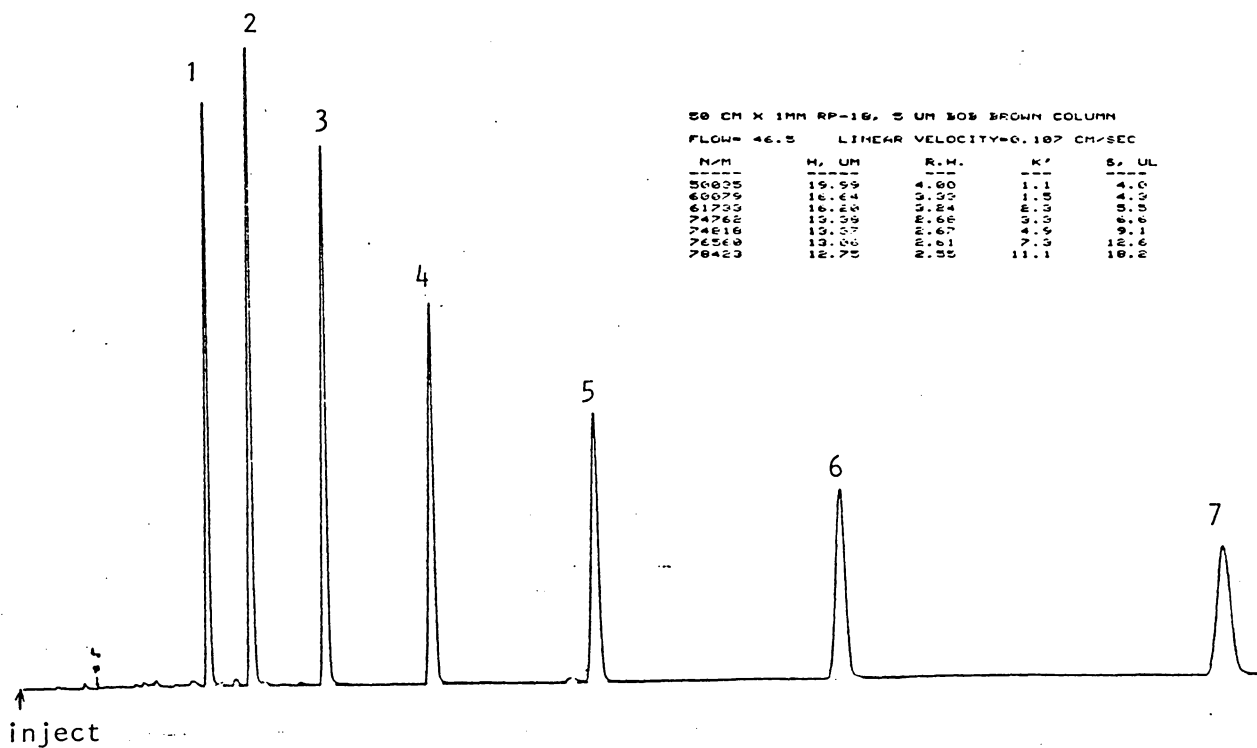


Figure 37. Chromatogram from a 50 cm, 5  $\mu$ m LiChrosorb RP-18 column made using the temperature programmed column packing technique.

Mobile Phase - 80/20 MeCN/H<sub>2</sub>O  
 Flow Rate - 50  $\mu$ l/min.  
 Pressure - 3800 psi  
 Sample - C<sub>1</sub>-C<sub>7</sub> alkyl benzenes

(numbers refer to number of carbon atoms in alkyl side chain)

perature bath and measured with the total immersion thermometer inside the water jacket surrounding the column, to the nearest 0.5° C. Retention times were recorded with a CDS-111 integrator (Varian Associates, Walnut Creek, CA.) to the nearest 0.01 minute (0.6 second). The mobile phase was allowed to equilibrate with the column at each new temperature for at least 30 minutes with flow. The Rheodyne 7410 0.5 µl internal loop injector was used to inject samples. The detector was set at the optimal wavelength for each sample (Table VII, p. 116), and was operated with the lowest time constant available (0.05 seconds).

#### 4.4.3.1 CALCULATIONS

Retention times from duplicate runs were averaged and entered into the computer. The retention volumes were calculated by multiplying the measured retention time by the flow rate. A temperature-density correction factor was used to adjust all the apparent retention volumes to volumes at a single temperature (25° C). The computer program used to manipulate the data is given in Appendix B.

#### 4.4.4 ADSORPTION ISOTHERM STUDY

A batch extraction method was used to measure the adsorption isotherm of methanol/water mixtures on LiChrosorb® RP-18, similar to a procedure used by Yonkers et. al. (133). The instrumentation used in the column extraction is shown in Figure 38. Five different mobile phases were used, with nominal concentrations of 90/10, 70/30, 50/50, 30/70 and 10/90 methanol/water, mixed by volume at 20° C. The three column temperatures investigated were 25°, 50° and 75° C. A preconditioned 25 cm microbore column packed with 10 µm LiChrosorb RP-18 was equilibrated at 250 µl/min with each methanol-water mixture at each temperature for 20 minutes. It was then extracted with 1 ml n-propanol at 100 µl/min for 10 minutes. This extraction volume was shown to be adequate, since a second milliliter of n-propanol failed to extract any additional methanol or water from the column. Care was taken to prevent any component evaporation during the extraction process. The extract was transported from the column through the top septa of an ice-chilled, 2 ml GC autosampler vial using a syringe needle. A 100 µl automatic pipette was used to add acetonitrile as an internal standard. Rather than trusting the auto pipette completely, the amount of acetonitrile added was determined by weighing the vial before and after addition to

## EXTRACTION SYSTEM

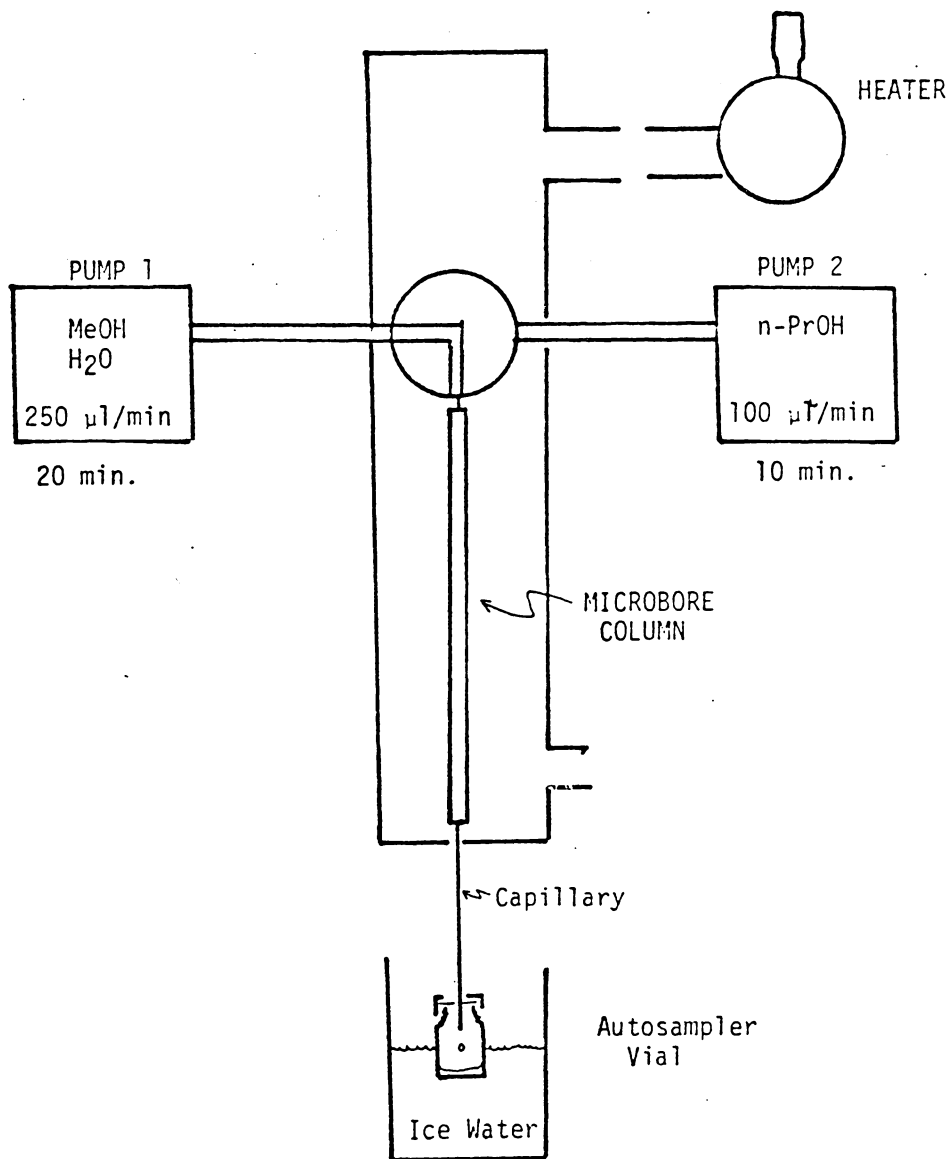


Figure 38. Batch extraction system for isotherm determination.

the nearest 0.1 mg. A new septa was placed on the vial before loading it on the autosampler.

A Varian 3700 GC (Varian Associates, Walnut Creek, CA.) equipped with a Varian autosampler was used to analyse this mixture. Conditions are given in Figure 39. A Varian CDS-111 integrator under control of the autosampler was started upon sample injection. The integrator was programmed to calculate the weight of methanol and water extracted from the column referenced to the internal standard peak (acetonitrile). All vials were analysed in triplicate. Duplicate extracts were performed at each temperature and mobile phase composition. Samples were prepared from the original mobile phases by pipetting 150  $\mu$ l from the solvent reservoir, adding 850  $\mu$ l n-propanol and 100  $\mu$ l acetonitrile. Weighed standards close to the concentrations of the analytes were also prepared. Figure 39 shows a typical chromatogram. Reproducibility for multiple injections of a single mixture was seen to be worse with a program rate of 10° C per minute (methanol - 0.8% RDS, water - 1.4% RDS; N = 27) than it was at 5° per minute (methanol - 0.26% RDS, water - 0.185% RDS; N = 35) explaining why the latter was used.

GC CONDITIONS

Column : Porapak Q  
6 ft x 1/8"

Detector : Thermal Conductivity

Program : 90° - 190° C at 5° C/min.

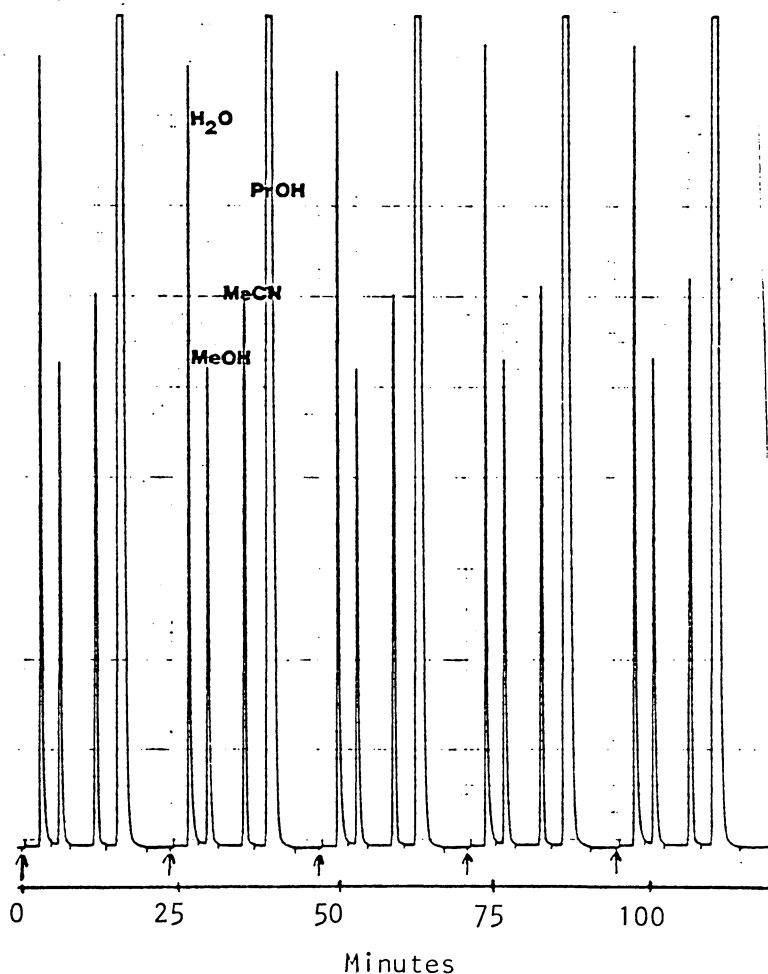


Figure 39. Conditions of analysis and a typical chromatogram of the column extract (arrows mark injection point).

#### 4.4.4.1 CALCULATIONS

The weight values supplied by the CDS-111 were adjusted for the actual weights of the internal standards contained in each sample, and then adjusted to the response factors of the weighed standards run concurrent with the samples. These weights were expressed as molar concentrations of methanol in water, and the change in concentration resulting from adsorption on the RP-18 was calculated. The computer program for this is listed in Appendix C.

#### 4.4.5 DENSITY DATA

The density of the three mobile phases was measured by picnometry at temperatures from  $-20^{\circ}$  C to  $75^{\circ}$  C, and is given in Table VIII and Figure 40. Since all mobile phases used boil between  $75^{\circ}$  and  $100^{\circ}$  C, density at  $100^{\circ}$  C was extrapolated from data in Figure 40. Measured data agrees with published data (134) to within 1%.

#### 4.4.6 EMPTY COLUMN VOLUME

The volume of the 25 cm x 1 mm ID column was determined by measuring the volume of water it took to fill it with a syringe

Table VIII

Density as a function of temperature  
for methanol/water mixtures.

Temp. (° C)	Composition (MeOH/H <sub>2</sub> O)		
	90/10	70/30	50/50
-20	.860	.913	.949
0	.843	.899	.938
25	.824	.879	.921
50	.800	.859	.903
75	.778	.836	.886
100	(.754)	(.814)	(.865)

Figure 40

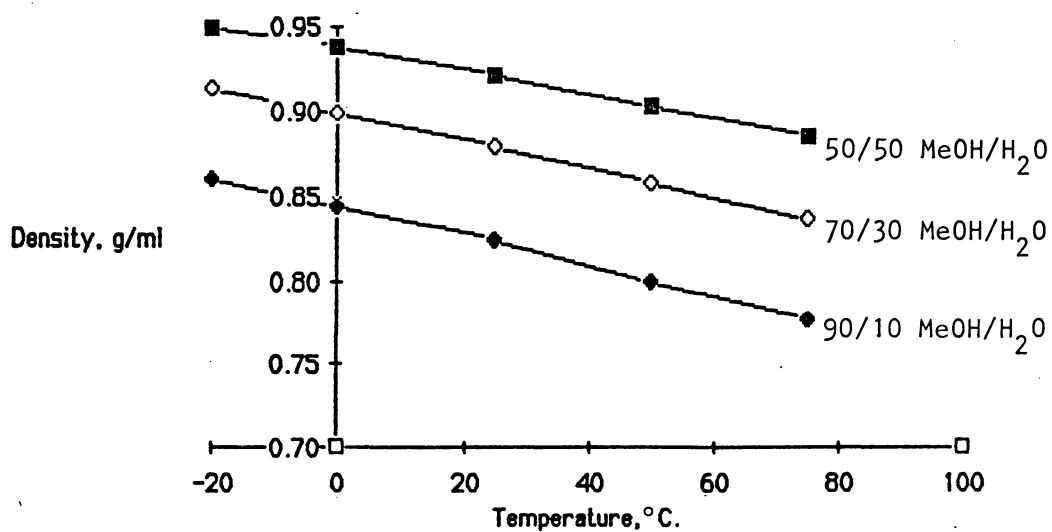


Figure 40. Density versus temperature for 50/50, 70/30 and 90/10 methanol/water mixtures.

(208.4  $\mu\text{l}$   $\pm$  5.2  $\mu\text{l}$ ), filling it with mercury and weighing the mercury (214  $\mu\text{l}$   $\pm$  1.4  $\mu\text{l}$ ) and by the difference in weight between an empty column with two parafilm plugs and a water filled column with two parafilm plugs (215.4  $\mu\text{l}$   $\pm$  1.0  $\mu\text{l}$ ). This gives a calculated tube ID of 1.047 mm, suggesting that 23  $\mu\text{m}$  of the tube wall was removed during the polishing process.

The volume of the tubing connecting the injector to the column and the column to the detector was measured by replacing the column with a ZDV fitting and measuring the length of time it took a sample to travel from the injector to the detector at 27  $\mu\text{l}/\text{min}$ . This volume was calculated to be 14.9  $\mu\text{l}$   $\pm$  0.5  $\mu\text{l}$ .

The volume contained in the empty column and all connection tubing was therefore 230.3  $\mu\text{l}$   $\pm$  1.5  $\mu\text{l}$ .

#### 4.4.7 PACKED COLUMN VOLUME

The difference in the weight of the column packed with 10  $\mu\text{m}$  LiChrosorb® RP-18 filled with methanol (density = 0.7914 g/cc) and  $\text{CCl}_4$  (density = 1.59 g/cc) gave the difference in the densities of these two solvents times the volume.

$$\begin{aligned} W_1 &= W_{\text{sol}} + D_1V \\ - W_2 &= W_{\text{sol}} + D_2V \end{aligned}$$

$$\Delta W_{1-2} = D_{1-2}V$$

$$V = W_{1-2}/D_{1-2} \quad (18)$$

where  $D_1$  and  $D_2$  are the solvent densities,  $W_{sol}$  is the fixed weight of the column and sorbent,  $V$  is the fluid volume and  $W_1$  and  $W_2$  are the weights of the column filled with the different solvents. Assuming the volume accessible to both solvents was equal, this gave the total calculated liquid volume of the packed column as 140.3  $\mu$ l, indicating that 65% of the column is filled with liquid and the rest is taken up by the sorbent.

#### 4.4.8 COLUMN CONDITIONING

The first time the temperature of a column packed with LiChrosorb RP-18 was raised above 90° C, a waxy substance washed off it, and if it was connected to the detector cell (at room temperature), this waxy material solidified inside the cell and stopped the flow, producing both high back pressure and off scale absorbance (Figure 41). This wax can be safely removed by conditioning the column disconnected from the rest of the system. The column is heated to 150° C with the pump delivering 80/20 MeOH/H<sub>2</sub>O at 2000 psi (constant pressure mode) for 15 minutes. The flow rate at this pressure was ca. 2.5 ml/min. This waxy substance is insoluble in MeOH/H<sub>2</sub>O and the high flow rate supplied the necessary shear forces to disperse

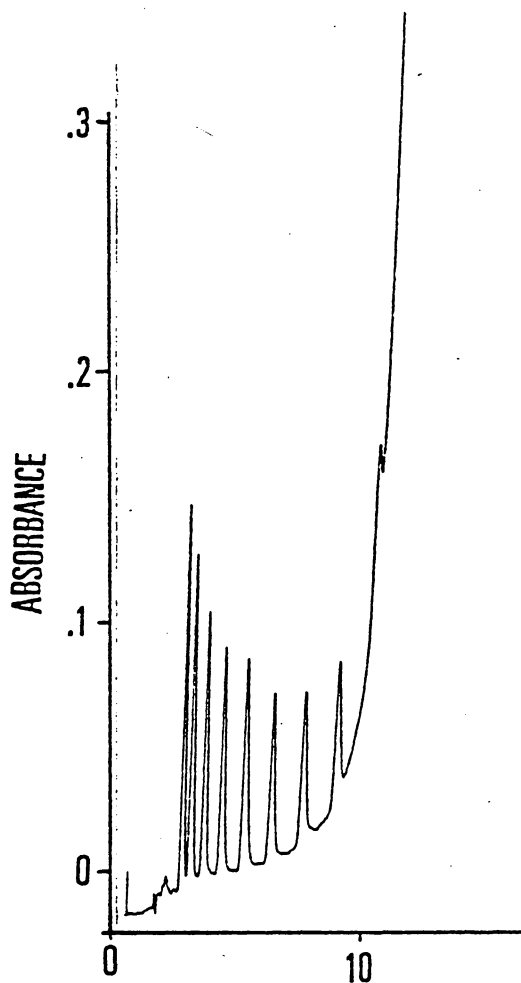


Figure 41. Temperature programmed chromatogram showing the effects of detector cell blockage by wax solidifying inside the detector cell.

Column - 25 cm x 1 mm ID  
 Sorbent - LiChrosorb RP-18, 10  $\mu$ m  
 Mobile Phase - 90/10 MeOH/H<sub>2</sub>O  
 Flow Rate - 100  $\mu$ l/min.  
 Initial Temp. - 30° C.  
 Program Rate - 5° C./min.  
 Sample - C<sub>1</sub>-C<sub>9</sub> Alkyl Benzenes

it as tiny droplets and carry it off the column bed. Approximately 1.4 mg was removed per 25 cm microbore column (100 mg sorbent). It had a melting point of 90° C but gives no GC peaks up to 350°C. from an OV-101 column. The infrared spectrum of this waxy material contained bands at 940 and 1210  $\text{cm}^{-1}$  (Si-OR) and 1100  $\text{cm}^{-1}$  (Si-OCH<sub>2</sub>CH<sub>3</sub>) which were consistent with the silane (octadecyltriethoxy silane) used to derivatize the base silica. It is either labile bonded groups on the silica or residual derivatizing material that was not washed off the sorbent with THF during manufacture (48).

Once it was removed, the problem of filling the detector cell with wax was removed. Column failure with 10  $\mu\text{m}$  material comes from the eventual dissolution of the silica backbone and the formation of a void at the head of the column. Column failure from 5  $\mu\text{m}$  material comes from the inability to remove this wax before it seals off either the column outlet frit or the column itself.

#### 4.4.9 FLOW MEASUREMENT

A variation on a syringe displacement technique was used where a valve directed the mobile phase from the detector to either a waste container or into a graduated (0.010 ml) 1 ml

pipette (Figure 42). The ID of the pipette was chosen to enable insertion of a standard pipe cleaner to dry the walls between measurements. Without this, a 5% flow rate difference was observed between a dry tube measurement and a wet tube measurement.

#### 4.4.10 TEMPERATURE RESPONSE TIME

The temperature response time was measured for a 25 cm long, 1/4" OD x 4.6 mm ID conventional bore column tube and a 525 cm long 1/16" OD x 1 mm ID microbore column tube. The internal volumes of both columns were equal. They were filled with methanol, one end was sealed and the other was attached to a methanol filled 0-30 psi pressure gauge. A calibration curve of temperature versus pressure was generated by placing these fluid filled tubes into a GC oven at different temperatures (40-110° C) and allowing them equilibrate for 15 minutes. Both columns at 25° C were then placed into an oven at 110° C and the pressure rise versus time was measured. This was related back to the temperature with the calibration curve.

The temperature response times for microbore and conventional bore columns are shown in Figure 43. The greater mass of stainless steel in the column walls, the greater volume of sol-

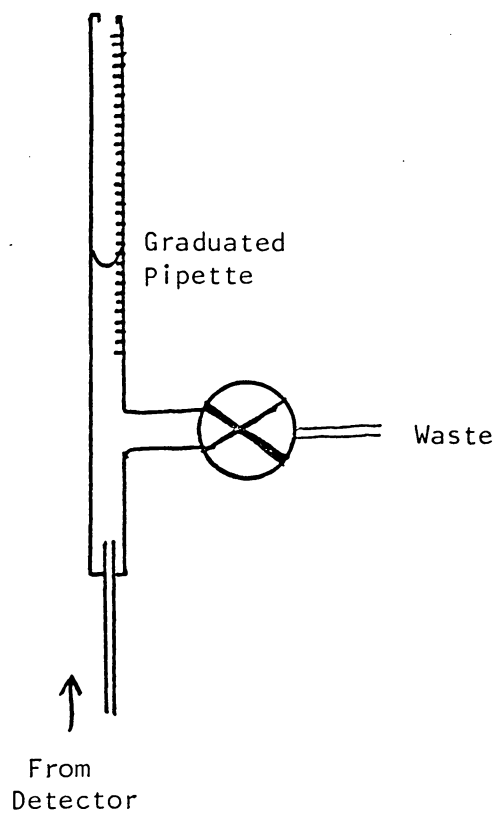


Figure 42. Side-arm pipette used to measure low flow rates.

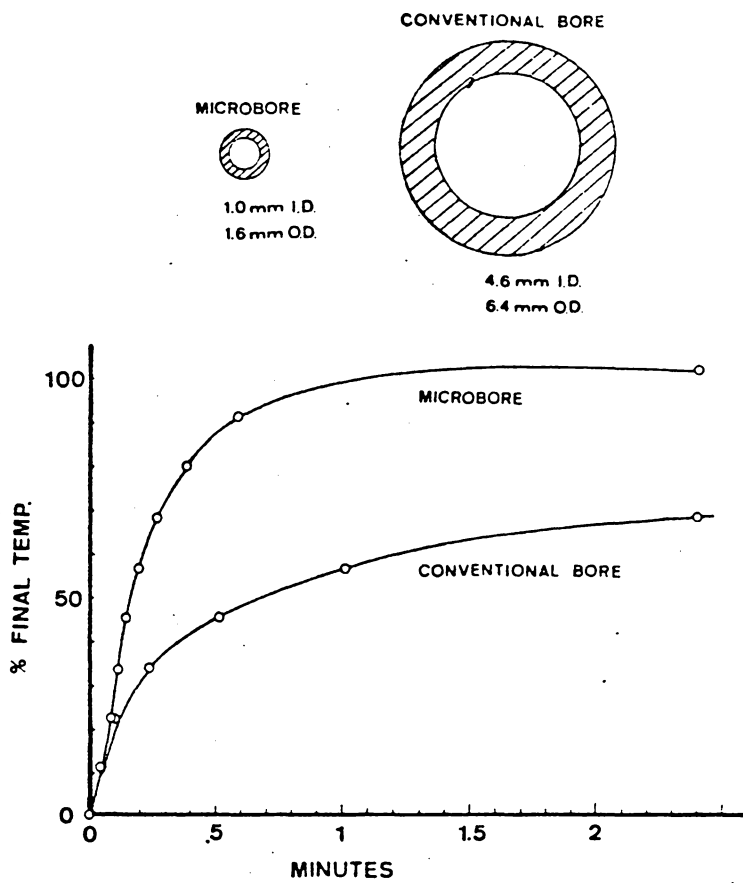


Figure 43. Temperature response times for conventional 4.6 mm ID columns and 1 mm ID microbore columns.

vent in the column and the lower surface-to-volume ratio of conventional columns are responsible for the slower response time.

A tacit assumption was made that the sorbent has the same heat capacity as methanol, but since the column is 70-80% solvent when packed, this serves as an approximation.

## 5.0 RESULTS AND DISCUSSION

This section first addresses the performance of microbore instrumentation without considering temperature. The requirements of injector and detector volumes are examined. Methods of increasing injection volume without decreasing column efficiency are dealt with in detail. The magnitude of resolution loss using conventional detector cells with microbore columns is presented. The importance of a smooth inner wall for microbore columns is stressed.

Temperature is then introduced. Thermal response times for conventional and microbore columns are contrasted. The effect of temperature on the retention volume of a large body of samples is reported, and difficulties encountered converting these volumes to thermodynamically meaningful data is discussed. The effect of temperature on column efficiency is examined. Experimental results are presented on how temperature affects the adsorbed layer of solvent on the stationary phase. Temperature programmed LC is illustrated, with resolution, analysis time and range of sample retentions accessible with a single solvent being key issues. Temperature and solvent gradients are contrasted.

## 5.1 MICROBORE EQUIPMENT PERFORMANCE

### 5.1.1 INJECTION VOLUME

The effect of injection volume was investigated by measuring the number of theoretical plates ( $N$ ) obtained as a function of the injection volume. Various volumes were obtained through partial loop injection. These were determined by dividing the measured peak area from partial loop injection by the peak area from total loop injection (giving the fraction transferred) and then multiplying by the loop volume ( $1 \mu\text{l}$ ). A 25 cm Whatman glass lined microbore column packed with  $10 \mu\text{m}$  Partisil ODS-3 (Whatman, Clifton, NJ) was operated at the optimum linear velocity ( $\mu_{\text{opt}}$ ) with 80/20 acetonitrile/water. The samples were benzene ( $k' = 1$ ) and anthracene ( $k' = 3$ ). Figure 44 shows the effect of sample volume on  $N$  resulting from injecting between  $0.31 \mu\text{l}$  to  $1.0 \mu\text{l}$ . The early peak ( $k' = 1$ ) was much more sensitive to injection volume than the later peak ( $k' = 3$ ). A sharp drop in  $N$  was observed for total loop injection. A  $1 \mu\text{l}$  loop provides sharply defined injection profiles for up to 50% loop transfer (65), but laminar flow broadens the remaining 50% and reduces observed column performance (see Figure 6, p. 39). High performance from microbore columns requires less than  $1 \mu\text{l}$  injection volumes from loop injectors, and the best perform-

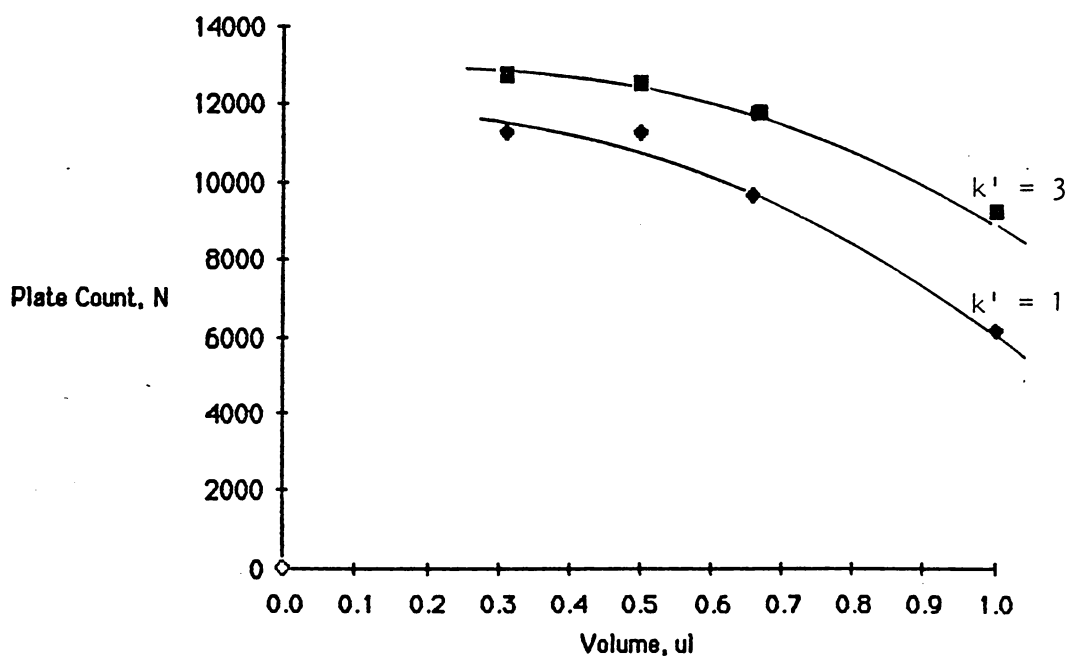


Figure 44. Efficiency versus injection volume for microbore columns.

ance is observed through partial loop injection.

### 5.1.2 WEAK SOLVENT (MOBILE PHASE)

The use of strong and weak solvents will be examined in this section for their ability to eliminate the band broadening effects caused by the injection volume. The strength of a solvent in reversed phase LC is proportional to the concentration of organic modifier it contains. A predominantly aqueous mobile phase is a weak solvent since sample species move through the column slower than they would if one used a less aqueous mobile phase. Pure methanol would be a strong solvent.

Small injection volumes severely reduce the sensitivity for microbore columns. Methods of eliminating the band broadening effects of larger sample volumes and laminar flow profiles during injection were sought. In gas chromatography, one means of accomplishing this is to cool the column inlet so that a large volume of vaporized sample condenses onto a short length of the column. Subsequent heating of this zone will revaporize the sample giving it a narrower profile than it originally had. This band compression gives sharper peaks.

Solvent strength in LC being roughly equivalent to temper-

ature in GC, an LC step gradient system was constructed where the initial eluting strength of the mobile phase was low. Following injection, a sharp solvent strength increase was effected by switching in a stronger solvent using a valve (step-gradient). The resulting chromatogram is shown in Figure 45, and the plate counts for this injection scheme and one using the stronger solvent throughout the run are given in Table IX. The step gradient technique did not work for the following reasons.

In GC, sample molecules of moderate vapor pressure are dispersed in large volumes of fixed gases of fairly high vapor pressures. Upon injection into a cooled inlet, the sample molecules collide with the cool walls of the column, lose energy, slow down and eventually condense, while the carrier remains as a gas and rapidly diffuses away from the sample. In LC, the sample components and their carrier rapidly separate from each other.

In LC, for solubility considerations, most samples are dissolved in either pure organic solvents (like MeOH or MeCN) or the current column mobile phase. In either case, the solvent strength is greater than or equal to that of the mobile phase. Upon injection, the sample solvent remains with the sample

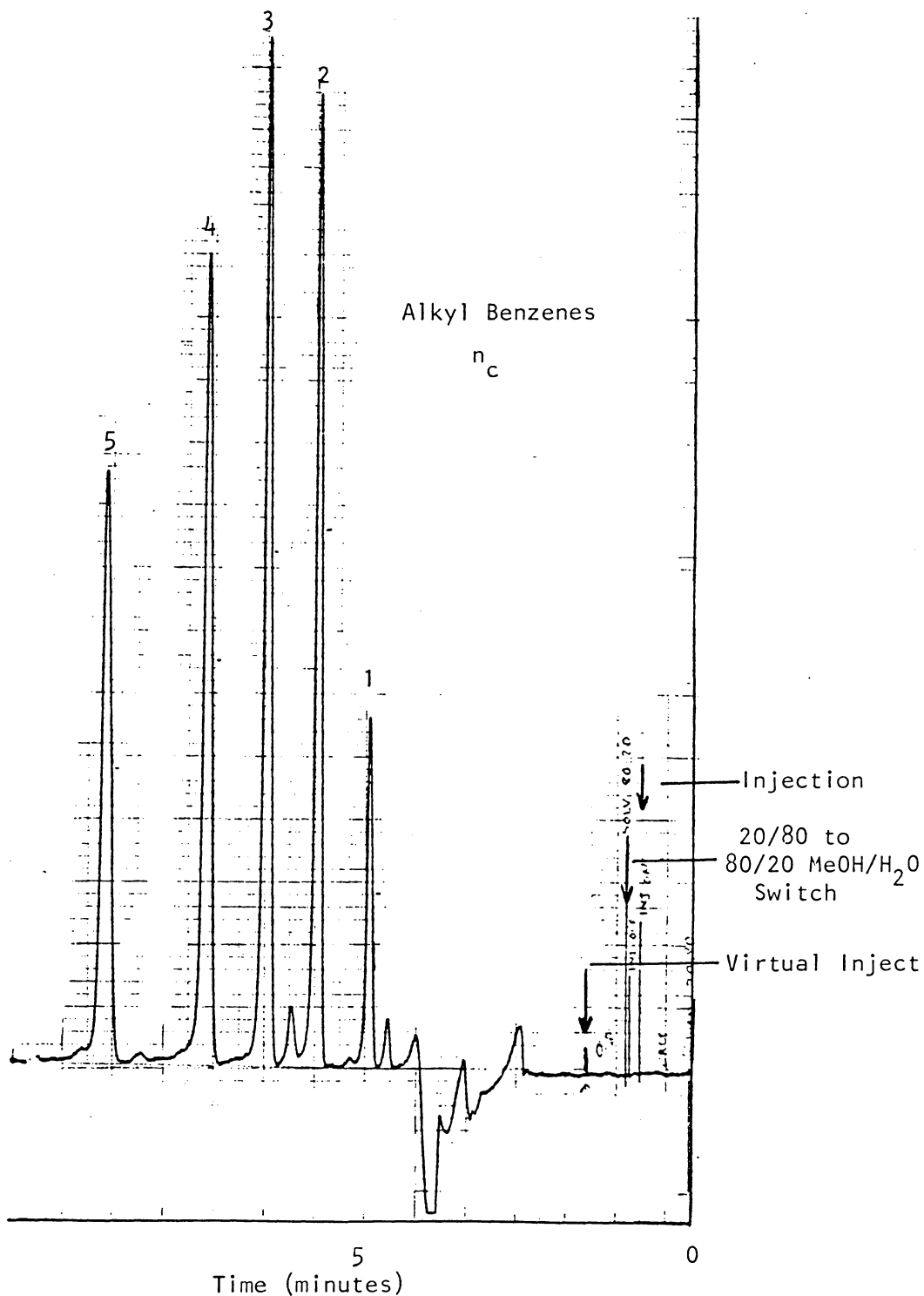


Figure 45. Step gradient chromatogram.

Initial Solvent - 20/80 MeOH/H<sub>2</sub>O  
 Step Gradient - 80/20 MeOH/H<sub>2</sub>O  
 Sample Solvent - 100% MeOH

Table IX

Plate counts for constant solvent and step  
gradient solvent injection techniques.

$k'$	N(con.)	N(step)
0.33	6610	8270
0.64	9040	10600
0.94	9720	10560
1.33	10640	10520
1.95	11220	12880

since no mechanism exists to separate sample and solvent. In LC, the sample and its solvent do not separate. So regardless of the strength of the mobile phase in the column, the width of sample on the column at injection is controlled by the strength of the solvent in which it was originally dissolved.

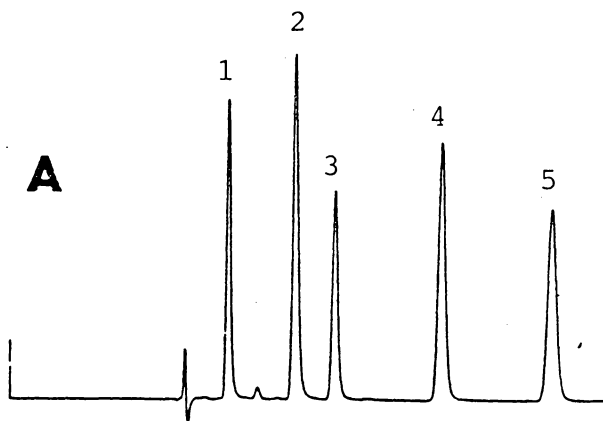
### 5.1.3 WEAK SOLVENT (SAMPLE SOLVENT)

From the previous section, it is obvious that in order to compress the injection band width in LC, the sample solvent must be weaker than the mobile phase.

Figure 46 demonstrates the non-eluting solvent effect. In Figure 46 a, a 0.5  $\mu$ l injection was made in an eluting solvent. An eluting solvent is one whose strength is equal to or greater than the mobile phase used in the separation. Figure 46 b shows the effect of increasing this sample volume 10-fold with the same eluting solvent while keeping the sample mass constant - (the original 0.5  $\mu$ l sample volume was increased to 5.0  $\mu$ l with MeOH). This larger sample volume resulted in the initial sample band on the column being excessively wide giving broader, flatter peaks at the detector. Column efficiency had been greatly reduced. Figure 46 c shows an injection of this same 5  $\mu$ l volume with the same sample mass, but in this case the sample

SOLVENT EFFECT IN  
MICROBORE HPLC  
80:20 MeOH:H<sub>2</sub>O

SIZE 0.5 UL  
SOLVENT 100 % MeOH



SIZE 5.0 UL  
SOLVENT 100 % MeOH



SIZE 5.0 UL  
SOLVENT 50/50 MeOH/H<sub>2</sub>O

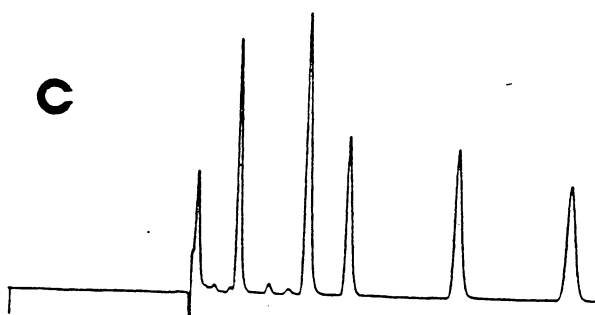


Figure 46. Non-eluting solvent effect.

Column - 50 cm x 1 mm ID  
Sorbent - LiChrosorb RP-18, 10  $\mu$ m  
Flow Rate - 50  $\mu$ l/min.  
Sample - 1) Phenol; 2) 2-Ethyl Phenol;  
3) Anisole; 4) Benzene; 5) Toluene.

was dissolved in a non-eluting solvent (50/50 MeOH/H<sub>2</sub>O). This solvent was weaker than the mobile phase, and during the injection process, sample components did not move down the column but were adsorbed into a narrow band at the head of the column. Elution began only when the stronger mobile phase came in behind the sample.

Figure 47 shows the effect that changing the sample solvent strength relative to a fixed mobile phase strength had on the plate count delivered by the column for samples of varying degrees of retention. It is seen that the narrower, less retained peaks benefit more from the non-eluting solvents than the broader, more retained ones.

Non-eluting solvents also allow large volumes to be injected without loss in resolution. Figure 48 shows a very high resolution separation of PTH-Amino Acids in which 25  $\mu$ l of sample was injected onto a 50 cm long, 5  $\mu$ m RP-18 column (N = 45,000 on peak 7). This excellent chromatogram was obtained even though the volume used represented 50 times the usual maximum injection volume using eluting sample solvents.

An important consideration in reducing the sample solvent strength is the solubility of the sample in this weaker

Column - 25 cm x 1 mm ID  
Mobile Phase - 75/25 MeCN/H<sub>2</sub>O  
Injection Volume - 25  $\mu$ l

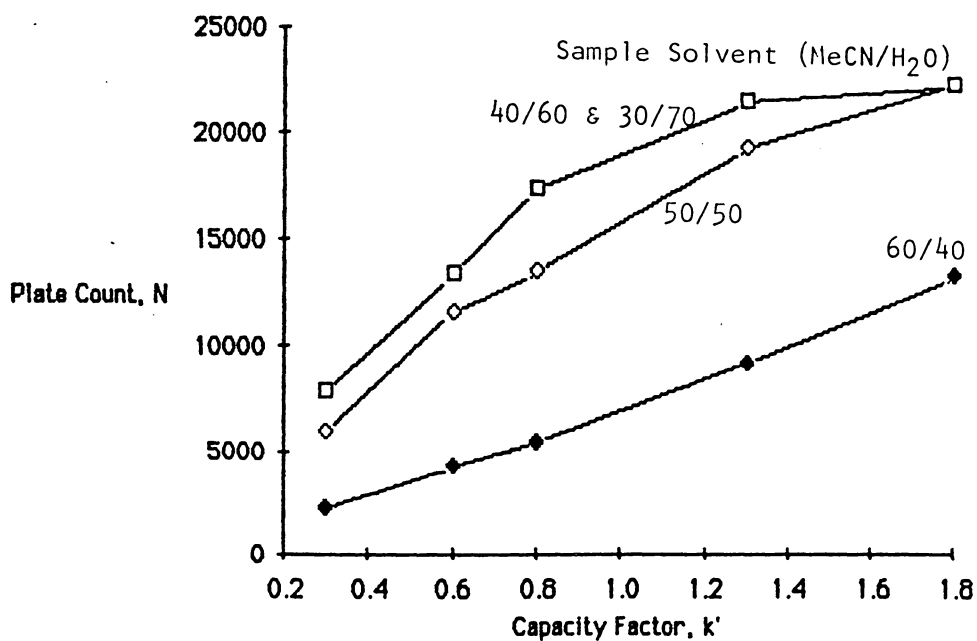


Figure 47. Effect of the difference between the mobile phase and sample solvent strength on observed efficiency as a function of capacity factor.

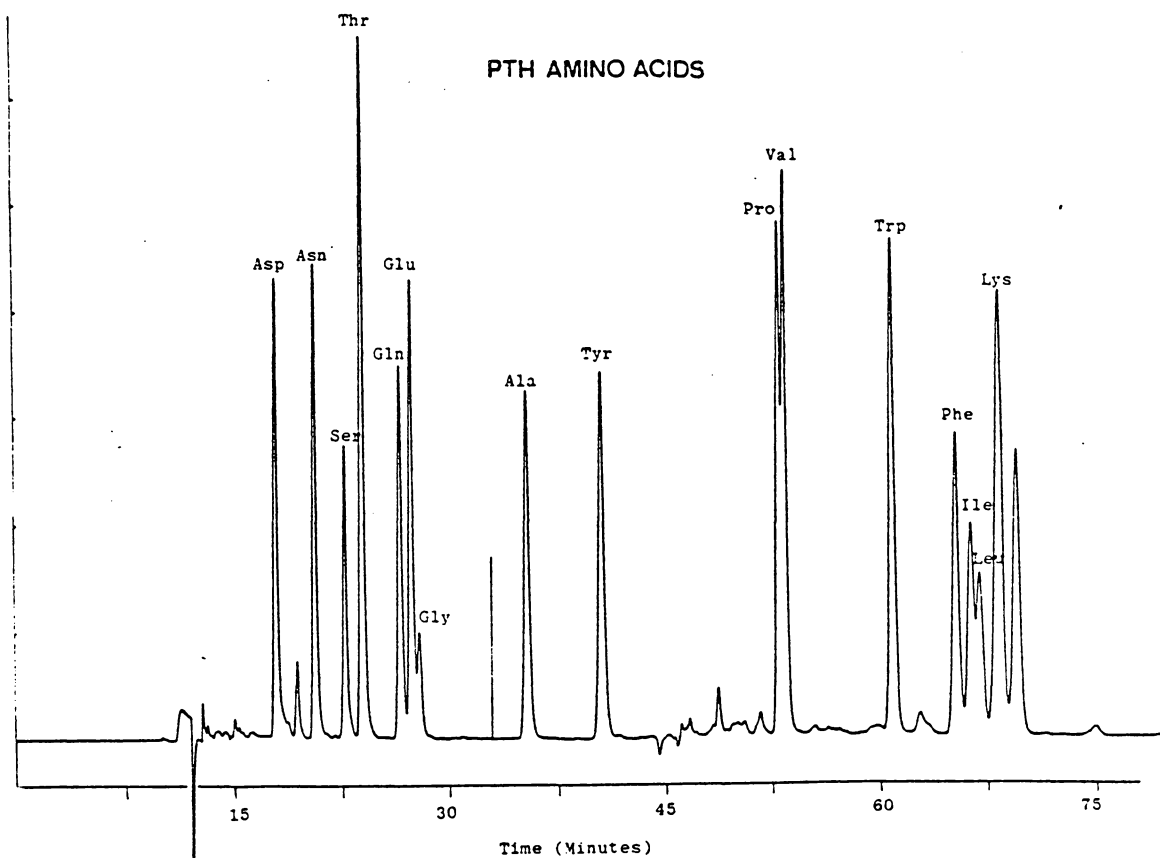


Figure 48. PTH-amino acid analysis using a large volume injection (25  $\mu$ l) on a 50 cm microbore column.

Sorbent - LiChrosorb RP-18, 5  $\mu$ m

Mobile Phase - Initial - 22/78 MeOH/Buffer  
 Final - 50/50 MeOH/Buffer  
 (step gradient at 32 minutes)

Sample Solvent - 10/90 MeOH/H<sub>2</sub>O

solvent. It is sometimes difficult to get a sample into solution in a weak, binary solvent. Taking up the sample in a pure organic solvent first and then diluting with water is often successful.

#### 5.1.4 DETECTOR CELL VOLUME

Microbore columns may be used with conventional detector cells provided that all excess volume between the column outlet and the optical path of the cell is reduced as much as possible. Figure 49 shows two chromatograms of the same sample with the same solvent on a microbore column attached to a 0.5  $\mu$ l cell and an 8.0  $\mu$ l cell. The cell pathlengths were 1 and 10 mm respectively. Note the difference in the sensitivity scales. Figure 50 shows plate counts using both detectors, showing that the major losses in resolution occur only for the early eluting peaks ( $k' < 2$ ).

#### 5.1.5 POLISHED VERSUS NON-POLISHED TUBING PERFORMANCE

A direct comparison of polished and non-polished tubing was performed to illustrate the advantage of polished tubing for high performance microbore columns. Two 25 cm columns were packed using identical procedures and tested with the same sam-

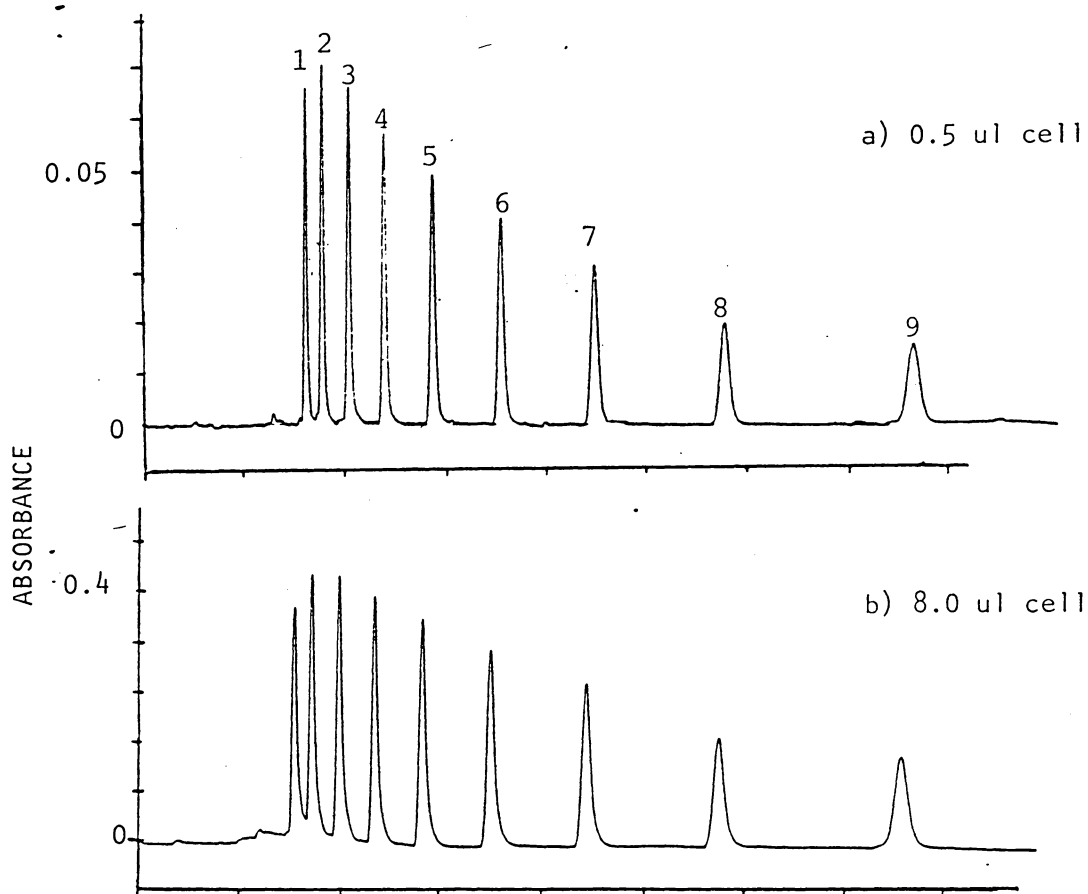


Figure 49. Chromatograms from a microbore column using  
 a) 0.5 and b) 8.0  $\mu$ l cells.

Column - 25 cm x 1 mm ID  
 Sorbent - LiChrosorb RP-18, 7  $\mu$ m  
 Solvent - 80/20 MeCN/H<sub>2</sub>O  
 Sample - C<sub>1</sub>-C<sub>9</sub> Alkyl Benzenes.

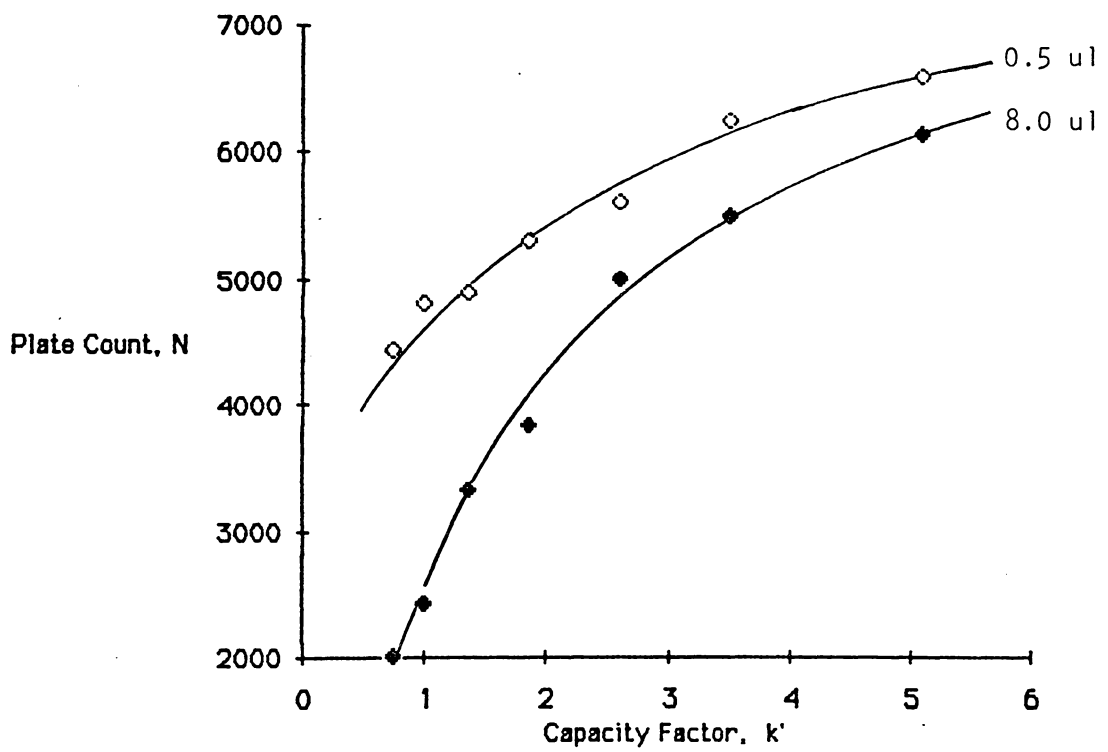


Figure 50. Observed column efficiency versus  $k'$  from 0.5 and 8.0  $\mu$ l cells.

ple and mobile phases. Their only difference was in the finish of the inside walls of the tubing. Figure 51 shows a Van Deemter plot (plate height  $H$  versus linear velocity  $u$ ) for these two tubes. The polished tube consistently gave a lower plate height and therefore generated more plates during the separation than the non-polished tube.

After several hours operation, the unpolished column developed a 1.8 cm void at the top of the column, and this resulted in an even greater plate height.

A recent publication (135) discounted the need for polished tubing, showing no effect of inside tube finish on column performance. It should be stressed that they only examined conventional 4.6 mm ID tubing, where the effects of wall finish are apt to be less important than for microbore columns. Consistently low microbore column performance was observed when non-polished 1/16" stainless steel tubing was used.

## 5.2 TEMPERATURE EFFECTS

### 5.2.1 EFFECT OF TEMPERATURE ON RETENTION

The retention volumes measured for the various homologous

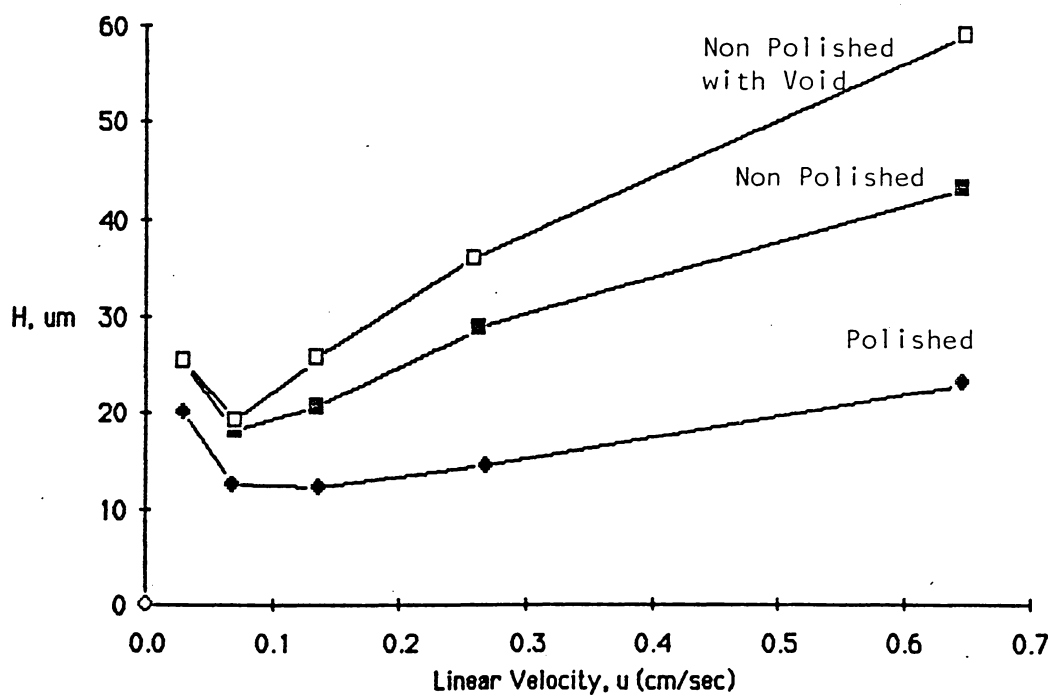


Figure 51. Van Deemter Plots from microbore columns constructed from polished and non-polished tubing.

Column - 25 cm x 1 mm ID  
 Sorbent - LiChrosorb RP-18, 5  $\mu$ m  
 Solvent - 80/20 MeCN/H<sub>2</sub>O  
 Sample - Octyl Benzene ( $k'$  = 7)

series members at the different temperatures and mobile phase compositions are given in Appendix D. These data were used to calculate void volumes ( $V_0$ 's) by each of the three methods (89,99,106) described in Appendix A and the results are given in Table X.

### 5.2.2 EXCESSIVE VOID VOLUME ESTIMATES

At the colder temperatures and with the weaker (more aqueous) mobile phases, the predicted  $V_0$ 's frequently exceeded the total empty column volume of 230  $\mu$ l. This is illogical, since the void volume can never exceed the total column volume. The possible causes for this unexpected result were examined.

#### 5.2.2.1 PENDANT GROUP EFFECTS

A pendant group effect occurs where the alkyl chain is so short that the magnitude of the  $\Delta G$  contribution resulting from the addition of a methylene group is altered by the base group via some type of shielding mechanism. Since the linearity of the  $\ln k'$  vs  $n_c$  relationship is based on equal  $\Delta G$  contributions to retention by each additional methylene group, this pendant group interference distorts the  $\ln k'$  vs  $n_c$  linearity and leads to curvature in this relationship for the earlier members in

Table X

$V_0$  estimates from homologous series  
as a function of temperature and mobile  
phase composition. Volumes in  $\mu\text{l}$ .

AKB = Alkyl Benzenes            PAR = Parabens  
BZT = Benzoates                ACE = Acetates  
PHE = Phenones                 KET = Ketones

$V_0$  Estimates by the Mockel Method (89).

90/10 Methanol-Water

Temp.	AKB	BZT	PHE	PAR	ACE	KET
-20	215	197	240	179	170	176
0	196	174	184	159	168	160
25	180	172	154	136	160	143
50	170	145	157	60	143	154
75	159	142	130	-	-	-
100	178	-	60	-	-	-

70/30 Methanol-Water

-20	381	335	304	214	167	166
0	322	239	193	186	167	167
25	238	193	168	163	161	162
50	192	174	146	-	160	158
75	177	162	155	160	159	158
100	169	161	151	130	145	146

50/50 Methanol-Water

-20	-	520	320	477	246	178
0	520	497	292	298	201	161
25	509	324	264	203	194	156
50	254	228	201	165	153	152
75	216	178	164	151	137	148
100	180	159	152	146	197	149

Table X (cont.)

V<sub>0</sub> Estimates by the Grobler Method (106).

## 90/10 Methanol-Water

Temp.	AKB	BZT	PHE	PAR	ACE	KET
-20	150	197	-	179	169	176
0	199	174	-	159	168	160
25	186	171	-	136	165	143
50	175	145	-	28	144	154
75	159	142	-	-	-	-
100	177	-	-	-	-	-

## 70/30 Methanol-Water

-20	392	335	149	206	166	161
0	315	230	107	187	163	142
25	264	197	98	170	166	178
50	210	179	23	-	166	163
75	190	166	98	195	172	165
100	173	165	126	128	141	177

## 50/50 Methanol-Water

-20	-	737	320	494	246	164
0	944	461	220	295	201	145
25	575	317	237	208	199	145
50	254	324	184	183	151	147
75	224	193	100	162	143	138
100	201	168	134	150	126	151

Table X (cont.)

$V_0$  estimates using the Berendsen method (99).

90/10 Methanol-Water

Temp.	AKB	BZT	PHE	PAR	ACE	KET
-20	291	202	-	179	173	176
0	206	178	-	161	164	163
25	175	169	-	136	160	145
50	167	151	-	28	154	154
75	158	142	-	-	-	-
100	174	-	-	-	-	-

70/30 Methanol-Water

-20	409	336	197	227	172	171
0	344	247	217	189	175	167
25	234	187	169	156	163	167
50	172	166	141	-	159	160
75	169	158	151	169	156	163
100	166	158	147	135	148	175

50/50 Methanol-Water

-20	-	737	320	417	246	187
0	706	557	388	319	200	173
25	395	336	118	203	168	158
50	253	231	204	143	156	152
75	209	160	169	138	94	187
100	166	148	156	140	384	148

the series. The calculations were carried out only on the latter ( $n_c \geq 5$ ) members and while it reduced the problem it did not eliminate it (Table XI). A computer program was written where void volumes calculated by Berendsen's method (99) were carried out on every conceivable combination of homologs. Table XII shows that the  $V_0$  estimates varied widely depending on which members of the series were used for the estimate.

#### 5.2.2.2 PRECISION OF RETENTION VOLUME MEASUREMENTS

Each of the  $V_0$  estimation procedures used a different mathematical approach to predict the void volume. They weigh errors in measured retention volumes differently and therefore produce slightly different  $V_0$  estimates. When a synthetic data array was constructed in which the log of the capacity factor versus the carbon number was perfectly linear, all three  $V_0$  estimation algorithms gave exactly the same answer. Referring to the retention time of a single homolog as a 'term', the influence that introducing a 1% error in a single term had on the  $V_0$  estimate was examined as a function of the position that term occupied in the array, and is shown in Figure 52. It is seen that Berendsen's method (102) shows a  $\pm 10\%$  error if either of the last two terms had a 1% error, but was less sensitive to errors in the earlier terms. Grobler's method (109) was exact-

Table XI.

$V_0$  Estimation using the Mockel method (89)  
using  $n_c \geq 5$ .

90/10 Methanol-Water

Temp.	AKB	BZT	PHE	PAR	ACE	KET
-20	329	218	240	179	174	176
0	219	194	191	165	166	160
25	163	159	154	136	144	143
50	163	154	157	60	145	154
75	158	142	130	-	-	-
100	169	-	60	-	-	-

70/30 Methanol-Water

-20	-	-	-	245	184	195
0	520	284	-	199	190	180
25	234	179	175	147	166	163
50	168	153	142	-	163	159
75	154	149	157	-	154	162
100	160	151	147	151	149	159

50/50 Methanol-Water

-20	-	-	-	-	-	-
0	-	-	-	-	-	216
25	-	-	-	222	-	170
50	-	289	-	114	150	155
75	224	152	138	124	60	170
100	154	137	143	139	365	148

Table XII

Void volume prediction using Berendsens method  
for every conceivable combination of homologs.

Sample - Alkyl Benzenes  
Mobile Phase - 70/30 Methanol-Water  
Temperature - 50° C.

		Ending Homolog							
		3	4	5	6	7	8	9	10
1	Beginning Homolog	214	205	178	182	187	182	180	171
		2	196	155	172	183	178	176	167
			3	110	168	186	178	176	164
				4	221	215	190	168	151
					5	210	170	168	151
						6	129	153	134
							7	177	130
								8	84

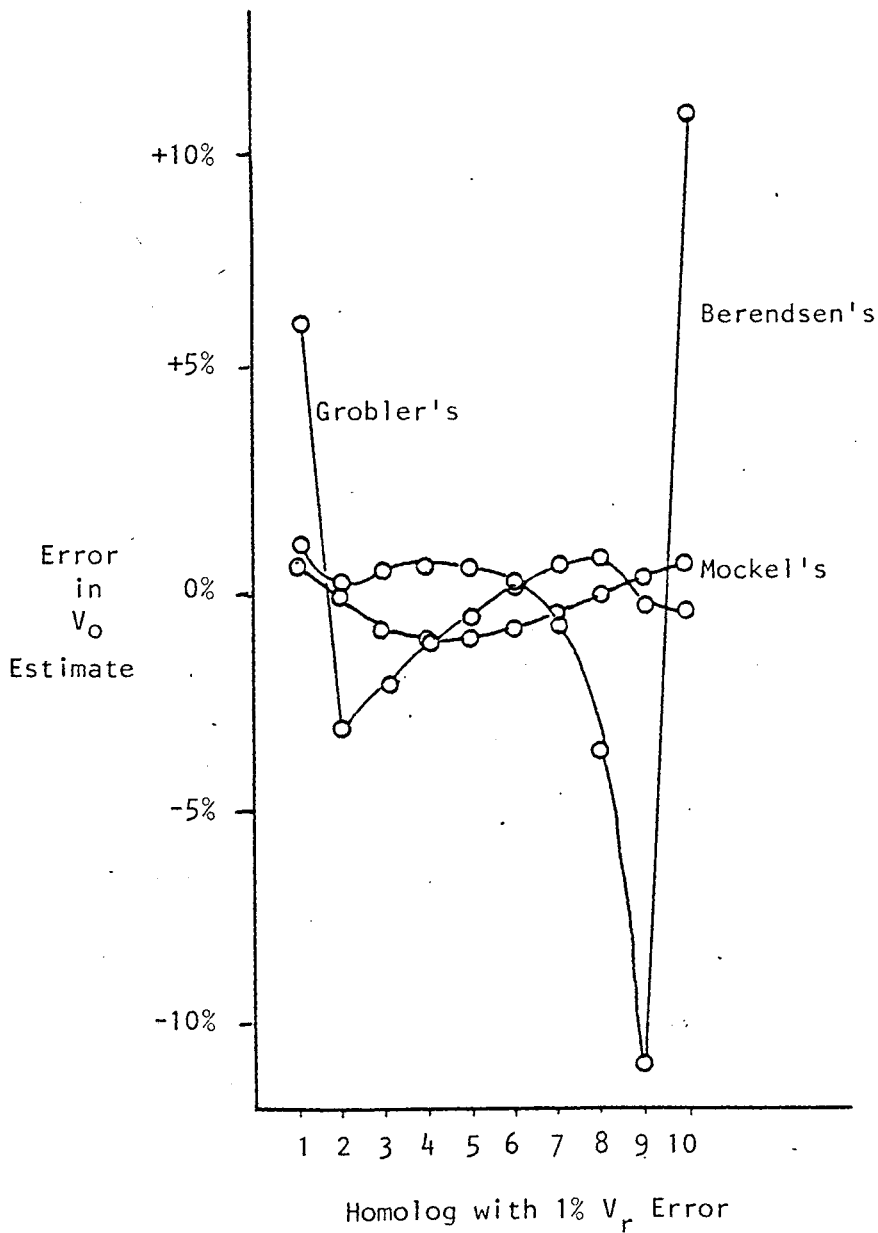


Figure 52. Effect of a 1% relative error in retention volume on the resulting  $V_0$  estimate.

ly the opposite, showing its peak sensitivity to errors in the first few terms. Mockel's method (92) was seen to be the best since a 1% error in the measured retention volume always translated to a  $\pm 1\%$  error in the  $V_0$  estimate. Unfortunately, Mockel's method involves thousands of calculations and takes the greatest amount of computer time to estimate  $V_0$ . (For a 10 term series, it takes 5 minutes of computations.)

The wide range of void volume estimates in Table XII ( $84 \mu\text{l} < V_0 < 221 \mu\text{l}$ ) can be accounted for by relatively minor adjustments in the original retention volume data. Table XIII shows that except for the first data point, errors sufficient to cause wide variations in the calculated void volumes are small and fall within the retention time variability of the system ( $\pm 0.5\%$ ).

#### 5.2.2.3 SORBENT CHANGE ON CONDITIONING

Solute retention on conditioned sorbent was little different from that of non-conditioned sorbent (Figure 53). The column showed slightly higher performance after conditioning ( $N$  before = 4400,  $N$  after = 6300) which may be attributed to a decrease in the thickness of the  $C_{18}$  layer, giving faster mass transfer, by the removal of excess silicone wax.

Table XIII

Adjustments to retention times to cause all combinations of homologs in table XII to predict the same void volume of 176  $\mu$ l.

Original Retention Times	Required Retention Times	% $\Delta$
1.72	1.669	-2.9
2.25	2.25	
3.13	3.136	-.2
4.56	4.539	+.5
6.76	6.771	+.2
10.30	10.325	+.2
15.98	15.98	
24.97	24.97	
39.27	39.27	
61.88	62.01	+.2

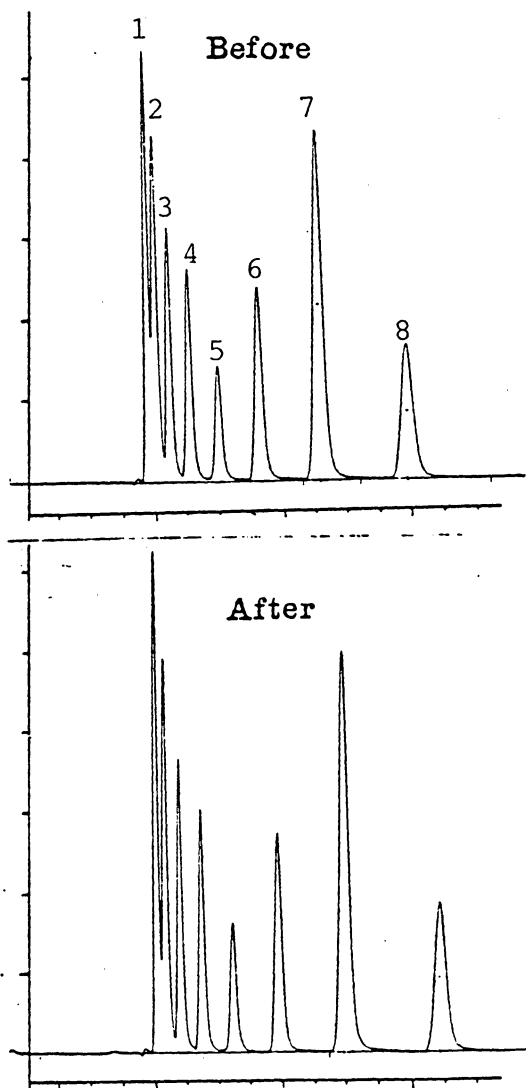


Figure 53. Effect of column conditioning on chromatographic performance.

Top - Before heat treatment  
 Bottom - After heating to 150° C  
 with 2.5 ml/min 80/20 MeOH/H<sub>2</sub>O  
 flowing through column for 15 min.

Sample - C<sub>1</sub>-C<sub>8</sub> Parabens

It could be proposed that either by oxidation of the alkyl side chain or through exposure of more surface silanol groups by the removal of bound  $C_{18}$  groups that the sorbent became more polar. This would lead to multiple retention mechanisms for homologous series with polar base groups, like the acetates and ketones. The longer alkyl chain members would be overall less polar than those with shorter chains, and this would result in abnormally high retention volumes for the earlier eluting members. The  $\ln k'$  vs  $n_c$  plot would be concave upwards and to straighten it out, the computer would be forced to pick larger  $V_0$ 's. However, this is precisely what is not seen. The void volume estimates from acetates and ketones are the most reasonable and lead to a single estimate of the void volume regardless of which members of the series (early or late) are used to predict the void volume.

#### 5.2.2.4 TEMPERATURE GRADIENTS

The flow rate used was fairly rapid (250  $\mu$ l/min) resulting in a rather short ( $\approx$ 30 second) residence time of the mobile phase within the controlled temperature zone. The entering mobile phase may not have had sufficient time to completely equilibrate with the temperature of the control bath. This could be considered as producing a cooler (or hotter) zone at

the head of the column compared to the rest of the column. The length of this zone would be a function of the flow rate, becoming longer at higher flow rates and shorter at lower ones. This would lead to a flow dependency in the measured retention volumes. Table XIV lists the observed retention volumes for alkyl benzenes in 90/10 MeOH/H<sub>2</sub>O mixtures at three different flow rates with the column at 100° C and the entering mobile phase at 25° C. As predicted by this model, a significant flow sensitivity in the retention volume was observed. The ratios of the retention volumes are also listed in Table XIV, and compared to 22  $\mu$ l/min, 85  $\mu$ l/min leads to a 7% increase in the retention volume while 224  $\mu$ l/min leads to a 13% increase.

The predicted  $V_0$ 's follow the same trend. The most interesting fact is that while the  $V_0$ 's depend on the flow rate, the  $k$ 's calculated using these  $V_0$ 's do not (Table XV). This is important. Even using a high flow rate, this study took over a month to conduct. It would take nearly a year to repeat it at 20  $\mu$ l/min. The results here suggests that while the  $V_0$  estimates obtained from this data were too high, the  $k$ 's calculated using them are none the less correct, being independent of the flow rate.

Table XIV

Retention volume as a function of flow rate.

Sample - Alkyl Benzenes  
 Solvent - 90/10 MeOH/H<sub>2</sub>O  
 Column Temperature - 100° C.  
 Solvent Temperature - 25° C.

nc	Flow Rate (μl/min.)		
	21	85	224
1	187	203	213
2	205	221	232
3	229	248	260
4	261	282	298
5	302	326	343
6	356	381	401
7	425	455	482
8	513	550	581
9	628	670	709
10	776	824	872

Percentage increase in retention volumes with flow rate.

nc	$V_{85}/V_{21}$	$V_{224}/V_{21}$
1	108.69	113.92
2	108.11	112.92
3	108.19	113.32
4	108.03	114.10
5	107.71	113.45
6	107.25	112.73
7	107.02	113.18
8	107.19	113.13
9	106.62	112.73
10	106.17	112.37

Table XV.

Void volume estimates from retention volume by the Berendsen method and resulting capacity factors.

Flow Rate ( $\mu\text{l}/\text{min}$ )	21	85	224
Void Volume ( $\mu\text{l}$ )	123	134	139
	Capacity Factors		
nc			
1	.52	.51	.52
2	.67	.65	.66
3	.87	.85	.87
4	1.13	1.10	1.15
5	1.46	1.43	1.47
6	1.90	1.85	1.89
7	2.47	2.40	2.47
8	3.18	3.10	3.18
9	4.12	3.99	4.10
10	5.32	5.14	5.27

### 5.2.3 TEMPERATURE EQUIVALENCE TO COMPOSITION

The  $\ln k'$  vs  $n_c$  plots at different temperatures for alkyl benzenes at two different mobile phase compositions are shown in Figure 54. One way of illustrating the temperature equivalence to composition is to superimpose these Figures and note what temperatures cause the same members of a homologous series at two different mobile phase compositions to line up. For example, the 50/50 MeOH/H<sub>2</sub>O data at 100° C lines up with the 70/30 MeOH/H<sub>2</sub>O data at 25° C. This means that a 20% increase in methanol content is equivalent to 75° C increase in temperature, or  $\Delta 3.75^\circ \text{C}$  equals a  $\Delta 1\%$  in methanol. Another way of correlating column temperature and mobile phase composition is to note that the slope of  $\ln k'$  vs  $n_c$  is equal to  $\ln \alpha$ , and  $\alpha$  (the methylene selectivity) is a measure of the solvent strength. Solvents with equal  $\alpha$ 's have equivalent strengths. A plot of  $\ln \alpha$  vs temperature is shown in Figure 55. Horizontal lines across this Figure connect solvents of equal elution strengths, showing the same 75° equivalence to a 20% change in methanol content. Given a practical temperature range of 150° C, this correlates to a 40% increase in methanol. Note that the lines are not exactly parallel, meaning there is not a fixed value for the temperature equivalence to solvent strength.

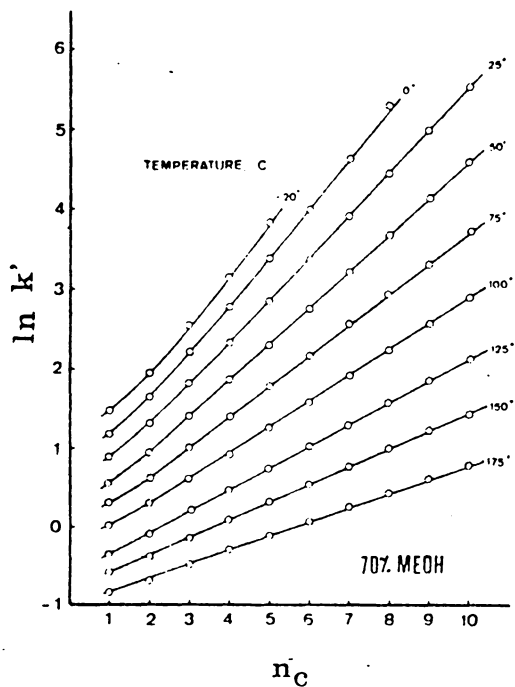
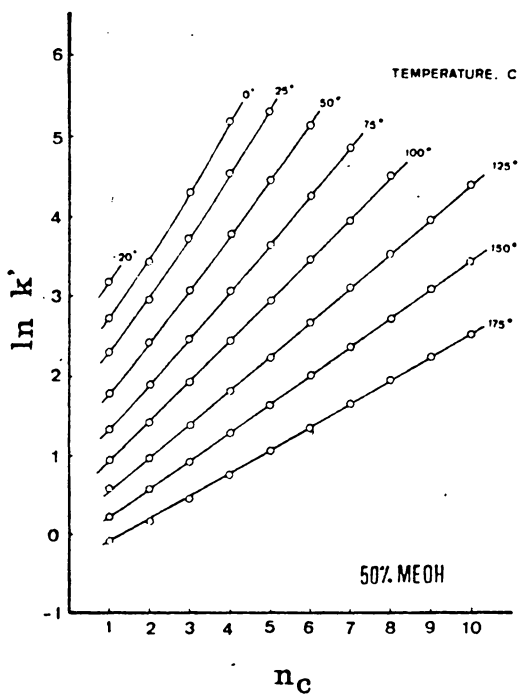


Figure 54.  $\ln k'$  versus  $n_c$  plots for alkyl benzenes as a function of temperature at two different mobile phase compositions.

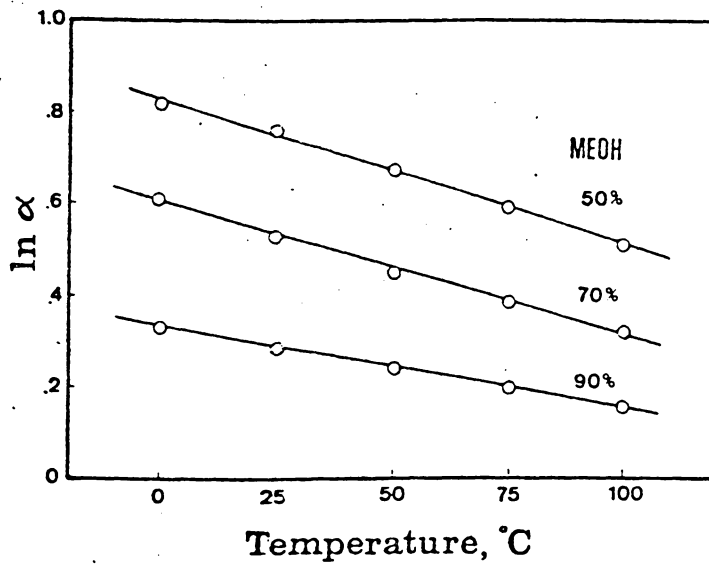


Figure 55.  $\ln \alpha$  versus temperature.

#### 5.2.4 EFFICIENCY VS TEMPERATURE

The effect of temperature on column efficiency was shown to be strongly influenced by preheating the mobile phase (37,38). Dramatic losses in column efficiency are observed unless both the entering mobile phase and the column are at the same temperature. For conventional bore columns, this is due to radial temperature profiles across the column bed, but for microbore columns, it can result from longitudinal temperature gradients from insufficient residence time of the solvent in the column. Excessive retention on "cold spots" are experienced by the more retained solutes.

The rate of heat transfer to an LC column by liquids is much faster than by gases due to the difference in the densities of liquids and gases. An air heating system cannot raise the temperature of the entering mobile phase as fast as the water jacket system, so air heating systems are expected to show reduced performance at high flow rates for later eluting peaks.

Figure 56 shows efficiency as a function of retention at different flow rates for a microbore column with the mobile phase at room temperature (18.8° C) and the column heated with air to 100° C. Column efficiency was dramatically reduced for

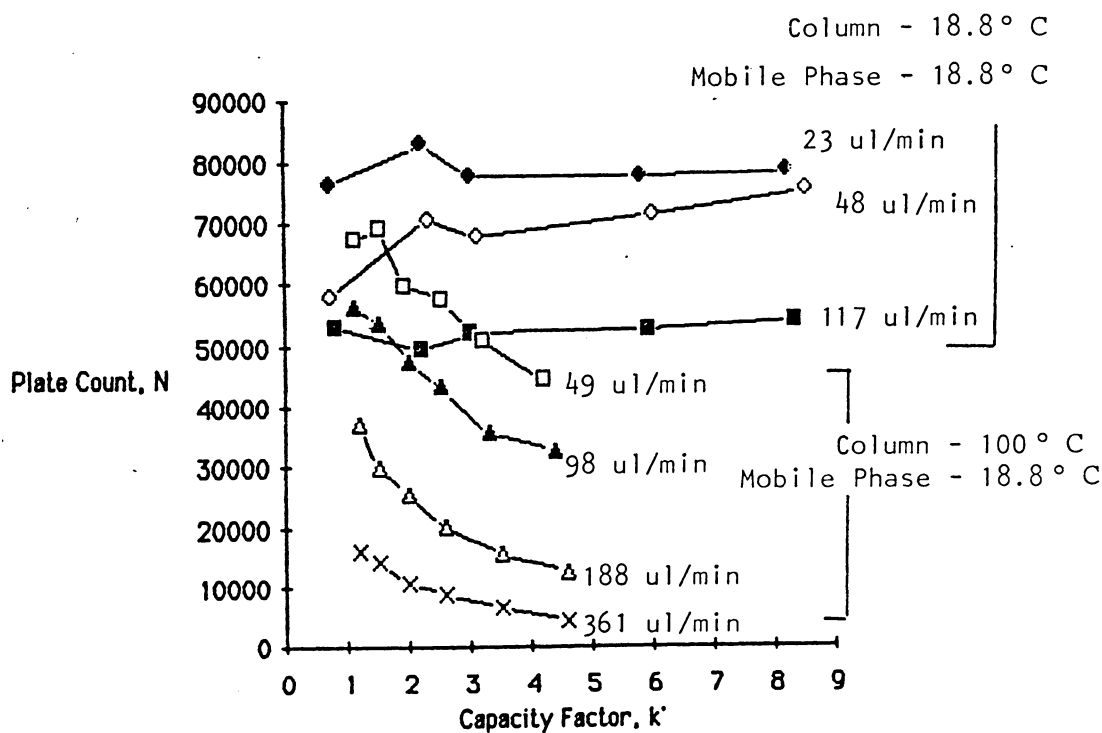


Figure 56. Observed column efficiency as a function of the flow rate, the capacity factor, and temperature of the column and the mobile phase using an air heating system.

Column - 25 cm x 1 mm ID  
 Sorbent - LiChrosorb RP-18, 10  $\mu$ m  
 Solvent - 90/10 MeOH/H<sub>2</sub>O  
 Sample - 18.8° - C<sub>1</sub>-C<sub>5</sub> Alkyl Benzenes  
 100° - C<sub>1</sub>-C<sub>6</sub> Alkyl Benzenes

the more retained components since retention on "cold spots"

within the column broaden these later peaks. In contrast, using the water jacket temperature control bath greatly accelerates the rate of thermal equilibration for the mobile phase as it enters the column, and does not show a reduction in efficiency with increased retention (Figure 57). In fact, efficiency actually improves with temperature due to improvements in the rate of mass transfer between the chromatographic phases.

#### 5.2.5 ADSORPTION ISOTHERM CHANGE WITH TEMPERATURE

When mixtures of aqueous and organic solvents are brought in contact with reversed phase sorbents, the organic component preferentially adsorbs to the non-polar surface (82,83), giving rise to a partition retention mechanism. To describe the effect temperature on retention, both changes in the partition coefficients of the solutes and changes in the phases into which they partition must be addressed. This study measured adsorption isotherm of methanol/water mixtures on LiChrosorb RP-18 as a function of temperature and composition.

A method of presenting binary solvent adsorption isotherm

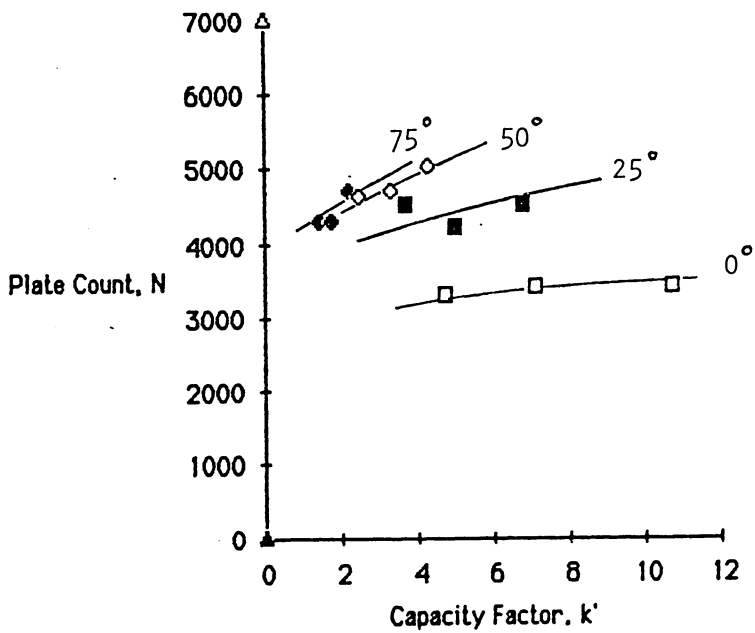


Figure 57. Column efficiency versus temperature for a water jacketed microbore column.

Column - 25 cm x 1 mm ID  
 Sorbent - LiChrosorb RP-18, 10  $\mu$ m  
 Solvent - 90/10 MeOH/H<sub>2</sub>O  
 Flow Rate - 100  $\mu$ l/min.  
 Sample - C<sub>8</sub>-C<sub>10</sub> Alkyl Benzenes

data is to express the change in concentration resulting from exposing a known volume of binary solvent to a fixed weight of adsorbent. This is expressed as

$$\Gamma = V \Delta C / wt \quad (20)$$

where  $V$  is the volume,  $\Delta C$  is the concentration change and  $wt$  is the weight, and  $\Gamma$  is the apparent or composite surface excess (133). A plot  $\Gamma$  versus the equilibrium mole fraction of methanol in the mixtures at the three temperatures is shown in Figure 58.

The effect raising the temperature has on the composite isotherm is to reduce the magnitude of the change in concentration brought about by interaction with the surface. This means a smaller amount of the mobile phase is under control of the stationary phase. For low energy physical adsorption, the residence time of an individual molecule in the surface is brief. Net adsorption of one component over another means that one component is statistically more likely to be on the surface than the other. Thermal agitation causes the residence times of both species to decrease, which is consistent with the observed reduction in the composite isotherm with temperature. While the precision of most composite isotherm determinations makes detailed conclusions questionable, it is seen that no shift in the asymmetry of the composite adsorption isotherm

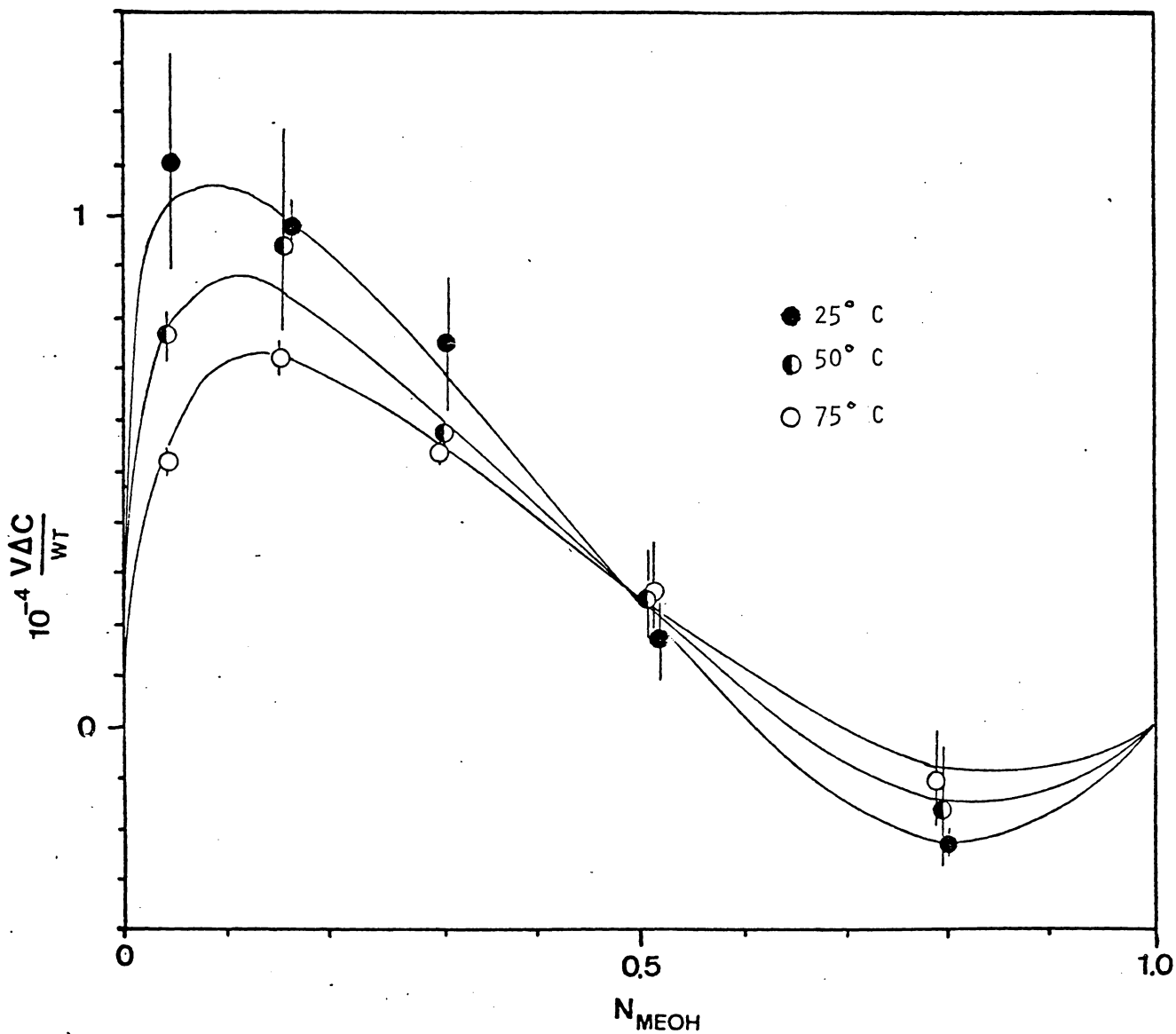


Figure 58. Composite adsorption isotherms for methanol/water mixtures on RP-18 as a function of temperature.

with temperature occurred, suggesting that the composition of the adsorbed layer remains fairly constant with temperature. Reduction in capacity factors with temperature can be accounted for by a change in the partition coefficient, a decrease in adsorption, a reduction in the stationary phase mass, but probably not by compositional change in the stationary phase.

#### 5.2.6 TEMPERATURE PROGRAMMING

Chromatograms obtained programming the temperature during a run are shown for different mobile phase compositions in Figure 59. Table XVI lists the isothermal and temperature programmed retention times, showing that with a greater room temperature retention (high  $\Delta H$ ), temperature has a much greater influence on retention times. Peak widths are nearly constant for the weaker (more aqueous) mobile phases, when retention becomes governed mainly by the column temperature (Table XVII).

#### 5.2.7 TEMPERATURE PROGRAMMING VS SOLVENT PROGRAMMING

The Varian 5000 gradient LC pump with the splitter provided a means of producing microbore gradients. This allowed a direct comparison to be made between solvent programming and

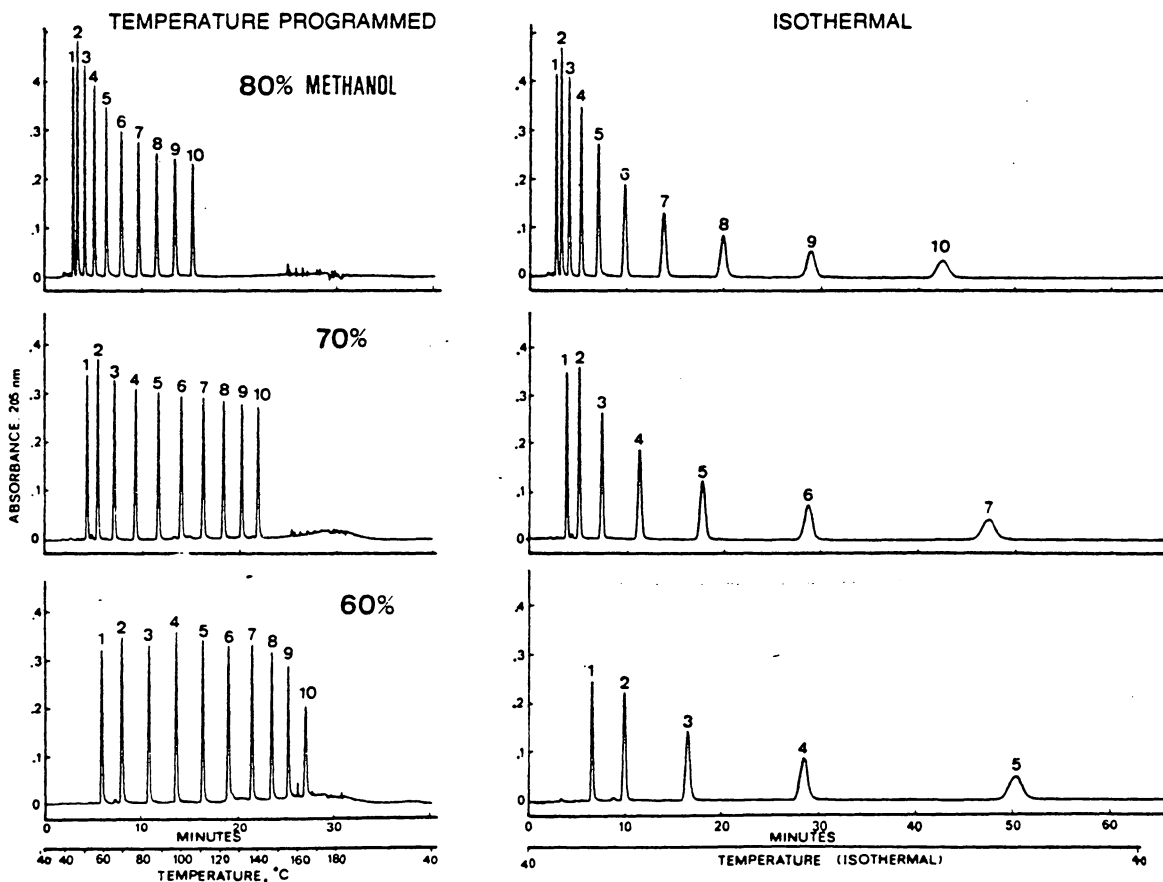


Figure 59. Temperature programmed microbore HPLC.

Column - 25 cm x 1 mm ID  
 Sorbent - LiChrosorb RP-18, 10  $\mu$ m  
 Sample - C<sub>1</sub>-C<sub>10</sub> Alkyl Benzenes

Left - Temperature Programmed at 5° C./min.  
 from 40° C. to 180° C.  
 Right - Isothermal at 40° C.

Table XVI

Temperature programmed versus isothermal retention times as a function of mobile phase composition.

Flow Rate - 100  $\mu$ l/min.  
 Isothermal Temperature - 20° C.  
 Temperature Program - 5°/min. from  
 20° to 150° C.

nc	90/10 MeOH/H <sub>2</sub> O			80/20 MeOH/H <sub>2</sub> O		
	IsoTh.	Tem. Pr.	%	IsoTh.	Tem. Pr.	%
1	2.47	2.48	100.5	3.23	3.27	101.2
2	2.66	2.68	100.7	3.83	3.85	100.5
3	2.97	2.98	100.3	4.80	4.73	98.5
4	3.39	3.40	100.2	6.28	5.91	94.1
5	3.93	3.94	100.2	8.45	7.42	87.8
6	4.67	4.60	98.5	11.70	9.28	79.3
7	5.68	5.44	95.8	16.61	11.42	68.8
8	7.02	6.45	91.9	23.89	15.94	66.7
9	8.79	7.63	86.8	34.80	15.94	45.8
10	11.15	8.96	80.4	51.19	18.12	35.4

nc	70/30 MeOH/H <sub>2</sub> O			60/40 MeOH/H <sub>2</sub> O		
	IsoTh.	Tem. Pr.	%	IsoTh.	Tem. Pr.	%
1	4.77	4.95	103.8	7.98	6.99	87.6
2	6.28	6.26	99.7	11.97	9.46	79.0
3	9.11	8.30	91.1	19.88	12.78	64.3
4	13.87	10.90	78.6	34.31	16.21	47.2
5	21.66	13.77	63.6	60.60	19.53	32.2
6	34.71	16.62	47.9	110.70	22.73	20.5
7	57.16	19.37	33.9	205.17	25.14	12.3
8	94.77	21.87	23.1	380.73	27.64	7.3
9	157.39	24.11	15.3	708.61	30.68	4.3
10	264.52	26.09	9.9	1320.10	34.20	2.6

Table XVII

Peak Widths ( $\sigma$ , in seconds) vs carbon number  
for alkyl benzenes in temperature programmed LC

nc	90/10	80/20	70/30	60/40
1	2.95	3.07	3.31	4.24
2	3.07	3.31	4.02	4.96
3	3.18	3.78	4.49	5.20
4	3.43	4.25	4.82	5.43
5	3.67	4.77	5.20	5.67
6	3.93	4.96	5.43	5.20
7	4.28	5.10	5.67	4.96
8	4.68	5.34	5.20	4.25
9	4.93	5.53	4.96	5.20
10	5.41	5.52	4.72	6.14

temperature programming. Conditions for the solvent gradient were 60/40 methanol-water to 100% methanol in 30 minutes, isothermally at 30° C. The temperature gradient conditions were 30° to 180° C at 5° C./min., run isocratically at 60/40 methanol. Both gradients start at exactly the same solvent strength and based on conclusions from previous sections, they both provide the same rate of solvent strength change during the run. The resulting chromatogram is shown in Figure 60. Temperature programming mimicked solvent programming during the first half of the run, but since the air heating system was required for temperatures above 100° C, the later peaks exhibit slightly longer and slightly broader retention due to extra retention on the slightly cooler initial portion of the column. A temperature programming using a liquid temperature control heating system would be expected to be capable of duplicating the solvent program chromatogram.

### 5.3 FUTURE WORK

A sealed, pressurized small volume liquid circulation temperature control system should be assembled and its temperature programmed performance tested. Columns should be packed with a buffer region on both ends comprised of small particle glass beads, which would provide the mobile phase more time to

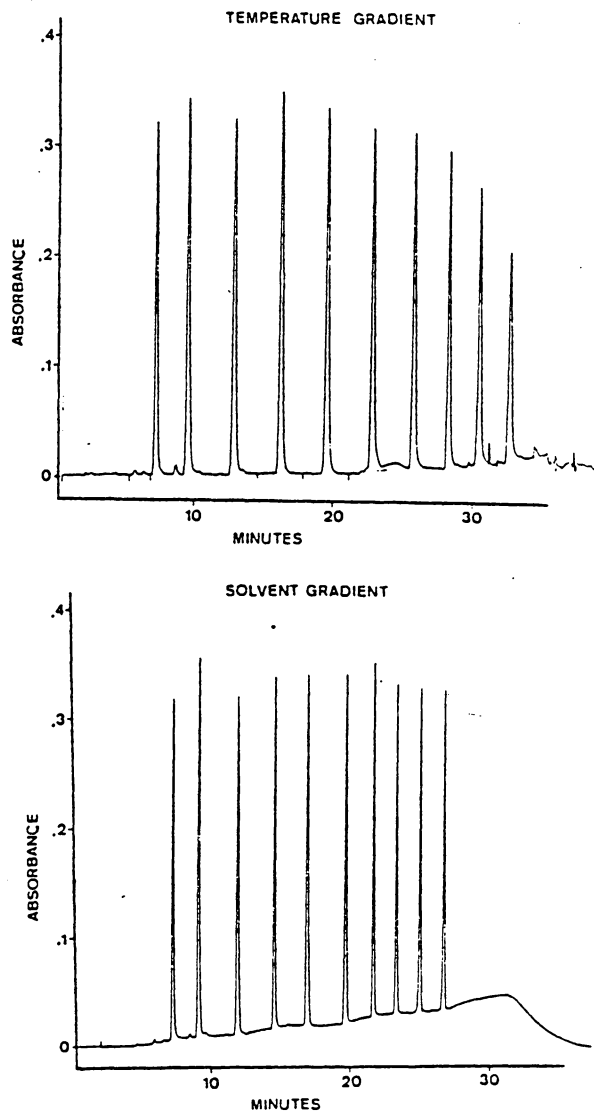


Figure 60. Comparison of solvent and temperature gradients.  
 Sample - C<sub>1</sub>-C<sub>10</sub> Alkyl Benzenes  
 Conditions in text.

come up to the column temperature, since it seems to be difficult to completely eliminate the cooling effects of the mobile phase when it flows through the injector. Megabore 0.51 mm ID fused silica columns would provide a lower thermal mass than 1/16" SST, and the importance of the thermal response time of the column tubing could be deduced by a comparison of the chromatographic performance obtained using either fused silica and stainless steel columns. Verification of the source of the waxy polymer removed from the column during conditioning, specifying whether it comes from chemical cleavage of the bound  $C_{18}$  groups or simple desorption of excess polymer adsorbed on the surface, would aid in assessing column stability. Some work has been done evaluating polymer based sorbents for temperature programmed work. Preliminary results suggest that with temperature programming, monomer cleavage from a polystyrene-divinyl benzene sorbent causes a rise in the UV absorbance of the mobile phase, limiting the maximum programmed temperature to 130° C. This maximum temperature depends to some extent to the original strength of the mobile phase. The rise in UV absorbance is inversely proportional to the flow rate, consistent with a fixed rate of dissolution of monomer. Complete results will be published shortly (136).

## 6.0 CONCLUSIONS

It was shown that microbore columns may be successfully used with conventional volume injectors and detectors. No loss in resolution was observed when non-eluting solvents were used during injection. Losses in resolution caused by 8  $\mu$ l detector cells were confined to the earliest eluting peaks ( $k' < 2$ ). This allows the utilization of microbore columns without the sensitivity loss of special low volume micro LC instrumentation. The use of polished tubing was shown to double the efficiency of a column compared to non-polished tubing. Polished tubing also provides stability against void formation.

Specification of the effect of temperature on retention was hindered by the failure of the linearization of homologous series to provide a single, unambiguous column void volume estimate, making calculated values for the  $k'$  uncertain. Effects on the  $V_0$  estimate by the influence of the pendant groups, the precision of the measured retention volumes, possible changes of the sorbent during conditioning and the existence of a temperature gradient along the column length were examined. While they were shown to influence the final  $V_0$  value, they could not completely account for the discrepancy

between the maximum possible  $V_0$  and that estimated by the various linearization procedures. Based on these results, it is concluded that the relationship between the log of the capacity factor and the number of carbon atoms in the alkyl side chain of a homologous series is non-linear at lower temperatures, with weaker mobile phases, and for more retained homologous series. This conclusion has been reached by other investigators (93, 95, 98) and casts serious doubt on the validity of the linearization of homologous series when used to provide a reliable estimate of the void volume. As with the use on "non-retained" species for  $V_0$  estimates (73, 106, 109),  $V_0$  values by linearization of homologous series are valid only over a limited range of solvent strengths.

A possible explanation for this non-linearity other than the pendant group effect might be that different members in a series experience different void volumes depending on the degree of interaction they have with the stationary phase. Very long homologs ( $n_c > 20$ ) may be partially excluded from the pore structure of the sorbent. Another source of size exclusion may come from the ability of different sample molecules to penetrate the adsorbed layer of solvent on the stationary phase to varying degrees. Non-polar solutes are expected to have the most affinity for the non-polar stationary phase and experi-

ence a greater  $V_0$  than polar molecules which are more repelled from this region. This is consistent with the data in Table XI, where the more non-polar series provide larger  $V_0$  estimates. The series are listed left-to-right in the order of the most retained to the least retained series. While the volume of a monolayer of methanol, assuming a methyl surface area of  $20 \text{ \AA}^2$  and a  $250 \text{ M}^2/\text{g}$  surface area of the underivatized sorbent, is only  $8 \text{ \mu l}$ , solvation of each of the  $\text{C}_{18}$  chains bound to the surface greatly increases the available surface area of the sorbent and thus the volume that this monolayer occupies. If all molecular interactions are confined to a region with only monolayer dimensions, changes in the dimensions of the sample species on the atomic scale are apt to play an important role in the retention of those species. The non-linearity of  $\ln k'$  vs  $n_c$  within a single series may possibly come about through the decreased ability of the longer homologs to completely fit within this region in all statistically probable orientations compared to the smaller members. This exclusion of the larger members from the monolayer would mean that the smaller members see a slightly larger  $V_0$  and this would result in an upward curvature in  $\ln k'$  vs  $n_c$  plots if the  $V_0$  estimates from the longer homologs was used to calculate the  $k'$ s for the shorter members. The linearization procedure will counter this curvature by increasing the  $V_0$  estimate beyond what is reasonable.

With polar homologous series, the large potential  $V_0$  for the smaller members is restricted by their repulsion from the non-polar stationary phase, and is replaced by steric exclusion for longer members. In this way, the void volume experienced by polar solutes do not appear to depend as much on carbon number, and the  $\ln k'$  vs  $n_c$  plots give reasonable  $V_0$  estimates. It should be stressed these are merely rationalizations of the observations made in this study, and other factors such as the pendant group effects also play an important role in the observed non-linearity.

An examination of the change in the adsorbed layer of mobile phase with temperature showed that a decreased amount of mobile phase was under the control of the sorbent. This is reasonable based on simple energetics considerations. Higher temperatures lead to decreased adsorption for all species.

The equivalence of temperature to mobile phase composition was demonstrated, showing that the maximum increase in temperature would be equivalent to a 40% increase in methanol content of the mobile phase. While this illustrates the superiority of solvent programming, not all analyses require a gradient program with the maximum change in solvent strength for optimal elution. Temperature programming was shown to provide a

14-fold reduction in analysis time for a mixture of  $C_1$ - $C_{10}$  n-alkyl benzenes in 60/40 methanol/water going from 40° C to 180° C. For many analyses, this improvement in speed (and sensitivity) is sufficient justification for the use of temperature gradients in LC. These improvements comes about using simple, inexpensive instrumentation and avoid the high cost of a microbore solvent gradient system.

An increase in efficiency with temperature was seen only for a liquid bath temperature control system. The failure of the air circulation system to provide improvements with temperature were attributed to its inability to transfer heat to the column rapidly enough to eliminate the formation of a "cold spot" at the head of the column, which exaggerated the retention of more retained sample components. The liquid circulation system could not be used for temperature programming since its maximum program rate was too slow to provide noticeable chromatographic improvements at typical flow rates. This highlighted the need to construct a liquid temperature control system with a faster response time than currently available instrumentation for temperature programmed LC. While a direct comparison of solvent and temperature programmed LC showed chromatograms that were very similar, the temperature programmed chromatogram showed slightly lower performance due to

the debilitating effects of a cold spot at the head of the column using the air temperature control system. Small volume liquid temperature control systems should be employed to obtain the highest performance for temperature programmed microbore LC.

## VOID VOLUME DETERMINATION

### Appendix A.

Three methods were used to deduce the column void volume  $V_0$  from the retention volumes measured for members of homologous series. They have been used by Berendsen (102), Grobler (109) and Mockel (92) and for ease of reference these names will be used as labels in describing them. While they all rely on the existence of a linear relationship between the log of the capacity factor and the number of carbon atoms in the alkyl side chain of the homolog ( $n_c$ ), they each reduce the data by different pathways and non-linearities in the original data set will influence the final  $V_0$  in different ways.

Berendsen's method and Grobler's method both require retention volumes for consecutive members in the series, and as such can not be easily used whenever intermediate members of a series are missing. Mockel's method can be used without a complete set of homologs, but it requires much longer computational times than either Berendsen's or Grobler's methods.

## BERENDSEN'S METHOD

$k'_1$  = capacity factor of the  $n^{\text{th}}$  homolog

$k'_2$  = capacity factor of the  $n+1^{\text{th}}$  homolog

$$\alpha = k'_2/k'_1$$

$V_{r1}$  = retention volume for the  $n^{\text{th}}$  homolog

$V_{r2}$  = retention volume for the  $n+1^{\text{th}}$  homolog

$V_0$  = the void volume

Given:  $k'_2 = (V_{r2} - V_0)/V_0$

$$k'_1 = (V_{r1} - V_0)/V_0$$

$$\alpha = k'_2/k'_1$$

Then:  $\alpha = (V_{r2} - V_0)/(V_{r1} - V_0)$

$$\alpha V_{r1} - \alpha V_0 = V_{r2} - V_0$$

$$\alpha V_{r2} - V_0 + V_0 = V_{r2}$$

$$\alpha V_{r2} - (\alpha - 1)V_0 = V_{r2}$$

Plot:  $V_{r2}$  vs  $V_{r1}$

$$\text{Slope} = \alpha$$

$$\text{Intercept} = (\alpha - 1)V_0$$

$$V_0 = \text{Intercept}/(\text{Slope} - 1)$$

## GROBLER'S METHOD

$nc_1$  = carbon number for the  $n^{\text{th}}$  homolog

$nc_2$  = carbon number for the  $(n+1)^{\text{th}}$  homolog

$C_1, C_2$  = constants

Assume: 
$$V_{r2} = V_0 + C_1 e^{C_2 nc_2}$$

$$V_{r1} = V_0 + C_1 e^{C_2 nc_1}$$

$$V_{r2} - V_{r1} = C_1 (e^{C_2 nc_2} - e^{C_2 nc_1})$$

$$\ln(V_{r2} - V_{r1}) = \ln C_1 + C_2(nc_2 - nc_1)$$

Plot:  $\ln(V_{r2} - V_{r1})$  vs  $nc$

Slope =  $C_2$

Again: 
$$V_r = V_0 + C_1 e^{C_2 nc}$$

Plot:  $V_r$  vs  $e^{C_2 nc}$

Intercept =  $V_0$

## MOCKEL'S METHOD

Mockel's method assumes that when the correct value for the  $V_0$  is chosen, a perfectly straight line will describe the relationship between  $\ln k'$  and the number of carbon atoms in the alkyl side chain of the homolog,  $n_c$ . The correlation coefficient,  $r$ , gives the degree of linearity of a line, and when  $r = 1$ , the line is perfectly straight. The  $V_0$  value producing an  $r$  value closest to 1 is assumed to be the best  $V_0$  estimate.

Numerically, the procedure first requires a reasonable range for  $V_0$  be defined. Next, that range is divided into a number of points and each of those points is used to calculate the log of the capacity factor.

$$\ln k' = \ln (V_r - V_0)/V_0$$

With  $X = n_c$ ,  $Y = \ln k'$ , and  $N =$  the number of data points in the regression analysis, the correlation coefficient is calculated using the following equations:

$$A = N\sum X^2 - (\sum X)^2$$

$$B = (N\sum XY - \sum X\sum Y)/A$$

$$C = (\sum X^2\sum Y - \sum X\sum XY)/A$$

$$D = (\sum Y^2 - B\sum XY - C\sum Y)/(N-2)$$

$$E = (N\sum Y^2 - (\sum Y)^2)/N(N-1)$$

$$r = \sqrt{1 - (D/E)}$$

A means of decreasing the computation time was used, in which an initially wide range of  $V_0$  values was divided into 20 points. The  $V_0$  value giving the largest  $r$  value in that range was used to center the next range and  $\pm 1$  point from that center was divided into 20 points. This was repeated a third time, so that the precision of 2000 analyses requires only 60 regression analyses.

## B.0 HOMOLOGOUS SERIES PROGRAM

The following program, written in Basic, reduces the retention times measured for the homologous series and calculates void volumes by the three linearization methods.

```
2 DIM V(3,6,6,11)
6 FOR X=1 TO 3
10 FOR Y=1 TO 6
14 FOR Z=1 TO 6
18 FOR W=1 TO 11
22 V(X,Y,Z,W)=0
26 NEXT W
30 NEXT Z
34 NEXT Y
38 NEXT X
42 OPEN "O",#1,"PRNT:"
46 FOR X=1 TO 3
50 FOR Y=1 TO 6
54 READ D(X,Y)
58 NEXT Y
62 NEXT X
66 DATA .8602,.84337,.82438,.79958,.77784,.754
70 DATA .91305,.89853,.87919,.85857,.83639,.814
74 DATA .94915,.93822,.92167,.90332,.88619,.865
78 FOR X=1 TO 3
82 FOR Y=1 TO 6
86 FOR Z=1 TO 6
90 READ F,N
94 FOR W=1 TO N
98 READ U
102 READ V
106 V(X,Y,Z,U)=(V*F*D(X,Y))/(D(X,3)*1000)
110 NEXT W
114 NEXT Z
118 NEXT Y
122 NEXT X
126 DEFDBL B-J
130 M=5
134 X1=2:Y1=1:Z1=1
135 PRINT X1,Y1,Z1,M
138 GOTO 603
142 B=0:C=0:D=0:E=0:F=0:G1=0:G2=0
146 S1=0:S2=0:S3=0:S4=0:S5=0:S6=0:S7=0:S8=0
150 FOR N=M TO 10
154 X=V(X1,Y1,Z1,N):Y=V(X1,Y1,Z1,N+1):Z=N
158 Q1=0:Q2=0
162 IF X>0 THEN 170
166 Q1=1
```



```

382 K1# = LOG( (V(X1, Y1, Z1, N) / T#) - 1 )
386 G3 = G3 + 1
390 B = B + N
394 C = C + K1#
398 D = D + N * K1#
402 F = F + (N * N)
406 F = F + (K1# * K1#)
410 NEXT N
414 O = G3
418 G = ( (O * F) - (B * B) )
422 IF G3 <= 2 THEN 458
426 S# = ( (O * D) - (B * C) ) / G
430 U# = ( (E * C) - (B * D) ) / G
434 S2# = ( (O * F) - (C * C) ) / (O * (O - 1))
438 S1# = ( (F - (U# * C) - (S# * D) ) / (O - 2) )
442 R1# = ( 1 - (S1# / S2#) )
446 IF R1# > K# THEN 454
450 GOTO 458
454 K# = R1# : Q# = T# : S3# = S# : I3# = U# : G5 = G3
458 T# = T# + J
462 IF T# >= I THEN 470
466 GOTO 370
470 T1 = T1 + 1
474 GOTO 334
478 IF G5 >= 2 THEN 478
476 PRINT #1, "NO MOCKEL DATA"
477 GOTO 550
478 PRINT #1, USING "MOCKEL EST V0=#.###" ; Q#;
482 PRINT #1, USING "LOG A=#.###"; S#;
486 PRINT #1, USING " LOG B=#.###"; U#
488 PRINT #1
490 PRINT #1, "R="; K#
494 PRINT #1
498 PRINT #1, " K' LOG K' "
502 FOR N=1 TO 11
510 K3 = (V(X1, Y1, Z1, N) / Q#) - 1
522 PRINT #1, USING " ## "; N;
542 IF K3 > 0 THEN 550
546 PRINT #1
547 GOTO 554
550 PRINT #1, USING "###.## ###.###" ; K3;
LOG(K3)
554 NEXT N
558 Y1 = Y1 + 1
562 IF Y1 = V THEN 568
566 GOTO 135
568 Y1 = 1
570 Z1 = Z1 + 1
574 IF Z1 = V THEN 580
578 GOTO 135
580 Z1 = 1
582 X1 = X1 + 1
586 IF X1 = 4 THEN 594
590 GOTO 135

```

```

594 X1=1
595 M=5
596 GOTO 135
603 PRINT #1
604 PRINT #1
605 PRINT #1
606 IF Z1=1 THEN PRINT #1, "ALKYL BENZENES";
610 IF Z1=2 THEN PRINT #1, "BENZOATES";
614 IF Z1=3 THEN PRINT #1, "PHENONES";
618 IF Z1=4 THEN PRINT #1, "PARABENS";
622 IF Z1=5 THEN PRINT #1, "ACETATES";
626 IF Z1=6 THEN PRINT #1, "KETONES";
630 IF X1=1 THEN PRINT #1, "    90/10 ";
634 IF X1=2 THEN PRINT #1, "    70/30 ";
638 IF X1=3 THEN PRINT #1, "    50/50 ";
642 PRINT #1, "METHANOL/WATER  "
643 PRINT #1, "TEMPERATURE=";
644 IF Y1=1 THEN PRINT #1, "-20"
645 IF Y1=2 THEN PRINT #1, "0"
646 IF Y1=3 THEN PRINT #1, "25"
647 IF Y1=4 THEN PRINT #1, "50"
648 IF Y1=5 THEN PRINT #1, "75"
649 IF Y1=6 THEN PRINT #1, "100"
650 GOTO 142
654 FOR M=1 TO 10
658 PRINT #1, USING"## ";M;
662 FOR Y=1 TO 6
666 P1=0:P2=0
670 IF V(X,Y,Z,M)-Q>0 THEN 678
674 GOTO 682
678 P1=1
682 IF V(X,Y,Z,M+1)-Q>0 THEN 690
686 GOTO 694
690 P2=1
694 IF P1+P2=2 THEN 706
698 PRINT #1, "    ";
702 GOTO 710
706 PRINT #1, USING "##.### "; LOG(V(X,Y,Z,M)-Q)
-LOG(V(X,Y,Z,M+1)-Q);
710 NEXT Y
714 PRINT #1
718 NEXT M
722 PRINT #1
726 PRINT #1
730 PRINT #1
734 PRINT #1
738 PRINT #1
742 NEXT Z
746 PRINT#1
750 PRINT #1
754 NEXT X
1110 DATA 221, 10, 1, 1.155, 2, 1.27, 3, 1.49, 4, 1.79, 5,
2.31
1111 DATA 6, 3.06, 7, 4.53, 8, 6.895, 9, 12.15, 10, 23.17

```

1120 DATA 221, 6, 3, 1.195, 4, 1.37, 5, 1.675, 6, 2.14, 7,  
2.945, 8, 4.325  
1130 DATA 221, 4, 5, 1.205, 7, 1.43, 9, 2.495, 11, 6.69  
1140 DATA 221, 5, 4, 1.105, 5, 1.27, 6, 1.54, 7, 1.985, 8,  
2.71  
1150 DATA 221, 6, 4, .93, 5, 1.015, 6, 1.16, 7, 1.36, 8, 1.  
75, 9, 2.39  
1160 DATA 221, 4, 6, 1.06, 7, 1.22, 8, 1.49, 9, 1.95  
1210 DATA 234, 10, 1, 1.10, 2, 1.205, 3, 1.39, 4, 1.65, 5,  
2.03  
1211 DATA 6, 2.57, 7, 3.41, 8, 4.60, 9, 6.47, 10, 9.29  
1220 DATA 234, 6, 3, 1.11, 4, 1.265, 5, 1.49, 6, 1.795, 7,  
2.26, 8, 2.93  
1230 DATA 234, 5, 4, 1.095, 5, 1.255, 7, 1.83, 9, 3.095, 1  
1, 6.23  
1240 DATA 234, 5, 4, .98, 5, 1.10, 6, 1.265, 7, 1.5, 8, 1.8  
4  
1250 DATA 234, 6, 4, .9, 5, .975, 6, 1.09, 7, 1.25, 8, 1.50  
5, 9, 1.845  
1260 DATA 234, 4, 6, .995, 7, 1.125, 8, 1.30, 9, 1.565  
1310 DATA 239, 10, 1, 1.025, 2, 1.11, 3, 1.25, 4, 1.44, 5,  
1.69  
1311 DATA 6, 2.04, 7, 2.525, 8, 3.165, 9, 4.035, 10, 5.21  
5  
1320 DATA 239, 6, 3, 1.025, 4, 1.135, 5, 1.28, 6, 1.485, 7  
, 1.76, 8, 2.125  
1330 DATA 239, 4, 5, 1.095, 7, 1.445, 9, 2.07, 11, 3.175  
1340 DATA 239, 3, 6, 1.06, 7, 1.20, 8, 1.38  
1350 DATA 239, 6, 4, .85, 5, .905, 6, 1.00, 7, 1.12, 8, 1.2  
7, 9, 1.485  
1360 DATA 239, 4, 6, .915, 7, 1.01, 8, 1.13, 9, 1.29  
1410 DATA 243, 10, 1, .93, 2, .995, 3, 1.09, 4, 1.225, 5, 1  
.385  
1411 DATA 6, 1.59, 7, 1.87, 8, 2.22, 9, 2.67, 10, 3.25  
1420 DATA 243, 6, 3, .91, 4, 1.00, 5, 1.095, 6, 1.225, 7, 1  
.39, 8, 1.60  
1430 DATA 243, 4, 5, .98, 7, 1.2, 9, 1.56, 11, 2.14  
1440 DATA 243, 3, 6, .92, 7, 1.01, 8, 1.11  
1450 DATA 243, 4, 6, .91, 7, 1.00, 8, 1.09, 9, 1.23  
1460 DATA 243, 3, 7, .905, 8, .99, 9, 1.1  
1510 DATA 239, 8, 3, .99, 4, 1.075, 5, 1.18, 6, 1.31, 7, 1.  
47, 8, 1.67, 9, 1.915, 10, 2.215  
1520 DATA 239, 3, 6, 1.06, 7, 1.16, 8, 1.28  
1530 DATA 239, 3, 7, 1.045, 9, 1.27, 11, 1.59  
1540 DATA 240, 1, 1, 0  
1550 DATA 241, 1, 1, 0  
1560 DATA 241, 1, 1, 0  
1610 DATA 240, 3, 3, .905, 4, .954, 5, 1.015, 6, 1.088, 7,  
1.183, 8, 1.2975, 9, 1.4305, 10, 1.591  
1620 DATA 240, 2, 7, .97, 8, 1.045  
1630 DATA 240, 3, 7, .91, 9, 1.06, 11, 1.23  
1640 DATA 241, 1, 1, 0  
1650 DATA 241, 1, 1, 0  
1660 DATA 241, 1, 1, 0

2110 DATA 113.1, 5, 1, 6.69, 2, 9.88, 3, 17.06, 4, 30.17,  
 5, 53.78  
 2120 DATA 113.1, 5, 1, 5.79, 2, 8.67, 3, 14.605, 4, 26.84  
 , 5, 52.08  
 2130 DATA 113.1, 4, 1, 2.77, 2, 3.92, 3, 5.44, 4, 9.01  
 2140 DATA 113.1, 8, 1, 2.69, 2, 3.4, 3, 4.93, 4, 7.80, 5, 1  
 3.56, 6, 25.23, 7, 48.94, 8, 97.13  
 2150 DATA 113.1, 7, 1, 1.77, 2, 1.995, 3, 2.47, 4, 3.345,  
 5, 5.06, 6, 8.52, 7, 15.535  
 2160 DATA 113.1, 5, 2, 1.005, 3, 2.09, 5, 3.64, 6, 5.645,  
 7, 9.825  
 2210 DATA 234, 8, 1, 2.82, 2, 4.04, 3, 6.59, 4, 11.15, 5, 1  
 9.83, 6, 36.04, 7, 68.37, 8, 129.28  
 2220 DATA 234, 8, 1, 1.69, 2, 2.26, 3, 3.34, 4, 5.33, 5, 9.  
 05, 6, 16.01, 7, 29.46, 8, 54.59  
 2230 DATA 234, 6, 1, 1.230, 2, 1.64, 3, 2.20, 4, 3.24, 5, 5  
 .48, 7, 17.35  
 2240 DATA 234, 8, 1, 1.10, 2, 1.34, 3, 1.81, 4, 2.66, 5, 4.  
 24, 6, 7.17, 7, 12.66, 8, 22.91  
 2250 DATA 234, 9, 1, .85, 2, .95, 3, 1.15, 4, 1.51, 5, 2.17  
 , 6, 3.375, 7, 5.65, 8, 9.985, 9, 18.21  
 2260 DATA 234, 6, 2, .87, 3, 1, 5, 1.62, 6, 2.35, 7, 3.73, 9  
 , 11.15  
 2310 DATA 235, 10, 1, 2.21, 2, 3.03, 3, 4.555, 4, 7.17, 5,  
 11.585  
 2311 DATA 6, 19.19, 7, 32.525, 8, 55.26, 9, 94.56, 10, 16  
 2.30  
 2320 DATA 235, 8, 1, 1.38, 2, 1.77, 3, 2.445, 4, 3.625, 5,  
 5.6, 6, 8.99, 7, 14.79, 8, 24.615  
 2330 DATA 235, 7, 1, 1.065, 2, 1.34, 3, 1.73, 4, 2.42, 5, 3  
 .61, 7, 9.085, 9, 25.025  
 2340 DATA 235, 8, 1, .91, 2, 1.05, 3, 1.32, 4, 1.78, 5, 2.5  
 6, 6, 3.9, 7, 6.17, 8, 10.01  
 2350 DATA 235, 9, 1, .815, 2, .895, 3, 1.06, 4, 1.32, 5, 1.  
 77, 6, 2.525, 7, 3.835, 8, 6.05, 9, 9.87  
 2360 DATA 235, 6, 2, .83, 3, .92, 5, 1.39, 6, 1.87, 7, 2.71  
 , 9, 6.49  
 2410 DATA 237, 10, 1, 1.72, 2, 2.24, 3, 3.125, 4, 4.555, 5  
 , 6.755  
 2411 DATA 6, 10.305, 7, 15.985, 8, 24.99, 9, 39.37, 10, 6  
 1.93  
 2420 DATA 237, 8, 1, 1.175, 2, 1.435, 3, 1.86, 4, 2.55, 5,  
 3.635, 6, 5.35, 7, 8.055, 8, 12.29  
 2430 DATA 237, 8, 1, .9, 2, 1.1, 3, 1.36, 4, 1.78, 5, 2.45,  
 7, 5.22, 9, 12.16, 11, 29.34  
 2440 DATA 241, 1, 1, 0  
 2450 DATA 237, 8, 2, .785, 3, .845, 4, .975, 5, 1.17, 6, 1.  
 465, 7, 1.94, 8, 2.7, 9, 3.9  
 2460 DATA 237, 6, 2, .795, 3, .875, 5, 1.215, 6, 1.535, 7,  
 2.045, 9, 4.10  
 2510 DATA 240, 10, 1, 1.4, 2, 1.715, 3, 2.225, 4, 2.99, 5,  
 4.095  
 2511 DATA 6, 5.76, 7, 8.245, 8, 11.9, 9, 17.31, 10, 25.33

2520 DATA 240, 8, 1, 1.02, 2, 1.19, 3, 1.46, 4, 1.86, 5, 2.  
44, 6, 3.3, 7, 4.57, 8, 6.42  
2530 DATA 240, 8, 1, .88, 2, 1.02, 3, 1.195, 4, 1.46, 5, 1.  
855, 7, 3.29, 9, 6.39, 11, 13.105  
2540 DATA 240, 5, 1, .765, 2, .815, 3, .925, 4, 1.085, 7, 2  
.135  
2550 DATA 240, 9, 1, .75, 2, .785, 3, .885, 4, 1.02, 5, 1.2  
15, 6, 1.5, 7, 1.94, 8, 2.57, 9, 3.51  
2560 DATA 240, 6, 2, .76, 3, .82, 5, 1.06, 6, 1.26, 7, 1.57  
, 9, 2.69  
2610 DATA 242, 10, 1, 1.165, 2, 1.36, 3, 1.645, 4, 2.05, 5  
, 2.60  
2611 DATA 6, 3.375, 7, 4.455, 8, 5.945, 9, 8.03, 10, 10.9  
25  
2620 DATA 242, 8, 1, .915, 2, 1.02, 3, 1.185, 4, 1.415, 5,  
1.715, 6, 2.14, 7, 2.735, 8, 3.54  
2630 DATA 242, 8, 1, .8, 2, .89, 3, 1.005, 4, 1.165, 5, 1.3  
85, 7, 2.125, 9, 3.52, 11, 6.18  
2640 DATA 242, 7, 2, .72, 3, .8, 4, .9, 5, 1.025, 6, 1.195,  
7, 1.435, 8, 1.76  
2650 DATA 242, 8, 2, .74, 3, .82, 4, .91, 5, 1.03, 6, 1.205  
, 7, 1.45, 8, 1.785, 9, 2.25  
2660 DATA 242, 5, 3, .755, 5, .93, 6, 1.055, 7, 1.24, 9, 1.  
84  
3110 DATA 89, 1, 1, 41.44  
3120 DATA 89, 3, 1, 22.58, 2, 43.98, 3, 97.96  
3130 DATA 89, 4, 1, 10.23, 2, 20.14, 3, 45.11, 4, 107.99  
3140 DATA 89, 4, 1, 12.12, 2, 21.99, 3, 48.14, 4, 111.10  
3150 DATA 89, 3, 3, 12.88, 4, 31.17, 5, 82.8  
3160 DATA 107, 6, 1, 1.96, 2, 2.4, 3, 3.43, 4, 6.06, 5, 13.  
35, 6, 33.21  
3210 DATA 218, 4, 1, 11.47, 2, 22.58, 3, 52.48, 4, 124.92  
3220 DATA 218, 5, 1, 5.88, 2, 11.09, 3, 23.40, 4, 53.59, 5  
, 128.68  
3230 DATA 218, 5, 1, 3, 2, 5.51, 3, 10.4, 4, 23.2, 5, 55.64  
3240 DATA 218, 5, 1, 2.82, 2, 4.845, 3, 9.84, 4, 21.6, 5, 5  
0.85  
3250 DATA 218, 5, 1, 1.459, 2, 2.26, 3, 4.3, 4, 9.46, 5, 22  
.54  
3260 DATA 218, 7, 1, .87, 2, 1.05, 3, 1.47, 4, 2.46, 5, 4.9  
7, 6, 11.19, 7, 27.18  
3310 DATA 224, 5, 1, 7.37, 2, 13.65, 3, 28.78, 4, 62.44, 5  
, 137.07  
3320 DATA 224, 6, 1, 3.76, 2, 6.59, 3, 12.83, 4, 26.70, 5,  
57.42, 6, 125.92  
3330 DATA 224, 5, 2, 3.07, 3, 6.35, 4, 12.71, 5, 27.13, 7,  
132.2  
3340 DATA 224, 7, 1, 1.72, 2, 2.7, 3, 4.89, 4, 9.75, 5, 20.  
46, 6, 44.11, 7, 96.49  
3350 DATA 224, 4, 3, 3.23, 4, 6.23, 5, 13.25, 6, 28.87  
3360 DATA 224, 8, 1, .82, 2, .98, 3, 1.31, 4, 2.03, 5, 3.67  
, 6, 7.28, 7, 15.49, 8, 33.71  
3410 DATA 227, 6, 1, 4.51, 2, 7.95, 3, 14.86, 4, 28.73, 5,  
56.58, 6, 112.49

3420 DATA 227,7,1,2.53,2,4.06,3,7.14,4,13.36,5,2  
 5.64,6,50.15,7,99.29  
 3430 DATA 227,6,1,1.65,2,2.45,3,4.02,4,7.18,5,13  
 .56,7,52.2  
 3440 DATA 227,8,1,1.25,2,1.76,3,2.8,4,4.87,5,8.9  
 7,6,17.06,7,33.05,8,64.07  
 3450 DATA 227,5,3,2.4,4,4.16,5,7.66,6,14.73,7,28  
 .93  
 3460 DATA 227,9,1,.78,2,.91,3,1.16,4,1.64,5,2.64  
 ,6,4.6,7,8.57,8,16.46,9,32.23  
 3510 DATA 227,7,1,3.08,2,4.87,3,8.19,4,14.29,5,2  
 5.47,6,45.9,7,83.35  
 3520 DATA 227,8,1,1.85,2,2.72,3,4.34,4,7.31,5,12  
 .66,6,22.32,7,39.90,8,71.42  
 3530 DATA 227,7,1,1.32,2,1.86,3,2.75,4,4.41,5,7.  
 45,7,23.03,9,73.97  
 3540 DATA 227,8,1,1.01,2,1.29,3,1.84,4,2.81,5,4.  
 58,6,7.74,7,13.45,8,23.5  
 3550 DATA 227,6,3,1.84,4,2.84,5,4.66,6,8,7,14.09  
 ,8,24.52  
 3560 DATA 227,9,1,.76,2,.87,3,1.06,4,1.4,5,2.02,  
 6,3.14,7,5.21,8,8.33,9,15.71  
 3610 DATA 227,8,1,2.23,2,3.19,3,4.91,4,7.8,5,12.  
 56,6,20.57,7,34.04,8,56.47  
 3620 DATA 227,8,1,1.45,2,1.96,3,2.84,4,4.33,5,6.  
 77,6,10.03,7,17.6,8,28.74  
 3630 DATA 227,7,1,1.12,2,1.46,3,1.99,4,2.89,5,4.  
 41,7,11.12,9,29.62  
 3640 DATA 227,8,1,.87,2,1.04,3,1.33,4,1.83,5,2.6  
 5,6,3.99,7,6.22,8,9.86  
 3650 DATA 227,7,3,1.47,4,2.055,5,3.035,6,4.675,7  
 ,7.415,8,11.35,9,24.35  
 3660 DATA 227,9,1,.74,2,.82,3,.96,4,1.19,5,1.59,  
 6,2.24,7,3.33,8,5.14,9,8.16

## C.0 ISOTHERM PROGRAM

The following program reduces the GC data from the column extract study and calculates the difference in concentration between the original mobile phase and that within the column.

```
10 OPEN "O", #1, "PRNT:
20 DIM I<5,8>,W<5,8,3>,M<5,8,3>,A<5,8,2>,T<5,8>,
   O<5,8>,C<5,8,3>,H<5,3>,V<5,8,3>,J<5,3>
30 FOR Y=1 TO 5
40 FOR X=1 TO 8
50 READ I<Y,X>
60 NEXT X
70 NEXT Y
80 FOR Y=1 TO 5
90 FOR X=1 TO 8
100 FOR N=1 TO 3
110 READ W<Y,X,N>,M<Y,X,N>
120 W<Y,X,N>=W<Y,X,N>*(I<Y,X>/.0759)
130 M<Y,X,N>=M<Y,X,N>*(I<Y,X>/.0759)
140 NEXT N
150 NEXT X
160 NEXT Y
200 Y=1
210 FOR X=1 TO 8
220 FOR N=1 TO 3
230 W<Y,X,N>=W<Y,X,N>/.9722000
240 M<Y,X,N>=M<Y,X,N>/.994417
250 NEXT N
260 NEXT X
270 FOR Y=2 TO 3
280 FOR X=1 TO 8
290 FOR N=1 TO 3
300 W<Y,X,N>=W<Y,X,N>/1.01674
310 M<Y,X,N>=M<Y,X,N>/1.03124
320 NEXT N
330 NEXT X
340 NEXT Y
350 FOR Y=4 TO 5
360 FOR X=1 TO 8
370 FOR N=1 TO 3
380 W<Y,X,N>=W<Y,X,N>/.990940
390 M<Y,X,N>=M<Y,X,N>/.990187
400 NEXT N
410 NEXT X
420 NEXT Y
```

```

430 GOTO 1200
500 FOR Y= 1 TO 5
510 READ K,D
520 FOR X=0 TO 8
530 READ G
540 T(Y,X)=D*(1-((K/1000)*G))
550 NEXT X
560 NEXT Y
600 FOR Y=1 TO 5
610 FOR X=1 TO 8
615 S1=0
620 FOR N=1 TO 3
625 S1=W(Y,X,N)+M(Y,X,N)+S1
626 NEXT N
627 IF X<3 THEN 660
630 PRINT #1, USING ".#### ",S1/(3*T(Y,X))
660 NEXT X
670 PRINT #1
680 NEXT Y
700 FOR Y=1 TO 5
710 FOR X=1 TO 8
720 S1=0:S2=0
730 FOR N=1 TO 3
740 S1=S1+W(Y,X,N)
750 S2=S2+M(Y,X,N)
760 NEXT N
770 A(Y,X,1)=S1/3
780 A(Y,X,2)=S2/3
790 NEXT X
800 NEXT Y
810 FOR Y=1 TO 5
820 FOR X=1 TO 8
830 S1=0:S2=0
840 FOR N=1 TO 3
850 S1=S1+((A(Y,X,1)-W(Y,X,N))^2)
860 S2=S2+((A(Y,X,2)-M(Y,X,N))^2)
870 NEXT N
880 S(Y,X,1)=(S1^.5)/2
890 S(Y,X,2)=(S2^.5)/2
900 NEXT X
910 NEXT Y
1000 FOR Y=1 TO 5
1010 FOR X=1 TO 8
1020 PRINT #1, USING "##### .##### ##.## ",A(Y
,X,1),S(Y,X,1),S(Y,X,1)*100/A(Y,X,1)
1030 NEXT X
1040 PRINT #1
1050 NEXT Y
1060 PRINT #1
1070 FOR Y=1 TO 5
1080 FOR X=1 TO 8
1090 PRINT #1, USING "##### .##### ##.## ",A(Y
,X,2),S(Y,X,2),S(Y,X,2)*100/(A(Y,X,2))
1100 NEXT X

```

```

1110 PRINT #1
1120 NEXT Y
1200 FOR Y=1 TO 5
1210 FOR X=1 TO 8
1220 FOR Z=1 TO 3
1260 V<Y,X,Z>=(M<Y,X,Z>/.7914)+(W<Y,X,Z>/.9985)
1270 NEXT Z
1280 NEXT X
1290 NEXT Y
1300 FOR Y=1 TO 5
1310 FOR F=1 TO 3
1311 I=0:Q=0:I1=0:Q1=0
1320 FOR X=(2*F+1) TO (2*F+2)
1330 FOR Z=1 TO 3
1340 FOR D=1 TO 3
1350 FOR E=1 TO 2
1360 I=I+W<Y,X,Z>-<W<Y,E,D>*<V<Y,X,Z>/V<Y,E,D>>>
1361 I1=I1+M<Y,X,Z>-<M<Y,E,D>*<V<Y,X,Z>/<V<Y,E,D>
>>>
1370 NEXT E
1380 NEXT D
1390 NEXT Z
1400 NEXT X
1410 H<Y,F>=I/36
1411 J<Y,F>=I1/36
1420 FOR X=(2*F)+1 TO (2*F)+2
1430 FOR Z=1 TO 3
1440 FOR D=1 TO 3
1450 FOR E=1 TO 2
1460 Q=Q+((<H<Y,F>-<W<Y,X,Z>-<W<Y,E,D>*<V<Y,X,Z>/
V<Y,E,D>>>)^2)
1461 Q1=Q1+((<J<Y,F>-<M<Y,X,Z>-<M<Y,E,D>*<V<Y,X,Z>
>/<V<Y,E,D>>>)^2)
1470 NEXT E
1480 NEXT D
1490 NEXT Z
1500 NEXT X
1510 S=(Q/35)^.5
1511 S1=(Q1/35)^.5
1520 PRINT #1, USING "# # ###.## ###.##";Y,F,H
<Y,F>*9407.34,S*9407.34
1521 PRINT #1, USING " ###.## ###.##";J<Y,F
>*9407.34,S1*9407.34
1530 NEXT F
1531 PRINT #1
1540 NEXT Y
2000 DATA .0773,.0757,.0780,.0764,.0768,.0771,.0
763,.0756
2010 DATA .0748,.0771,.0757,.0752,.0776,.0776,.0
753,.0788
2020 DATA .0763,.0748,.0770,.0769,.0774,.0774,.0
759,.0775
2030 DATA .0762,.0752,.0758,.0750,.0767,.0767,.0
771,.0783

```

2040 DATA .0762, .0750, .0742, .0781, .0770, .0783, .0  
 782, .0785  
 2050 DATA .01456, .10510, .01463, .10527, .01462, .10  
 532  
 2060 DATA .01505, .10935, .01529, .10961, .01512, .10  
 970  
 2070 DATA .01726, .11597, .01726, .11603, .01714, .11  
 632  
 2080 DATA .01725, .11693, .01737, .11699, .01737, .11  
 710  
 2090 DATA .01565, .11344, .01565, .11353, .01688, .11  
 374  
 2100 DATA .01707, .11406, .01703, .11413, .01698, .11  
 426  
 2110 DATA .01590, .10966, .01592, .10966, .01539, .10  
 997  
 2120 DATA .01651, .10919, .01657, .10932, .01664, .10  
 945  
 2130 DATA .04248, .08328, .04249, .08336, .04249, .08  
 324  
 2140 DATA .03842, .07525, .03916, .07535, .03932, .07  
 542  
 2150 DATA .04738, .09370, .04710, .09388, .04728, .09  
 380  
 2160 DATA .04783, .09529, .04700, .09546, .04793, .09  
 564  
 2170 DATA .04565, .09113, .04481, .09059, .04494, .09  
 074  
 2180 DATA .04484, .09150, .04527, .09160, .04522, .09  
 181  
 2190 DATA .04499, .08979, .04431, .08988, .04497, .09  
 011  
 2200 DATA .04314, .08759, .04327, .08763, .04333, .08  
 761  
 2210 DATA .07138, .05320, .07062, .05746, .07157, .05  
 814  
 2220 DATA .06954, .05675, .06956, .05668, .06972, .05  
 670  
 2230 DATA .07324, .06593, .07342, .06600, .07338, .06  
 595  
 2240 DATA .07643, .06672, .07643, .06671, .07625, .06  
 670  
 2250 DATA .07476, .06480, .07470, .06481, .07469, .06  
 481  
 2260 DATA .07473, .06507, .07496, .06516, .07502, .06  
 521  
 2270 DATA .07490, .06486, .07532, .06492, .07512, .06  
 492  
 2280 DATA .07318, .06336, .07406, .06401, .07408, .06  
 416  
 2290 DATA .10213, .03444, .10290, .03445, .10253, .03  
 451  
 2300 DATA .09117, .03055, .09114, .03046, .09009, .03  
 045

2310 DATA .10639, .04081, .10618, .04073, .10547, .04  
 053  
 2320 DATA .10757, .04077, .10781, .04104, .10793, .04  
 130  
 2330 DATA .10564, .04073, .10287, .04050, .10325, .04  
 077  
 2340 DATA .10698, .03986, .10733, .03981, .10669, .03  
 981  
 2350 DATA .10473, .03877, .10528, .03885, .10495, .03  
 897  
 2360 DATA .10388, .03827, .10386, .03834, .10370, .03  
 829  
 2370 DATA .14873, .01372, .14881, .01366, .15039, .01  
 369  
 2380 DATA .11908, .01078, .12047, .01096, .12124, .01  
 102  
 2390 DATA .14049, .01642, .13980, .01627, .13940, .01  
 633  
 2400 DATA .13101, .01689, .13158, .01697, .13020, .01  
 691  
 2410 DATA .13363, .01524, .13297, .01524, .13448, .01  
 523  
 2420 DATA .13312, .01501, .13303, .01500, .13319, .01  
 501  
 2430 DATA .13155, .01396, .13152, .01399, .13135, .01  
 396  
 2440 DATA .13122, .01387, .13135, .01389, .13174, .01  
 388  
 2450 DATA 1.0577, .8450  
 2460 DATA 27.2, 27.2, 48, 48.5, 79.5, 79.5  
 2470 DATA .9219, .9  
 2480 DATA 22.6, 23.4, 48.5, 48.5, 79.0, 78.5  
 2490 DATA .7754, .9416  
 2500 DATA 25.3, 25.3, 49.2, 48.5, 78.5, 78.8  
 2510 DATA .6038, .9714  
 2520 DATA 22.5, 23.3, 49.4, 49.2, 80.2, 80.3  
 2530 DATA .4547, .9938  
 2540 DATA 23.6, 24, 50, 49.9, 80.8, 80.8

## RETENTION VOLUMES

### Appendix D.

The following tables list the retention volumes, in  $\mu\text{l}$ , for each member of the homologous series, observed from a 25 cm x 1 mm ID column packed with LiChrosorb RP-18, as a function of column temperature and mobile phase composition.

All measured flow rate values were corrected for changes in density with temperature, and the retention volumes were calculated by multiplying this flow rate by the observed retention time.

Total column volume measured by picnometry was 140  $\mu\text{l}$ . Total extracolumn volume was measured as 15  $\mu\text{l}$ . Extracted volume by GC was 158  $\mu\text{l}$ . Column void volumes estimated from the following data are listed in Table XI.

- $n_c$  - Carbon Number
- Alkbnzs - Alkyl Benzenes
- Bnzoates - Benzoic Acid Esters
- Phenones - Alkyl Phenones
- Parabens - Para Hydroxy Benzoic Acid Esters
- Acetates - Acetic Acid Esters
- Ketones - 2-Ketones

		90/10 MeOH/H <sub>2</sub> O		Temperature = -20° C.		
nc	Alkbnzs	Bnzoates	Phenones	Parabens	Acetates	Ketones
1	245					
2	269					
3	316	253				
4	379	290		234	197	
5	489	355	255	269	215	
6	648	453		326	246	225
7	959	624	303	420	288	258
8	1460	916		574	371	316
9	2573		528		506	413
10	4907					
11			1417			

		90/10 MeOH/H <sub>2</sub> O		Temperature = 0° C.		
nc	Alkbnzs	Bnzoates	Phenones	Parabens	Acetates	Ketones
1	252					
2	276					
3	318	254				
4	377	289	250	224	206	
5	464	341	287	252	223	
6	588	411		289	249	228
7	780	517	419	343	286	257
8	1052	670		421	344	297
9	1480		708		422	358
10	2125					
11			1425			

		90/10 MeOH/H <sub>2</sub> O		Temperature = 25° C.		
nc	Alkbnzs	Bnzoates	Phenones	Parabens	Acetates	Ketones
1	245					
2	265					
3	299	245				
4	344	271			203	
5	404	306	262		216	
6	488	355		258	239	219
7	603	421	345	287	268	241
8	756	508		330	304	270
9	964		495		355	308
10	1246					
11			759			

		90/10 MeOH/H <sub>2</sub> O		Temperature = 50° C.		
nc	Alkbnzs	Bnzoates	Phenones	Parabens	Acetates	Ketones
1	233					
2	249					
3	273	228				
4	307	251				
5	347	274	246			
6	398	307		230	228	
7	469	348	301	253	251	227
8	556	401		278	273	248
9	669		391		308	276
10	814					
11			536			

		90/10 MeOH/H <sub>2</sub> O		Temperature = 75° C.		
nc	Alkbnzs	Bnzoates	Phenones	Parabens	Acetates	Ketones
1						
2						
3	251					
4	272					
5	299					
6	332	268				
7	372	294	265			
8	423	324				
9	485		322			
10	561					
11			403			

		90/10 MeOH/H <sub>2</sub> O		Temperature = 100° C.		
nc	Alkbnzs	Bnzoates	Phenones	Parabens	Acetates	Ketones
1						
2						
3	237					
4	250					
5	266					
6	285					
7	310	255	239			
8	340	274				
9	375		278			
10	417					
11			323			

		70/30 MeOH/H <sub>2</sub> O		Temperature = -20° C.		
nc	Alkbnzs	Bnzoates	Phenones	Parabens	Acetates	Ketones
1	729	631	302	293	193	
2	1076	944	427	370	217	197
3	1858	1591	592	537	269	228
4	3286	2923	981	849	364	
5	6401	5672		1477	551	396
6				2748	928	615
7				5330	1692	1070
8				10578		
9						
10						
11						

		70/30 MeOH/H <sub>2</sub> O		Temperature = 0° C.		
nc	Alkbnzs	Bnzoates	Phenones	Parabens	Acetates	Ketones
1	646	387	282	252	195	
2	925	517	376	307	218	199
3	1509	765	504	414	263	229
4	2553	1220	742	609	346	
5	4540	2072	1255	971	497	371
6	8252	3666		1642	773	538
7	15654	6745	3973	2899	1294	854
8	29600	12499		5246	2286	
9					4169	2553
10						
11						

		70/30 MeOH/H <sub>2</sub> O		Temperature = 25° C.		
nc	Alkbnzs	Bnzoates	Phenones	Parabens	Acetates	Ketones
1	519	324	250	214	192	
2	712	416	315	247	210	195
3	1070	575	407	310	249	216
4	1685	852	569	418	416	
5	2722	1316	848	602	593	327
6	4510	2113		917	901	439
7	7643	3476	2135	1450	1422	637
8	12986	5785		2352	2319	
9	22222		5881			1525
10	38141					
11						

		70/30 MeOH/H <sub>2</sub> O			Temperature = 50° C.	
nc	Alkbnzs	Bnzoates	Phenones	Parabens	Acetates	Ketones
1	417	285	218			
2	544	348	267		191	193
3	758	451	330		205	212
4	1105	619	432		237	
5	1639	882	595		284	295
6	2501	1298			356	373
7	3879	1955	1267		471	496
8	6065	2983			655	
9	9555		2951		946	995
10	15030					
11			7121			

		70/30 MeOH/H <sub>2</sub> O			Temperature = 75° C.	
nc	Alkbnzs	Bnzoates	Phenones	Parabens	Acetates	Ketones
1	353	257	222	193	189	
2	433	300	257	206	198	192
3	561	368	301	233	223	207
4	754	469	368	277	257	
5	1033	616	468		307	267
6	1453	833	830		378	318
7	2080	1153	1612	539	489	396
8	3002	1620	3306		648	
9	4367				886	679
10	6390					
11						

		70/30 MeOH/H <sub>2</sub> O			Temperature = 100° C.	
nc	Alkbnzs	Bnzoates	Phenones	Parabens	Acetates	Ketones
1	305	239	209			
2	355	267	233	188	193	
3	430	310	263	209	214	197
4	536	370	305	235	238	
5	680	448	362	268	269	243
6	882	559		312	315	276
7	1164	715	555	375	379	324
8	1554	925		460	467	
9	2099		920		588	481
10	2856					
11			1615			

		50/50 MeOH/H <sub>2</sub> O			Temperature = -20° C.	
nc	Alkbnzs	Bnzoates	Phenones	Parabens	Acetates	Ketones
1	3581	1951	884	1047		204
2		3801	1741	1900		249
3		8466	3899	4160	1113	356
4			9333	9602	2694	630
5					7156	1387
6						3451
7						
8						
9						
10						
11						

		50/50 MeOH/H <sub>2</sub> O			Temperature = 0° C.	
nc	Alkbnzs	Bnzoates	Phenones	Parabens	Acetates	Ketones
1	2456	1259	642	604	312	186
2	4836	2375	1180	1038	484	225
3	11239	5011	2227	2107	921	315
4	26752	11477	4968	4626	2026	527
5		27557	11916	10890	4827	1064
6						2396
7						5821
8						
9						
10						
11						

		50/50 MeOH/H <sub>2</sub> O			Temperature = 25° C.	
nc	Alkbnzs	Bnzoates	Phenones	Parabens	Acetates	Ketones
1	1651	842		385		184
2	3058	1476	688	605		220
3	6447	2874	1422	1095	724	293
4	13987	5981	2847	2184	1396	455
5	30704	12862	6077	4583	2968	822
6		28206		9881	6467	1631
7			29613	21614		3470
8						7551
9						
10						
11						

		50/50 MeOH/H <sub>2</sub> O		Temperature = 50° C.		
nc	Alkbnzs	Bnzoates	Phenones	Parabens	Acetates	Ketones
1	1045	586	382	290		181
2	1841	940	567	408		211
3	3442	1654	931	649	556	269
4	6654	3094	1663	1128	964	380
5	13105	5939	3141	2078	1774	611
6	26054	11615		3951	3412	1065
7		22997	12090	7655	6701	1985
8				14839		3812
9						7465
10						
11						

		50/50 MeOH/H <sub>2</sub> O		Temperature = 75° C.		
nc	Alkbnzs	Bnzoates	Phenones	Parabens	Acetates	Ketones
1	727	437	312	238		179
2	1150	642	439	305		205
3	1934	1025	649	434	434	250
4	3374	1726	1041	663	670	331
5	6013	2989	1759	1081	1100	477
6	10836	5269	5437	1827	1889	741
7	19678	9420		3175	3326	1230
8		16861	17463	5548	5789	1967
9						3709
10						
11						

		50/50 MeOH/H <sub>2</sub> O		Temperature = 100° C.		
nc	Alkbnzs	Bnzoates	Phenones	Parabens	Acetates	Ketones
1	539	351	271	210		179
2	772	474	353	252		198
3	1188	687	481	322	356	232
4	1887	1047	699	443	497	288
5	3038	1637	1067	641	734	385
6	4975	2619	2690	965	1131	542
7	8233	4257		1504	1793	805
8	13659	6951	7164	2385	2866	1243
9					5890	1974
10						
11						

## REFERENCES

1. R. P. W. Scott and P. Kucera, J. Chromatogr., 169 (1979) 51-72.
2. S. Rokushika, Z. Y. Qui, Z. L. Sun and H. Hatano, J. Chromatogr., 280(1983) 69-76.
3. M. G. Gore and P. M. Jordan, J. Chromatogr., 243 (1982) 323-328.
4. P. B. Hamilton Ann. N. Y. Acad. Sci., 102 (1962) 55.
5. J. Q. Walker, M. T. Jackson, Jr., and J. B. Maynard, Chromatographic Systems, Academic Press, New York, 1972
6. R. E. Majors, Anal. Chem., 44 (1972) 1722-1726.
7. R. W. Stout, J. J. DeStefano, L. R. Snyder, J. Chromatogr., 261 (1972) 189-212.
8. R. P. W. Scott, P. Kucera, J. Chromatogr., 185 (1979) 27-41.
9. J. Bowermaster, H. M. McNair, L. Chrom. Mag., 1 (1983) 362-364.
10. M. R. Silver, T. D. Trostler, M. R. Gould, J. E. Dickinson and G. A. Desotelle, J. Liq. Chromatogr., 7 (1984) 559-568.
11. R. P. W. Scott, P. Kucera, M. Munroe, J. Chromatogr., 186 (1979) 475-487.
12. J. H. Knox, J. Chromatogr. Sci., 18 (1980) 453-461.
13. R. Endeke, I. Halasz and K. Unger, J. Chromatogr., 99 (1974) 377-393.
14. P. Kucera, J. Chromatogr., 198 (1980) 93-109.

15. E. Katz, K. Ogan, R. P. W. Scott, J. Chromatogr., 260 (1983) 277-295.
16. L. R. Snyder, J. Chromatogr. Sci., 8 (1970) 692-706.
17. C. R. Powley, W. A. Howard and L. B. Rogers, J. Chromatogr., 299 (1984) 43-55.
18. M. Tswett, Bre. Deut. Bonstn Ges., 24 (1906) 316-384.
19. J. C. Giddings, J. Chem. Ed., 39 (1962) 569-572.
20. H. H. Strain, Ind. Eng. Chem. Anal. Ed., 18 (1946) 605-606.
21. A. L. LeRosen, C. A. Rivet Jr., Anal. Chem., 20 (1946) 1093-1094.
22. L. T. Chang, Anal. Chem., 25 (1953) 1235-1239.
23. R. J. Maggs, J. Chromatogr. Sci., 7 (1969) 145-151.
24. R. J. Maggs, T. E. Young, "Gas Chromatography 1968," C. L. A. Harborn, Ed.; Bartholomew Press, London, 1969; p. 234.
25. R. P. W. Scott, J. G. Lawrence, J. Chromatogr. Sci., 7 (1969) 65-71.
26. W. A. Aue, C. R. Hastings, J. Chromatogr., 42 (1969) 319-335.
27. J. J. Kirkland, J. J. DeStefano, J. Chromatogr. Sci., 8 (1970) 309-320.
28. L. T. Snyder, J. J. Kirkland, "Introduction to Modern Liquid Chromatography" 2nd Edition, Wiley-Interscience, New York, 1979.
29. M. J. Harvey, C. R. Lowe, P. D. G. Dean, Eur. J. Biochem., 41 (1974) 353-357.
30. M. Krejci, D. J. Kourilova, J. Chromatogr., 91 (1974) 151-160.
31. D. J. Kourilova, M. Krejci, V. Slavik, M. Deml, J. Chromatogr., 128 (1976) 79-86.

32. M. Krejci, D. J. Kourilova, J. Chromatogr., 138 (1977) 329-336.
33. E. J. Kikta Jr., A. E. Stange, S. Lam, J. Chromatogr., 138 (1977) 321-328.
34. J. Chmielowiec, H. Sawatzky, J. Chromatogr. Sci., 17 (1979) 245-252.
35. G. Hesse, H. Engelhardt, J. Chromatogr., 21 (1966) 228-238.
36. J. A. Schmit, R. A. Henry, R. C. Williams, J. F. Dieckman, J. Chromatogr. Sci., 9 (1971) 645-651.
37. A. Hashimoto, Anal. Chem., 51 (1979) 385-387.
38. W. A. Saner, J. R. Jadamec, R. W. Sager, Anal. Chem., 50 (1978) 749-753.
39. R. J. Perchalski, B. J. Wilder, Anal. Chem., 51 (1979) 774-776.
40. H. Poppe, J. C. Kraak, J. Chromatogr., 282 (1983) 399-412.
41. S. Abbott, P. Achener, R. Simpson, F. Klink, J. Chromatogr., 218 (1981) 123-135.
42. H. Poppe, J. C. Kraak, J. F. K. Huber, J. H. M. van den Berg, Chromatographia 14 (1981) 515-523.
43. Y. Hirata, E. Sumiya, J. Chromatogr., 267 (1983) 125-131.
44. J. Bowermaster, H. M. McNair, J. Chromatogr., 279 (1983) 431-438.
45. J. Bowermaster, H. M. McNair, J. Chromatogr. Sci., 22 (1984) 165-170.
46. J. G. Atwood, G. J. Schmidt, W. Slavin, J. Chromatogr., 171 (1979) 109-115.
47. M. G. Voronkov, V. P. Mileshevich, Yu. A. Yuzhelevskii, "The Siloxane Bond - Physical Properties and Chemical Transformations" Consultants Bureau, New York, 1987, p. 146.

48. Dr. Becker, E. Merck, Darmstadt, Personal Communication.
49. L. L. Lamparski, T. J. Nestruck, J. Chromatogr., 156 (1978) 143-151.
50. T. Welsh, H. Frank, J. Chromatogr., 267 (1983) 39-48.
51. H. Colin, C. Eon, G. Guiochon, J. Chromatogr., 122 (1976) 223-242.
52. H. Colin, J. C. Diez-Masa, G. Guiochon, T. Czajowska, I. Miediak, J. Chromatogr., 167 (1978) 41-65.
53. J. L. Vidal, P. Crouzet, A. Martens J. Chromatogr. Sci., 20 (1982) 252-255.
54. S. M. Fletcher, V. S. Handcock, J. Chromatogr., 206 (1981) 193-195.
55. A. J. P. Martin and R. L. M. Synge, Biochem. J., 35 (1941) 1358.
56. E. Grushka, M. N. Myers, P. D. Schettler, J. C. Giddings, Anal. Chem., 41 (1969) 889-892.
57. J. P. Foley, J. G. Dorsey, Anal. Chem., 55 (1983) 730-737.
58. R. P. W. Scott and C. F. Simpson, J. Chromatogr. Sci., 20 (1982) 62-66.
59. K. P. Hupe, R. J. Jonker, G. Rozing, J. Chromatogr., 285 (1984) 253-265.
60. C. E. Reese, R. P. W. Scott, J. Chromatogr. Sci., 18 (1980) 479-486.
61. W. Th. Kok, U. A. Th. Brinkman, R. W. Frei, H. B. Hanekamp, F. Nooitgedacht, H. Poppe, J. Chromatogr., 237 (1982) 357-369.
62. C. H. Lochmuller, M. Summer, J. Chromatogr. Sci., 18 (1980) 159-165.
63. H. H. Lauer, G. P. Rozing, Chromatographia 14 (1981) 641-647.

64. G. Taylor, Proc. Royal Soc., 219 (1953) 186-203.
65. R. Aris, G. Taylor, Proc. Royal Soc., 223 (1956) 446.
66. R. P. W. Scott, P. Kucera, J. Chromatogr. Sci., 9 (1971) 641-644.
67. J. C. Sternberg, Adv. Chromatogr., 2 (1971) 206-270.
68. B. Coq, G. Cretier, J. L. Rocca, M. Porthault, J. Chromatogr. Sci., 19 (1981) 1-12.
69. M. Broquaire, P. R. Guinebault, J. Liq. Chromatogr., 4 (1981) 2039-2061.
70. P. R. Guinebault, M. Broquaire, J. Chromatogr., 217 (1981) 509-522.
71. K. Slais, D. Kourilova, M. Krejci, J. Chromatogr., 282 (1983) 363-370.
72. F. J. Yang, J. Chromatogr., 236 (1982) 265-277.
73. B. L. Karger, J. R. Gant, A. Hartkopf, P. H. Weiner, J. Chromatogr., 128 (1976) 65-78.
74. Cs. Horvath, W. Melander, I. Molnar, J. Chromatogr., 125 (1976) 129-156.
75. R. B. Hermann, J. Phys. Chem., 76 (1972) 2754-2759.
76. A. Leo, C. Hansch, P. Y. C. Jow, J. Med. Chem., 19 (1976) 611-615.
77. B. L. Karger, L. R. Snyder, C. Eon, J. Chromatogr., 125 (1976) 71-88.
78. P. J. Schoenmakers, Dissertation, Technische Hogeschool Delft, The Netherlands, 1981.
79. H. Hemetsberger, W. Maasfeld, H. Ricken, Chromatographia 9 (1976) 303-310
80. H. Hemetsberger, M. Kellermann, H. Ricken, Chromatographia 10 (1977) 726-730.
81. H. Hemetsberger, P. Behrensmeyer, J. Henning, H. Ricken, Chromatographia 12 (1979) 71-76.

82. N. Tanaka, K. Sakagami, M. Araki, J. Chromatogr., 199 (1980) 327-337.
83. M. C. Hennion, C. Picard, M. Caude, J. Chromatogr., 166 (1978) 21-35.
84. E. H. Slaats, W. Markovski, J. Fekete, H. Poppe, J. Chromatogr., 207 (1981) 299-323.
85. R. M. McCormick, B. L. Karger, Anal. Chem., 52 (1980) 2249-2257.
86. C. R. Yonker, T. A. Zwier, M. F. Burke, J. Chromatogr., 241 (1982) 257-280.
87. H. Colin, A. Krstulovic, G. Guiochon, Z. Yun, J. Chromatogr., 255 (1983) 295-309.
88. A. Nahum, Cs. Horvath, J. Chromatogr., 203 (1981) 53-63.
89. R. J. Laub, J. H. Purnell, J. Chromatogr., 161 (1978) 49-57.
90. S. R. Bakalyar, R. McIlwrick, E. Roggendorf, J. Chromatogr., 142 (1977) 353-365.
91. H. Colin, G. Guiochon, J. Chromatogr. Sci., 18 (1980) 54-63.
92. H. J. Mockel, T. Freyholdt, Chromatographia 17 (1983) 215-220.
93. H. Colin, G. Guiochon, z. Yun, J. C. Diez-Masa, J. Jandera, J. Chromatogr. Sci., 21 (1983) 179-184.
94. H. Colin, G. Guiochon, J. C. Diez-Masa, Anal. Chem., 53 (1981) 146-155.
95. H. Colin, A. M. Krstulovic, M. F. Gonnord, G. Guiochon, Z. Yun, P. Jandera, Chromatographia 17 (1983) 9-15.
96. P. Dufek, J. Chromatogr., 281 (1983) 49-58.
97. A. M. Krstulovic, H. Colin, A. Tchaplá, G. Guiochon, Chromatographia 17 (1983) 228-230.

98. A. Tchapla, H. Colin, G. Guiochon, Anal. Chem., 56 (1984) 621-625.
99. R. M. Smith, J. Chromatogr., 236 (1982) 313-320.
100. F. Murakami, J. Chromatogr., 178 (1979) 393-399.
101. A. M. Krstulovic, H. Colin, G. Guiochon, Anal. Chem., 54 (1982) 2438-2443.
102. G. E. Berendsen, P. J. Schoenmakers, L. de Galan, G. Vigh, Z. Varga-Puchony, J. Inczedy, J. Liq. Chromatogr., 3 (1980) 1669-1686.
103. W. R. Melander, J. F. Erard, Cs. Horvath, J. Chromatogr., 282 (1983) 211-228.
104. E. H. Slaats, J. C. Kraak, W. J. T. Brugman, H. Poppe, J. Chromatogr., 149 (1978) 255-270.
105. W. Melander, D. E. Campbell, Cs. Horvath, J. Chromatogr., 158 (1978) 215-230.
106. J. K. Johnson Jr., S. F. Cernosek Jr., R. M. Gutierrez-Cernosek, J. Chromatogr., 177 (1979) 277-311.
107. I. Vit, M. Popl, J. Fahrnich, J. Chromatogr., 281 (1983) 293-298.
108. B. Neidhart, K. P. Kringe, W. Brockmann, J. Liq. Chromatogr., 4 (1981) 1875-1886.
109. A. Grobler, G. Balizs, J. Chromatogr. Sci., 12 (1974) 57-58.
110. F. Helfferich, J. Chem. Ed., 41 (1964) 410-413.
111. J. F. K. Huber, J. Chromatogr. Sci., 7 (1969) 85-90.
112. C. R. Wilke, P. Chang, Am. Inst. Chem. Engr. J., 1 (1955) 264.
113. "International Critical Tables of Numerical Data, Physics, Chemistry and Technology," E. W. Washburn, Ed., McGraw-Hill, New York, 1928, Vol V, p. 11. New York
114. J. H. Knox, J. Chromatogr. Sci., 15 (1977) 352-364

115. D. McManigill, R. Board, D. R. Gere, Presented at the 1982 Pittsburg Conference, Atlantic City, NJ.
116. S. J. Van der Wal, F. J. Yang, J. High Resolut. Chromatogr. Chromatogr. Commun., 6 (1983) 216.
117. R. F. Meyers, R. a. Harwick, Anal. Chem., 56 (1984) 2211-2214.
118. ISCO, Lincoln, Nebraska, Patent Pending.
119. "International Critical Tables of Numerical Data, Physics, Chemistry and Technology," E. W. Washburn, Ed., McGraw-Hill, New York, 1928, Vol. III., pp. 210, 216, 233.
120. "UV Atlas of Organic Compounds," Plenum Press, New York, 1971.
121. George Buck, Handy and Harman Tube Co., Norristown, PA, personal Communication
122. Handy and Harman Tube Catalog, 1984, p7
123. J. Asshauser, I. Halasz, J. Chromatogr. Sci., 12 (1974) 139-147.
124. Extrudehone Co., Pittsburg, Pa.
125. D. Ishii, T. Tsuda, K. Hibi, T. Takeuchi, T. Nakanishi, J. High. Resolut. Chromatogr. Chromatogr., Commun., 2 (1979) 371-377.
126. H. Poppe, Presented at HPLC '84, New York City, May 23, 1984.
127. J. A. Apffel, Free University, Amsterdam, personal Communication.
128. R. E. Majors, Anal. Chem., 44 (1972) 1722-1726.
129. P. Bristow, P. N. Brittain, C. M. Riley, B. F. Williamson, J. Chromatogr., 131 (1977) 57-64.
130. T. J. N. Webber, E. H. McKerrell, Anal. Chem., 122 (1976) 243-258.

131. R. Meyer, Rutgers Univ., Piscataway, NJ, Personal Communication.
132. P. Kucera, G. Manius, J. Chromatogr., 216 (1981) 9-21.
133. C. R. Yonkers, Ph.D. Dissertation, Univ. of Ariz., 1982.
134. H. Colin, J. C. Diez-Masa, G. Guiochon, T. Czajkowska, I. Miedziak, J. Chromatogr., 167 (1978) 41-65.
135. J. W. Anderson, J. Chromatogr. Sci., 22 (1984) 332-334
136. J. Bowermaster, H. M. McNair, J. Chromatogr. Sci., to be published.

**The vita has been removed from  
the scanned document**